

**TRIQUINYLAMINES AS REGULATORS OF CALCIUM
HOMEOSTASIS OF NEURONAL CELLS**

Lois-May Bezuidenhout, B.Pharm

Dissertation submitted in partial fulfilment of the requirements for the degree
Magister Scientiae in Pharmaceutical Chemistry at the
North West University
Potchefstroom Campus

Supervisor: Prof. S.F. Malan
Co-supervisor: Prof. C.J. van der Schyf
Co-supervisor: Prof. W. Liebenberg

2007

Potchefstroom

CONTENTS

ABSTRACT.....	V
UITTREKSEL.....	VIII
CHAPTER 1: INTRODUCTION.....	1
1.1 POLYCYCLIC STRUCTURES AS ION CHANNEL MODULATORS..	1
1.2 RATIONALE.....	3
1.3 AIM OF THIS STUDY.....	4
CHAPTER 2: BACKGROUND.....	6
SUMMARY.....	6
ABBREVIATIONS.....	8
2.1 THE ROLE OF CALCIUM HOMEOSTASIS IN NEUROTOXICITY.....	9
2.1.1 The role of calcium in excitotoxicity.....	11
2.1.2 Calcium mediated neurotoxicity and the role of specific channel types.....	12
2.1.3 The role of glutamate in neurotoxicity.....	13
2.1.3.1 Glutamate receptors.....	14
2.1.3.2 Functioning and molecular structure of the NMDA receptors.....	16
2.1.4 Voltage-gated calcium channels.....	18
2.1.4.1 L-type calcium channels.....	19
2.2 DRUGS USED IN THE TREATMENT OF NEURODEGENERATIVE DISORDERS.....	20
2.2.1 L-type calcium channel blockers.....	20
2.2.2 NMDA receptor antagonists.....	22

2.2.2.1 Noncompetitive and uncompetitive NMDA receptor antagonists.....	23
2.2.3 Polycyclic compounds.....	26
2.2.3.1 Adamantane amines.....	26
2.2.3.2 Pentacycloundecylamines.....	28
2.2.3.3 Triquinylamines.....	38
2.2.3.3.1 Natural triquinanes.....	38
2.2.3.3.2 Synthesis of the triquinanes.....	39
2.3 SCREENING TECHNIQUES FOR EVALUATING L-TYPE CALCIUM CHANNEL ACTIVITY OF THE TRIQUINYLAMINES.....	43
2.3.1 Fluorescent microscopy.....	43
2.4 SCREENING THECHIQUES FOR EVALUATING NMDAR CHANNEL ACTIVITY OF THE TRIQUINYLAMINES.....	46
CHAPTER 3: SELECTION AND SYNTHESIS OF RELEVANT COMPOUNDS.....	48
3.1 INTRODUCTION.....	48
3.2 GENERAL APPROUCH.....	52
3.3 SYNTHESIS OVERVIEW.....	53
3.4 DEVELOPEMENT OF PYROLYSIS APPARATUS.....	55
3.5 SYNTHESIS.....	61
3.5.1 Pentacyclo[5.4.0 ^{2,6} .0 ^{3,10} .0 ^{5,9}]undecane-8,11-dione.....	61
3.5.2 Tricyclo[6.3.0.0 ^{2,6}]undecane-4,9-diene-3,11-dione.....	62
3.5.3 Tricyclo[6.3.0.0 ^{2,6}]undecane-3,11-dione.....	64
3.5.4 N-benzyl-3,11-azatricyclo[6.3.0.0 ^{2,6}]undecane (LB-1).....	66
3.5.5 N-cyclohexylmethyl-3,11-azatricyclo[6.3.0.0 ^{2,6}]undecane (LB-2).....	68
3.5.6 N-(3-methoxybenzyl)-3,11-azatricyclo[6.3.0.0 ^{2,6}]undecane(LB-3).....	70
3.5.7 N-(3-phenylpropyl)-3,11-azatricyclo[6.3.0.0 ^{2,6}]undecane (LB-4).....	72
3.5.8 N-methyl-3,11-azatricyclo[6.3.0.0 ^{2,6}]undecane (LB-5).....	75
3.5.9 N-(1-piridinyl)-3,11-azatricyclo[6.3.0.0 ^{2,6}]undecane (LB-6).....	76

3.6	CONCLUSION.....	78
3.7	COMPUTATIONAL STUDY.....	79
3.7.1	Problem statement.....	79
3.7.2	Computational calculations.....	81
3.7.3	Results.....	81
3.7.4	Conclusion.....	85
 CHAPTER 4: BIOLOGICAL EVALUATION.....		 86
SUMMARY.....		86
ABBREVIATIONS.....		86
 4.1 EVALUATION OF CALCIUM HOMEOSTASIS.....		 87
4.1.1	Introduction.....	87
4.1.2	Materials and methods.....	88
4.1.2.1	Cell cultures.....	88
4.1.2.2	Solutions.....	89
4.1.2.3	Loading cells with calcium-sensitive fluorescent indicators.....	90
4.1.2.4	Experimental single-cell recording.....	91
4.1.3	Results.....	92
4.1.3.1	Statistical analysis.....	92
4.1.3.2	Fluorescent calcium flux experiments.....	92
4.1.4	Discussion.....	99
 4.2 SCREENING OF THE TRIQUINYLAMINES FOR ACTIVITY AT THE NMDA RECEPTOR.....		 101
4.2.1	Introduction.....	101

4.2.2	Materials and methods.....	101
4.2.2.1	Animals.....	101
4.2.2.2	Materials.....	101
4.2.2.3	Radioligand binding assay.....	102
4.2.3	Results.....	103
4.2.3.1	Statistical analysis.....	103
4.2.3.2	Radioligand binding experiments.....	103
4.2.3.3	Dose-response curve.....	104
4.2.4	Discussion.....	105
4.2.5	Summary.....	106
CHAPTER 5: CONCLUSION.....		108
5.1	FINAL REMARK.....	113
REFERENCES.....		114
ACKNOWLEDGMENTS.....		128
APPENDISES		
APPENDIX A (ABBREVIATIONS).....		131
APPENDIX B (EXPERIMENTAL GRAPHS).....		133
APPENDIX C (SPECTRAL DATA).....		137

ABSTRACT

Neurodegenerative diseases include common and debilitating disorders such as Parkinson's disease (PD), Alzheimer's disease (AD), Huntington's disease (HD) and post-stroke neurodegeneration. Among these disorders, PD and AD have especially drawn attention because of their devastating impact on the elderly, their families, the health care system and society. These disorders are characterised by progressive and irreversible loss of neurons from specific regions of the brain. Among the mechanisms implicated to be responsible for neuronal cell death we focused our interest on excitotoxicity, which initiates a cascade of events resulting in neuronal injury as a result of excessive influx of Ca^{2+} through the *N*-methyl-D-aspartate receptor (NMDAR) and voltage gated calcium channels (VGCC).

The focus of the current study was to develop a novel group of multifunctional therapeutic agents that can be used in the treatment and/or prevention of neurodegenerative diseases. Several triquinylamine derivatives containing an endocyclic nitrogen atom (aza-bridged) and select side chains were synthesised by thermal [2 + 2] cycloreversion of the symmetric cage compound pentacyclo[5.4.0.0^{2,6}.0^{3,10}.0^{5,9}]undecane-8,11-dione. To be able to perform the thermal fragmentation reactions we designed and built a pyrolysis apparatus based on descriptions found in the literature. With this technology, the reaction was optimised to a yield approaching 80%. The symmetric *cis-syn-cis* triquinane scaffold obtained from the thermal fragmentation reaction underwent subsequent catalytic reduction, amination and hydride reduction to generate the series of compounds under study. The synthesised compounds were characterised using NMR, MS and IR techniques. Reductive amination produced very low yields of the desired products and we were also unable to isolate the *N*-methyl derivative, *N*-methyl-3,11-azatricyclo[6.3.0.0^{2,6}]undecane. A computational study was initiated to explain the apparent selectivity in the formation of the benzylamine derivative over the methylamine derivative. The computational study revealed that a significantly lower energy of formation and more favourable HOMO-LUMO overlap (indicating a

stronger covalent bond) might be an explanation for the selectivity in formation of the 3-benzyliminotricyclo[6.3.0.0^{2,6}]undecane-11-one intermediate over that of the 3-methyliminotricyclo[6.3.0.0^{2,6}]undecane-11-one intermediate.

In order to afford protection against excitotoxicity, new drug candidates have to attenuate the induced Ca²⁺ flux through the L-type calcium channels and demonstrate binding affinity for the NMDAR channels. Fluorescent microscopy was utilized to monitor Ca²⁺ flux through the L-type calcium channel after KCl-induced depolarisation (KCl at 140 mM) in the Mag-fura-2/AM preloaded N2α mouse neuroblastoma cell line. The *N*-(3-methoxybenzyl)-3,11-azatricyclo[6.3.0.0^{2,6}]undecane compound proved to be the most potent experimental compound with a reduction in fluorescence of approximately 55.9% and was the only compound that showed a statistically significant ($p < 0.05$) attenuation of Ca²⁺ flux. This data indicate that the introduction of electronic effects, such as the inductive effect with significant electron-withdrawing properties of the *N*-(3-methoxybenzyl)-3,11-azatricyclo[6.3.0.0^{2,6}]undecane compound, significantly influences the L-type calcium channel binding characteristics. The *N*-(phenylpropyl)-3,11-azatricyclo[6.3.0.0^{2,6}]undecane showed a reduction in fluorescence of 42.9 %, which indicated that, an increase in chain length leads to a commensurate increase in activity when compared to the benzylamine derivatives.

Radioligand binding studies were used to measure the displacement of [³H]MK-801 from NMDA/glycine-activated murine synaptoneurosome by the triquinylamine derivatives. The study indicated *N*-benzyl-3,11-azatricyclo[6.3.0.0^{2,6}]undecane to be the compound with the highest affinity, with an IC₅₀ value of 1.93 μM ($p < 0.05$), which is comparable to the clinically used drug memantine (IC₅₀ = 0.54 μM). None of the other triquinylamine compounds tested showed significant displacement, which indicated that these compounds do not strongly interact with the PCP binding site and possibly have a different site of interaction within the NMDA receptor/ion channel complex.

Our results demonstrate that the triquinylamines have the ability to simultaneously block both major neuronal calcium channels. Different binding characteristics were however found to be important for the two channels. Of the structure-activity

relationship parameters studied, geometric or steric constraints for interaction both at the VGCC and NMDAR channel appear to be dominant. However, binding characteristics for the VGCC were greatly improved with the introduction of inductive electronic effects. We conclude that the triquinylamines tested represent a novel group of dual-mechanistic agents that have potential as therapeutic agents in the treatment of neurodegenerative diseases.

UITTREKSEL

Neurodegeneratiewe siektes sluit toestande soos Parkinson-, Alzheimer- en Huntington se siekte asook beroerte in. Van hierdie toestande geniet veral Parkinson- en Alzheimer se siekte aandag vanweë hul verwoestende impak op bejaardes, hul familie, die gesondheidsorgstelsel en die gemeenskap. Hierdie toestande word gekarakteriseer deur progressiewe en onomkeerbare verlies van neurone in spesifieke areas van die brein. Verskeie meganismes is verantwoordelik vir die verlies van neurone, maar ons belangstelling in hierdie studie was gefokus op eksitotoksiteit, wat neuronale skade beskryf as gevolg van wanregulasie in Ca^{2+} fluks deur onder andere die *N*-metiel-D-aspartaat reseptorkanale (NMDAR-kanale) en die spanningsafhanklike kalsiumkanale.

Die fokus van hierdie studie was die ontwikkeling van 'n nuwe reeks multifunksionele terapeutiese verbindings wat gebruik kan word in die behandeling en/of die voorkoming van neurodegeneratiewe siektetoestande. Verskeie trikwinielamienderivate wat 'n endosikliese stikstofbinding (asa-brug) en verskeie sykettings bevat is gesintetiseer deur middel van 'n termiese [2 + 2] siklo-omkeringsreaksie vanaf die simmetriese "voëlhok" verbinding, pentasiklo[5.4.0.0^{2,6}.0^{3,10}.0^{5,9}]undeka-8,11-dioon. Om die termiese fragmenteringsreaksies uit te voer moes 'n pirolise-apparaat ontwerp en gebou word, gebaseer op beskrywings uit die literatuur. Deur gebruik van hierdie apparaat is die fragmenteringsreaksie geoptimaliseer tot 'n opbrengs van ~80 %. Die simmetriese *cis-syn-cis* trikwinaansistiem verkry vanaf die termiese fragmentasiereaksie het gedien as moederverbinding vir opeenvolgende katalitiese reduksie, aminering en hidriedreduksie om die reeks verbinding wat in hierdie studie ondersoek is, te lewer. Die verbindings wat gesintetiseer is, is gekarakteriseer deur KMR, MS en IR. Die reduktiewe amineringsreaksies het 'n baie lae opbrengs gelewer en *N*-metiel-3,11-asatrisiklo[6.3.0.0^{2,6}]undeka- kon nie geïsoleer word nie. 'n Rekenaarsmodelleringstudie is gebruik in 'n poging om die selektiewe vorming van die bensielamien, in stede van die metielamien, te verduidelik. Die modelleringstudie

het daarop gedui dat aansienlike laer vormingsenergie en meer gunstige HOMO-LUMO oorvleueling (wat sterker kovalente binding aandui) moontlik verantwoordelik kan wees vir die voorkeur in die vorming van die 3-bensielimienotrisiklo[6.3.0.0^{2,6}]undekaan-11-een oorgangsverbinding in stede van die 3-metielimienotrisiklo[6.3.0.0^{2,6}]undekaan-11-een oorgangsverbinding.

Die verbindings se vermoë om eksitotoksisiteit teen te werk is gemeet aan effektiewe Ca²⁺ fluks-onderdrukking in spanningsafhanklike kalsiumkanale, asook bepaling van die bindingsaffiniteit vir NMDAR-kanale. Fluoresensiemikroskopie in N2α muis neuroblastoomselle wat vooraf met Mag-fura-2/AM gelaai is, is gebruik om Ca²⁺ fluks deur kalsiumkanale te meet na KCl-geïnduseerde depolarisasie (KCl, 140 mM). Die *N*-(3-metoksiebensiel)-3,11-asatrisiklo[6.3.0.0^{2,6}]undekaan verbinding het die grootste effek getoon. Hierdie verbinding was die enigste wat 'n statisties-betekenisvolle ($p < 0.05$) onderdrukking van die Ca²⁺ fluks getoon het, met 'n vermindering in fluoressensie van ongeveer 55.9 %. Hierdie bevindings dui daarop dat die inkorporering van elektroniese effekte, soos die induktiewe effekte met beduidende elektron-onttrekkende einskappe waargeneem vir *N*-(3-metoksiebensiel)-3,11-asatrisiklo[6.3.0.0^{2,6}]undekaan verbinding, 'n betekenisvolle invloed op die bindingseienskappe aan die spanningsafhanklike kalsiumkanaal het. *N*-(fenielpropiel)-3,11-asatrisiklo[6.3.0.0^{2,6}]undekaan het 'n vermindering in fluoressensie getoon van ongeveer 42.9 %, wat daarop dui dat 'n toename in kettinglengte 'n gepaardgaande toename in aktiwiteit tot gevolg het.

Radioligandbindingstudies is gebruik om die verplasing van [³H]MK-801 vanaf NMDA/glisien geaktiveerde muis-sinaptoneurosome deur die trikwinielamienderivate te ondersoek. Die studie het getoon dat *N*-bensiel-3,11-asatrisiklo[6.3.0.0^{2,6}]undekaan die verbinding met die hoogste affiniteit was met 'n IC₅₀ waarde van 1.93 μM ($p < 0.05$). Hierdie waarde is vergelykbaar is met die klinies-gebruikte geneesmiddel memantien (IC₅₀ = 0.54 μM). Geen van die oorblywende trikwinielamiene wat in hierdie studie getoets is het enige betekenisvolle verplasing van [³H]MK-801 getoon nie. Dit dui daarop dat hierdie verbindings nie beskik oor sterk interaksie met die PCP bindingsetel nie en dus moontlik interageer met 'n ander setel binne die NMDA reseptor/ionkanaalkompleks.

Die resultate van hierdie studie dui daarop dat die trikwinielamiene oor die potensiaal beskik om gelyktydig die vernaamste neuronale kalsiumkanale te blokkeer, alhoewel dit duidelik is dat verskillende bindingskarakteristieke vir die spesifieke kanale van belang is. Die studie toon verder dat strukturaktiwiteitsverwantskappe vir interaksie met beide die spanningsafhanklike kalsiumkanale en NMDAR-kanale binne hierdie groep verbindings hoofsaaklik gedomineer word deur geometriese en steriese oorwegings. Verder blyk dit dat die bindingskenmerke vir interaksie met die spanningsafhanklike kalsiumkanale ook aansienlik verbeter met die inkorporering van induktiewe elektroniese effekte. Die trikwinielamiene wat ondersoek is in hierdie studie verteenwoordig 'n nuwe groep verbindings met 'n tweeledige werkingsmeganisme en wat oor die potensiaal beskik om as terapeutiese middels aangewend te word in die behandeling van neurodegeneratiewe siektetoestande soos Parkinson- en Alzheimer se siektes.

CHAPTER 1

INTRODUCTION

1.1 POLYCYCLIC STRUCTURES AS ION CHANNEL MODULATORS

In recent years many attempts have been made to extend the use of known Ca^{2+} channel blockers to areas other than pathological conditions of the cardiovascular system. Several studies identified disturbances in calcium homeostasis as one of the major contributors towards neurotoxicity and subsequent neuronal cell death (Lipton, 1999; Horn & Limburg, 2001; Kemp & McKernan, 2002). Two major pathways have been implicated to be responsible for the excessive influx of calcium into neurons during excitotoxicity; the voltage-gated calcium channels (VGCC) and *N*-methyl-D-aspartate receptor (NMDAR) channels (Choi, 1988; Choi, 1995; Sattler & Tymianski, 2000; Arundine, 2003).

To determine whether calcium channel blockers would be effective in the treatment of neuropathological disorders, researchers investigated the use of L-type calcium blockers such as nimodipine in the treatment of Ca^{2+} overload in the ischemic cascade following traumatic brain injury. Such application of these drugs has been reported to be effective (Feigin *et al.*, 1998; Horn & Limburg, 2001). The three main classes of selective L-type calcium channel blockers currently available for clinical use are the phenylalkylamines, the benzothiazepines, and the dihydropyridines (Mori *et al.*, 1996; Hockerman *et al.*, 1997). Polycyclic cage compounds, with NGP1-01 as a lead compound, were first established to be effective L-type calcium channel blockers by the group of Van der Schyf *et al.*, (1986). Further investigation led to the synthesis of several derivatives of NGP1-01 that showed good correlation with known L-type calcium channel blockers (Van der Schyf *et al.*, 1986; Van der Walt *et al.*, 1988; Malan *et al.*, 2000; Liebenberg *et al.*, 2000).

Several authors discussed the link between glutamate toxicity and Ca^{2+} influx through the NMDAR. The subsequent Ca^{2+} overload and observed excitotoxicity lead to the idea that glutamate toxicity participated in neuronal cell death. (Simon, 1984; Choi, 1985; Garthwaite *et al.*, 1986). This link also established a specific rationale for targeting the NMDAR for selective blockade of extraneous calcium fluxes, thus allowing subsequent reduction in glutamate-induced Ca^{2+} influx (Arundine, 2004). Several polycyclic compounds have been identified as NMDAR antagonists such as high-affinity noncompetitive NMDAR antagonists (MK-801 and PCP) and low-affinity uncompetitive NMDAR antagonists (amantadine, memantine and NGP1-01). The use of high-affinity noncompetitive NMDAR antagonists however, is limited in their use due to their undesirable psychotomimetic side effects. The use of low-affinity uncompetitive NMDAR antagonists such as amantadine and memantine, also polycyclic compounds, has been proven to be clinically well tolerated. This led to the evaluation of NGP1-01 for neuroprotective activity (Geldenhuis *et al.*, 2003; Grobler *et al.*, 2006; Geldenhuis *et al.*, 2006). NGP1-01 and several derivatives demonstrate favourable use-dependent and low-affinity uncompetitive block of the NMDAR channel.

It has become abundantly clear in diseases with multiple etiological causes of the observed pathology; clear benefits could be gained by employing so called “multifunctional” or “dual-mechanism” drugs as reported by several authors (Christiaans & Timmerman, 1996; Morphy *et al.*, 2004; Roth *et al.*, 2004; Morphy & Rankovic, 2005; Youdim & Buccafusco, 2005a,b; Van der Schyf *et al.*, 2006). Our interests in the polycyclic cage compounds eventually led to the evaluation of NGP1-01 for possible dual-mechanistic action on both the L-type calcium channel and NMDAR channel in the central nervous system (Kiewert *et al.*, 2006). The study by Kiewert established NGP1-01 as a promising lead structure for a new class of multifunctional drugs with great potential in the treatment of neurodegenerative diseases.

Further investigations to elucidate the mechanism by which NGP1-01 and its derivatives exert their pharmacological action led to the establishment of structure activity relationship correlations for series of these compounds on both the L-type calcium channel and NMDAR channel, both in the cardiovascular and in the central

nervous system (Malan *et al.*, 2000; Liebenberg *et al.*, 2000; Geldenhuys *et al.*, 2006). These structure activity relationships suggested that the pentacycloundecane skeleton may serve only as a bulk contributor for the biological activity of NGP1-01 and other polycyclic cage compounds (Malan *et al.*, 2000; Liebenberg *et al.*, 2000). Liebenberg *et al.*, (1996) synthesised thermal ring-opened derivatives of NGP1-01 in order to investigate the validity of this hypothesis. The compounds investigated showed favourable activity as calcium channel antagonists and the authors concluded that ring opening of the cage moiety did not diminish the potential to block the L-type calcium channel. The activity of these compounds as potential NMDAR antagonists still remains to be investigated. The possibility of yet another group of polycyclic compounds – the unique *cis-syn-cis* triquinane system – being identified as multimodal drug scaffolds, is an important concept lending impetus to the justification of studies that aim to further investigate these structures as drug scaffolds. To our knowledge no studies have been carried out to investigate derivatives of these polycycles as drug leads in the treatment of neurodegenerative diseases.

1.2 RATIONALE

Due to the fact that dysregulation of calcium homeostasis is implicated as one of the major contributors towards neurotoxicity and subsequent neuronal cell death (Lipton, 1999; Horn & Limburg, 2001; Kemp & McKernan, 2002), our focus in this study will be on the major pathways contributing toward the excessive calcium influx known as excitotoxicity. The VGCC and NMDAR channels have been implicated as two major pathways responsible for excessive Ca^{2+} influx and consequent Ca^{2+} accumulation and overload in neuronal cells (Choi, 1988; Choi, 1995; Sattler & Tymianski, 2000; Arundine, 2003). The link between excitotoxicity and these two major pathways established the rationale for targeting these channels for selective blockade in a use-dependent manner, thus regulating Ca^{2+} flux.

Our interest in the synthesis and pharmacological evaluation of the triquinylamines as possible neuroprotective drug candidates was prompted by:

- our search for fascinating new polycyclic structures that possess structural similarities to compounds with neuroprotective activity, specifically aimed at attenuating calcium flux through L-type calcium channels and NMDAR channels.
- the hypothesis that the pentacycloundecane cage moiety may serve only as a bulk contributor to the pharmacological action of NGP1-01 and other pentacycloundecane derivatives (Van der Schyf *et al.*, 1986; Malan *et al.*, 2000; Liebenberg *et al.*, 2000), thereby allowing a much more promiscuous approach towards chemical structure development for multimodal drugs. This theory was partially elucidated by Liebenberg *et al.*, (1996) through the syntheses of thermal ring-opened derivatives of NGP1-01 to yield triquinylamine structures. These compounds showed favourable activity as L-type calcium channel antagonists and the authors concluded that ring opening of the cage moiety did not diminish the potential to block the L-type calcium channel. The interaction of these compounds at the NMDAR needs to be investigated in order to establish the triquinane polycycle as a motif for multimodal drug design.
- the structural similarities between the triquinylamines and the pentacycloundecylamines. The later have been established as blockers of both the L-type calcium channels and NMDAR channels, (Van der Schyf *et al.*, 1986; Van der Walt *et al.*, 1988; Malan *et al.*, 2000; Liebenberg *et al.*, 2000; Geldenhuys *et al.*, 2003; Grobler *et al.*, 2006; Geldenhuys *et al.*, 2006; Kiewert *et al.*, 2006),

1.3 AIM OF THIS STUDY

The aim of this study was to synthesise a series of triquinylamines and to evaluate these novel structures as neuronal L-type calcium channel and NMDAR antagonists. This will be achieved by monitoring calcium movement into neuronal cells through the VGCC and by evaluating the affinity for the same binding site as MK-801 on the NMDAR channel. Fluorescence microscopic techniques will be utilized to measure calcium influx through the L-type calcium channel after KCl-induced depolarisation

in the N₂α mouse neuroblastoma cell line. To measure the affinity for the NMDAR channel we will utilize radioligand binding studies to evaluate the displacement of [³H]MK-801 from murine synaptoneurosomes in the presence and absence of the triquinylamine derivatives. The latter will evaluate whether these compounds compete with MK-801 and PCP for interaction with these ligands' specific binding sites inside the NMDAR channel, with a view to establish their mechanism of action on the NMDA receptor.

This study is part of an ongoing investigation into the biological activity of polycyclic amine derivatives and will further investigate the validity of the hypothesis that the pentacycloundecane skeleton may serve only as a bulk contributor to the activity of polycyclic compounds such as NGP1-01 and its derivatives. In order to be able to perform the thermal fragmentation reactions, a pyrolysis apparatus will be designed and built and the pyrolysis reactions reported in literature (Liebenberg *et al.*, 1996) that effected pathways towards the syntheses of triquinane-type scaffolds will be optimised. The triquinylamines synthesised will allow for direct comparison with previously synthesised and pharmacologically characterised pentacycloundecylamines that showed activity on both the L-type calcium channel and NMDAR channel.

CHAPTER 2

BACKGROUND

SUMMARY

Neurodegenerative diseases include common and debilitating disorders such as Parkinson's disease (PD), Alzheimer's disease (AD) and Huntington's disease (HD). These disorders are characterised by progressive and irreversible loss of neurons from specific regions of the brain. There are three mechanisms of neuronal cell death; excitotoxicity, metabolic compromise and oxidative stress, which may act separately or co-operatively to cause neurodegeneration (Lipton, 1999; Horn & Limburg, 2001; Kemp & McKernan, 2002). The focus in this study will be on excitotoxicity, which describes the neuronal injury that results from excessive influx of Ca^{2+} through the NMDA receptor channel and L-type calcium channel (Sattler & Tymianski, 2000; Arundine & Tymianski, 2003; Pringle, 2004).

Because of the NMDA receptor's large Ca^{2+} conductance, it has been a focus point of many research initiatives into excitotoxicity and neuronal death. However, the voltage gated calcium channel (VGCC) has also been established as a major pathway through which Ca^{2+} can enter the cell during the excitotoxic cascade. Thus, our focus in this study will primarily be on drug candidates that have shown neuroprotective activity by blocking these two major pathways.

Drug candidates that block the L-type calcium channels have primarily been studied for their pharmacological action in the cardiovascular system (Mori *et al.*, 1996). However, all L-type calcium channels share a common pharmacological profile, with a high sensitivity to several classes of drugs that have been used as selective L-type channel blockers including diltiazem, the prototype benzothiazepine; nimodipine, the prototype 1,4-dihydropyridine and verapamil, the prototype phenylalkylamine (Janis *et al.*, 1987; Hockerman, 1997; Triggle, 2003). These drugs can also be used to treat neurodegenerative diseases (Kobayashi & Mori, 1998; Pizzi *et al.*, 2002).

Drug candidates that prevent excessive activation of the NMDA receptor, termed NMDA receptor antagonists, reduce the potentially damaging and lethal influx of calcium into neurons. It is important to distinguish high and low-affinity uncompetitive NMDA receptor blockers from high-affinity noncompetitive receptor blockers such as MK-801 (dizocilpine) and PCP (phencyclidine). The latter exhibit behavioural side effects that limit their clinical usefulness. Low-affinity uncompetitive NMDA receptor blockers such as amantadine and memantine however, are clinically better tolerated because they modulate the receptor channel, rather than blocking it completely. Thus, the low-affinity uncompetitive NMDAR channel blockers operate in a use dependent manner that allows for normal neuronal functioning.

NGP1-01, the lead compound for the pentacycloundecanes, was first established as an L-type calcium channel blocker in the cardiac system (Van der Schyf *et al.*, 1986; Van der Walt *et al.*, 1988; Malan *et al.*, 2000; Liebenberg *et al.*, 2000). Further investigation led to the establishment of NGP1-01 and other pentacycloundecanes as uncompetitive low-affinity NMDA receptor antagonists with neuroprotective activity (Geldenhuys *et al.*, 2003; Grobler *et al.*, 2006; Geldenhuys *et al.*, 2006). Prompted by the interest in neuroprotective agents with multiple mechanisms of action, NGP1-01 was tested on L-type calcium channels and NMDA receptor channels by Kiewert *et al.*, (2006). This study established NGP1-01 as a promising lead structure for a new class of multifunctional drugs with great potential in the treatment of neurodegenerative diseases.

To further investigate the hypothesis that the pentacycloundecane skeleton serves only as a bulk contributor for the biological activity of NGP1-01, Liebenberg *et al.*, (1996) synthesised thermal ring-opened derivatives of NGP1-01 to obtain a *cis,syn,cis* triquinylamine system derived from the pentacycloundecane moiety. These compounds showed favourable activity as calcium channel antagonists and the investigators concluded that ring opening of the cage moiety of NGP1-01 did not diminish its potential to block the L-type calcium channel. This is an important concept in justifying further investigation of the triquinylamines, for to our knowledge

no studies have been carried out to determine their activity as possible drugs in the treatment of neurodegenerative diseases.

ABBREVIATIONS

AC	adenyl cyclase
AMPAR	α -amino-3-hydroxy-5-methylisoxazole-4-propionic acid receptor (also known as the quisqualate receptor)
AP	action potential
ATP	adenyl triphosphate
cAMP	cyclic adenosine-monophosphate
[Ca²⁺]_i	intracellular calcium concentration
[Ca²⁺]_e	extracellular calcium concentration
CNS	central nervous system
EAA	excitatory amino acid
ER	endoplasmic reticulum
GTP	guanosine triphosphate
Glu	glutamate
Gly	glycine
KA	kainate
MK-801	dizocilpine
NMDA	<i>N</i> -methyl-D-aspartate
NMDAR	<i>N</i> -methyl-D-aspartate receptor
NOS	nitric oxide synthases
PCP	phencyclidine
PLC	phospholipase-C
PKC	protein kinase-C
ROS	reactive oxygen species
SAR	structure-activity relationship
VGCC	voltage gated calcium channels

2.1 THE ROLE OF CALCIUM HOMEOSTASIS IN NEUROTOXICITY

In the search toward better understanding the mechanisms of cell death, several studies identified the disturbance in calcium metabolism as one of the major contributors towards neurotoxicity and subsequent neuronal cell death (Lipton, 1999; Horn & Limburg, 2001; Kemp & McKernan, 2002). McLean *et al.*, (1965) observed that liver that had been damaged by toxins accumulated calcium and suggested that calcium entry is responsible for tissue damage. Several other authors contributed to this theory when they reported the effect of calcium in tissue necrosis (Zimmerman & Hulsan, 1966; Schanne *et al.*, 1979). These authors arrived at the conclusion that Ca^{2+} influx into cells is a requirement for the observed toxicity. Further studies into these findings arrived at the conclusion that excessive Ca^{2+} influx (known as excitotoxicity) and subsequent accumulation in neuronal cells ultimately leads to cell death (Lipton, 1999; Horn & Limburg, 2001; Kemp & McKernan, 2002).

Calcium as an intracellular messenger is fundamental in the regulation of numerous cellular functions such as differentiation and growth, membrane excitability, exocytosis, and synaptic activity (Lipton, 1999; Tymianski & Tator, 1996). Neurons possess specialised homeostatic mechanisms to maintain calcium homeostasis by balancing the influx, extrusion and compartmentalisation of free calcium ions (Fig. 2.1). In their resting state, free intracellular calcium levels ($[\text{Ca}^{2+}]_i$) are maintained at low levels (100 μM) compared to approximately 1 mM in the extracellular space ($[\text{Ca}^{2+}]_e$). Thus, relatively small or localised $[\text{Ca}^{2+}]_i$ elevations can be used to trigger physiological events such as activation of enzymes or ion channels. Under physiological conditions the delicate interplay between Ca^{2+} influx, Ca^{2+} buffering, internal Ca^{2+} storage, and Ca^{2+} efflux allow multiple Ca^{2+} dependent signalling cascades to be regulated independently within the same cell. However, excessive Ca^{2+} influx or release from intracellular stores can elevate Ca^{2+} loads to levels that exceed the capacity of Ca^{2+} -regulatory mechanisms. This leads to the inappropriate activation of Ca^{2+} -dependent processes that are normally dormant or operate at low levels, causing metabolic derangements and eventual cell death. For example, over activation

of proteases, lipases, phosphatases, and endonucleases caused by excessive elevations in intracellular Ca^{2+} may directly damage cell structures or induce the formation of nitric oxide synthases (NOS) and other degradative enzymes that lead to formation of free radicals, necrosis or apoptosis (Lipton, 1999; Sattler & Tymianski, 2000; Kemp & McKernan, 2002; Arundine, 2003).

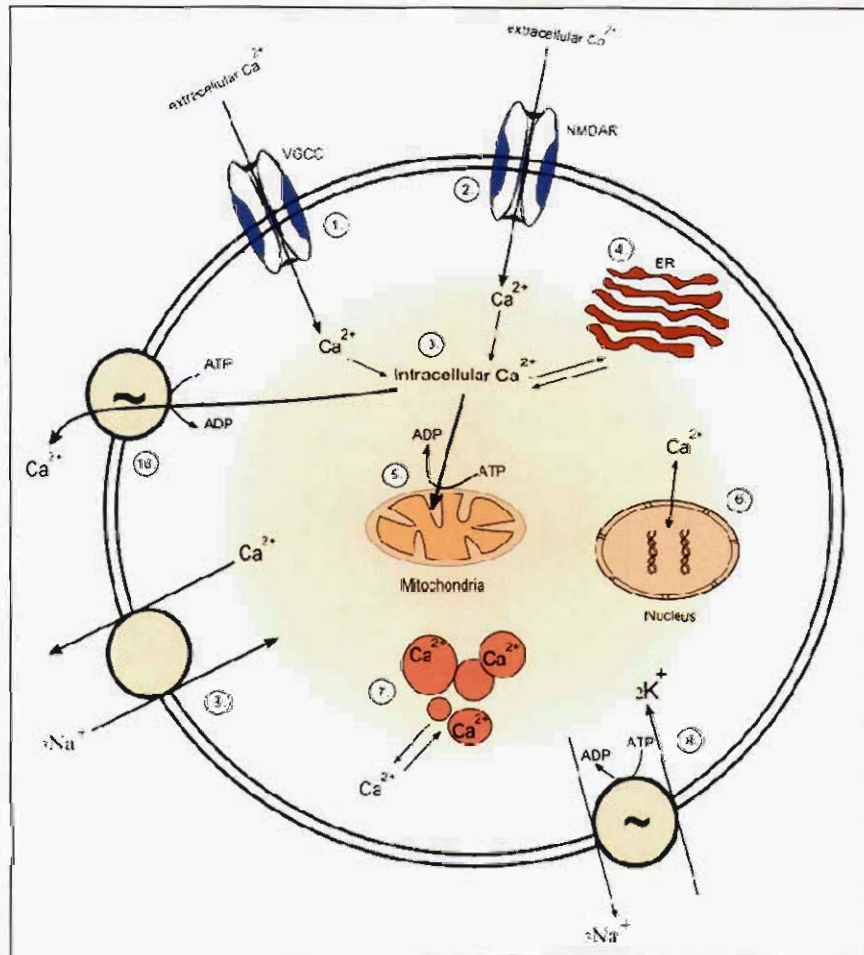


Figure 2.1: A schematic representation of Ca^{2+} homeostasis in neurons. Abbreviations: ER, endoplasmic reticulum; NMDAR, *N*-methyl-D-aspartate receptor; VGCC, voltage-gated calcium channels. (1) Ca^{2+} influx via VGCC; (2) Ca^{2+} influx via NMDAR; (3) accumulation of Ca^{2+} intracellular; (4) sequestration and release of Ca^{2+} by the ER; (5) sequestration of Ca^{2+} by the mitochondria; (6) sequestration of Ca^{2+} by the nucleus; (7) intracellular calcium buffering by Ca^{2+} binding proteins; (8) active transport via the Na, K-ATPase ionic pump; (9) Ca^{2+} extrusion via the Na/Ca-exchanger; (10) active transport via the Ca-ATPase ionic pump (adapted from Sattler and Tymianski, 2000).

2.1.1 THE ROLE OF CALCIUM IN EXCITOTOXICITY

As described earlier, calcium homeostasis is maintained by balancing the influx, extrusion and compartmentalisation of free calcium ions. Based on the model described in Fig. 2.1, the increase in $[Ca^{2+}]_i$ may arise through several separate sources. For the purpose of this study, we will focus on the two primary mechanisms by which calcium may enter the cell, i.e. NMDA receptors and VGCCs.

During traumatic brain injury, anoxic depolarisation has a biphasic effect: first, there is pre-synaptic calcium entry triggering the release of glutamate, and second, depolarisation in the post-synaptic neuron will cause opening of the VGCC with subsequent influx of calcium, whilst also acting as a trigger to remove the Mg^{2+} block of the NMDA receptor (NMDAR) (Pringle, 2004). Activation of the NMDAR leads to alterations in the concentration of intracellular ions, especially Ca^{2+} and Na^+ . The additional influx of Na^+ causes osmotic swelling and damage to cells. Choi and colleagues (Choi, 1987a & Choi *et al.*, 1987b) suggested that glutamate toxicity is primarily dependent on Ca^{2+} influx and, because of its large calcium conductance, the NMDAR has been a focus point of many research initiatives concerning excitotoxicity and neuronal diseases.

It is now well established that a strong relationship exists between excessive Ca^{2+} influx and glutamate-triggered neuronal injury (reviewed in Choi, 1988; Tymianski, 1996 & Tymianski *et al.*, 1996). Ca^{2+} overload can trigger many downstream neurotoxic cascades, including the generation of nitric oxide and other free radicals, which may cause lipid peroxidation and depletion of ATP stores in neurons. ATP depletion is a result of enhanced metabolic stress on mitochondria that leads to abnormal mitochondrial respiration and increased production of O_2^- , H_2O_2 , and OH^\cdot , i.e. reactive oxygen species (ROS). Calcium also stimulates the production of arachidonic acid metabolites. Finally, the elevation of intracellular calcium may result in the non-specific activation of many enzymes such as calpains and other proteases, protein kinases, nitric oxide synthase (NOS), calcineurins and endonucleases. This may cause abnormal control of signalling pathways and decreased integrity of

cytoskeletal elements and eventually cause activation of genetic signals leading to cell death (apoptosis) (Greene & Greenamyre, 1996; Arundine, 2003).

As mentioned earlier, the VGCC also largely contributes to the excess influx of calcium and subsequent increase in $[Ca^{2+}]_i$. The dramatic decrease in ATP concentration associated with these conditions leads to rapid depolarisation that is accompanied by large inward flux of calcium through the VGCC.

2.1.2 CALCIUM MEDIATED NEUROTOXICITY AND THE ROLE OF SPECIFIC CHANNEL TYPES

The excess entry of Ca^{2+} , and consequent Ca^{2+} overload, has been identified as one of the major mechanisms responsible for neuronal cell death through the variety of mechanisms previously discussed. A significant body of evidence is available to implicate calcium in neurotoxicity and several pathways have been identified to be involved in the excess entering of calcium into neuronal cells (Choi, 1988; Choi, 1995; Sattler & Tymianski, 2000; Arundine, 2003). Entry of calcium into neurons under normal physiological conditions is controlled predominantly by either VGCC or ligand-gated receptor-coupled channels, such as the NMDAR channels. Glutamate toxicity can be linked with Ca^{2+} influx through the NMDAR channel. The subsequent Ca^{2+} overload provided convergence between the idea that glutamate toxicity participated in hypoxic neuronal death, and other evidence suggesting that this death was associated with loss of Ca^{2+} homeostasis (Simon, 1984; Choi, 1985; Garthwaite *et al.*, 1986). This linkage also established a specific rationale for targeting the NMDAR for selective blockade allowing subsequent reduction in glutamate-induced Ca^{2+} influx (Arundine, 2004). Thus far, the focus for regulating calcium homeostasis in the central nervous system (CNS) has been mainly on the NMDAR channel. However, another major gateway for cellular Ca^{2+} entry is through voltage-gated calcium channels such as L-type calcium channels. In studies done on animal models of ischemia, the known L-type calcium channel blocker nimodipine has shown potential neuroprotective activity by blocking the influx calcium into the neuronal cell (Horn & Limburg, 2001).

The large array of neurodegenerative mechanisms and several potential drug targets as discussed above have made it difficult to propose a focused means of treating Ca^{2+} dependent neurodegeneration. Therapeutic strategies may have to address several processes simultaneously rather than a single drug target or neurotoxic mechanism. This has led to the concept of “dual-mechanistic drugs” that is supported by several scientists and clinicians (Morphy & Rankovic, 2005). In a recent review, Van der Schyf *et al.*, (2006) gave an overview of the therapeutic strategies and novel investigative drugs discovered or developed in the authors own, as well as other laboratories, that address multiple central nervous system etiological targets associated with an array of neuropsychiatric disorders. Of particular interest amongst the drugs discussed is the polycyclic cage compound NGP1-01, dizocilpine (MK-801) and memantine that act as NMDA antagonists and also as calcium channel blockers (Van der Schyf *et al.*, 2006).

2.1.3 THE ROLE OF GLUTAMATE IN NEUROTOXICITY

In a review by Arundine *et al.*, (2004) the authors described “The role of glutamate-dependent neurodegeneration in ischemic and traumatic brain injury”. The amino acid glutamate was described as major excitatory neurotransmitter in the mammalian CNS. Following glutamate release, postsynaptic responses occur through both metabotropic and ionotropic receptors. Metabotropic receptors mediate their actions through GTP-binding-protein-dependent mechanisms that cause mobilization of Ca^{2+} from internal stores. Activation of ionotropic receptors leads to permeability to sodium, potassium and/or calcium in associated ion channels. There are three types of ionotropic glutamate receptors: *N*-methyl-D-aspartate receptor (NMDAR), α -amino-3-hydroxy-5-methylisoxazole-4-propionic acid receptor (AMPA) and kainate receptor subtypes (Simon, 1984 & Ozyurt, 1988). Although glutamate receptor activation is required for various physiological and neuronal processes, pathologically enhanced glutamate receptor activity has been associated with neurotoxicity. In 1957, Lucas and Newhouse first described the capability of glutamate to act as an endogenous neurotoxin. Olney, (1969) coined the term “excitotoxicity” to represent EAA-mediated neurodegeneration. In 1978 Olney characterised the neurotoxic actions of

endogenous compounds like glutamate and aspartate as well as pharmacological agents such as kainate, quisqualate, and domoate that share the ability to activate excitatory amino acid receptors. Pathological glutamate receptor activity are involved in acute neurological conditions like stroke and epilepsy as well as chronic neurodegenerative disorders including Parkinson's disease, Alzheimer's disease, Huntington's chorea, and motor neuron disease. In this study our focus is on EAA-mediated neurodegeneration, with the NMDAR as a possible drug target.

2.1.3.1 Glutamate receptors

Michaelis, (1998) reviewed the pharmacological and physiological properties of neuronal glutamate receptors extensively. Johnston *et al.*, (1974) first proposed that glutamate receptors might exist in two different conformations; the ionotropic and metabotropic conformations, both of which are expressed in the membranes of neurons and glial cells. Ionotropic receptors transmit their signal upon activation by changing the membrane permeability of Na⁺ and Ca²⁺ ions. Metabotropic receptors are coupled to signal transduction cascades involving G-proteins and other multiple transduction mechanisms that modulate neuronal development, synaptic plasticity, and neuronal death (Kornhuber *et al.*, 1997).

The pharmacological and physiological characterisation of the various forms over the past two decades has led to the definition of three forms of ionotropic receptors, the kainate (KA), AMPA, and *N*-methyl-D-aspartate (NMDA) receptors; and two groups of metabotropic receptors: those that activate phospholipase-C (PLC), and those that inactivate adenylyl cyclase (AC). Both ionotropic and metabotropic receptors are linked to multiple intracellular messengers, such as Ca²⁺, cyclic AMP (cAMP) and reactive oxygen species that initiate multiple signalling cascades that determine neuronal growth, differentiation and survival (Michaelis, 1998). However, in this study our focus is on the ionotropic-NMDA receptors as possible target for neuroprotection. The compounds of interest, polycyclic amine derivatives, have also been proven to be active on the NMDA receptor (Kiewert *et al.*, 2006).

The NMDA receptors are spliced into various subunits e.g. NMDAR1, NMDAR2 and NMDAR3, with various splice variants. For the purpose of this study, we will not discuss further the subunits of the NMDA receptor, but will review the function and molecular structure of the NMDA receptor under section 2.1.3.2. A classification of the glutamate receptors can be seen in figure 2.2.

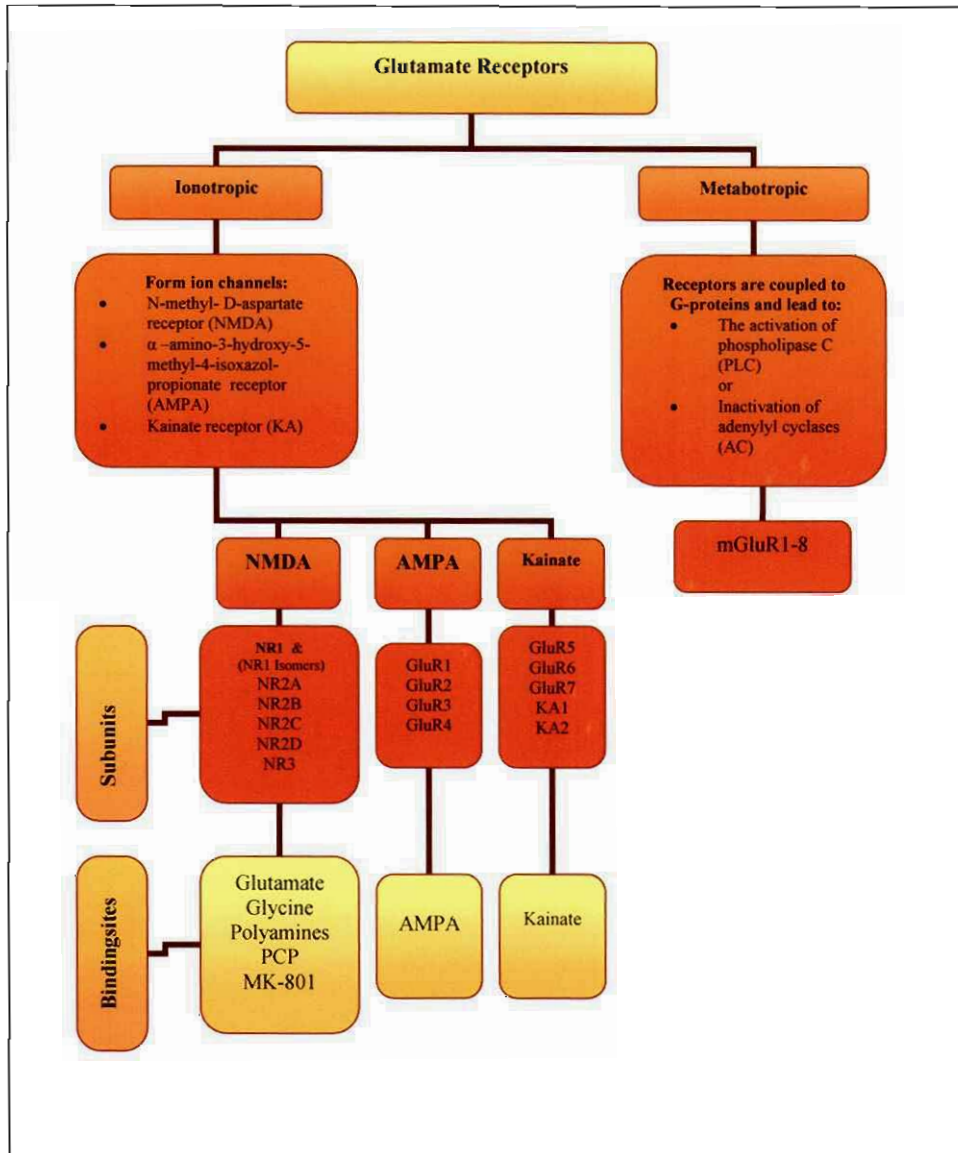


Figure 2.2: Classification of glutamate receptors. (adapted from Meador-Woodruff, 1999).

2.1.3.2 Functioning and molecular structure of the NMDA receptor

NMDA receptors are cationic channels gated by glutamate and have a high conductance and permeability to Ca^{2+} , which generate transient intracellular Ca^{2+} concentration increases, and are also permeable to Na^+ , which contribute to postsynaptic depolarisation. Activation of NMDARs in the synapse is initiated by the presynaptic release of glutamate, binding of both glutamate and glycine to NMDA receptors and subsequent opening of the ion channel (Michaelis, 1998). Several binding sites exist on the NMDAR (Fig. 2.3), of which two sites on the exterior of the cell are denoted for the agonist, glutamate (Glu) and co-agonist, glycine (Gly). Both sites must be occupied before the channel can open sufficiently. The NMDAR is not believed to function as a mediator of rapid synaptic transmission and, unlike KA and AMPA receptors, the NMDAR responds to glutamate more slowly and its contribution is primarily to the slow component of excitatory postsynaptic currents.

Several modulatory sites have been characterised (Fig. 2.3), which include sites for magnesium, zinc, polyamines, and binding of agonists and antagonists. A site denoted for magnesium binding is located on the exterior and interior of the channel. Magnesium normally occupies the exterior site while the interior site is probably unoccupied under biological conditions. At resting membrane potentials, the ion channel is blocked by extracellular Mg^{2+} , which prevents ion transduction even if glutamate and glycine are both bound to the receptor. This binding is due to electrostatic forces and the NMDAR has a unique status among ion channels, one which is not only ligand-gated, but also voltage-gated. Depolarization of the neuronal membrane relieves the voltage-dependent Mg^{2+} -block and facilitates receptor activation in the presence of glutamate and glycine. Subsequently Ca^{2+} can enter through the fully open channel. It is via this Ca^{2+} influx that NMDARs exert their intracellular physiological effects (Greene & Greenamyre, 1996; Michealis, 1998; Erowid, 2004). Thus, if the neuron is only slightly activated the NMDA channel may open partially but the magnesium ion will not be released from the binding site. The partially active channel will only allow Na^+ and K^+ to enter. However, if the neuron is rapidly or substantially activated by glutamate, the magnesium ion will be released and calcium can enter the cell.

Zinc ions (Zn^{2+}) also bind to the exterior of the channel and act in a poorly defined mechanism to inhibit receptor activation. Two binding sites on the interior of the receptor are denoted for the binding of polyamines like spermine and spermidine and another is sensitive to phosphorylation by PKC. (Greene & Greenamyre, 1996; Kornhuber & Weller, 1997; Michaelis, 1998; Erowid, 2004). The polyamine-binding site must not be confused with the binding site for the polycyclic amines. Polycyclic amines such as amantadine and memantine are low-affinity uncompetitive NMDAR channel blockers that bind to the PCP-binding site located within the ion channel of the receptor and are thus accessible for pharmacological modulation only in the open channel state. The PCP site is also the binding site for high-affinity noncompetitive NMDAR channel blockers like phencyclidine (PCP), ketamine, MK-801 (dizocilpine), DXM, and dextorphan.

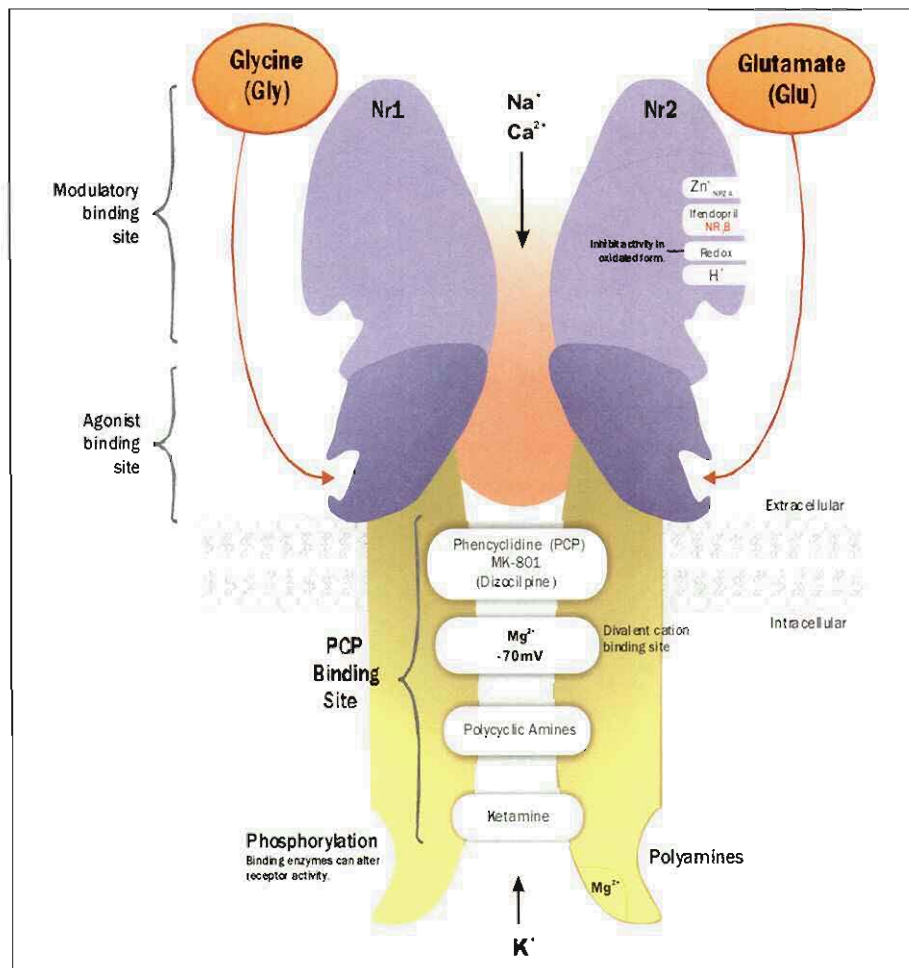


Figure 2.3: Representation of the binding sites associated with the NMDA receptor complex (adapted from Kemp and McKernan).

2.1.4 VOLTAGE-GATED CALCIUM CHANNELS

As previously mentioned the voltage-gated calcium channels constitute another major pathway for calcium entry into neurons and represent an attractive opportunity for therapeutic intervention. The voltage-gated Ca^{2+} channels are members of a family of ion channels that also include the Na^{+} and K^{+} channels which share significant structural and functional homology (Timin *et al.*, 2004; Triggle, 2006). Four types of Ca^{2+} channels exist (L, N, P, and T-type), that can be distinguished by their structure, subunit composition, location, biophysical properties and pharmacology. The channels consist of a central pore-forming α_1 subunit that expresses the major biophysical and functional properties of the channel. The auxiliary subunits, $\alpha_2\delta$, β and γ control the channel expression, membrane incorporation, and the drug binding and gating characteristics of the central unit (Triggle, 2006).

From an electrophysiological perspective, there are two classes of VGCCs; the low voltage- and high voltage-activated channels. The low voltage-activated channels belong to the T-class and are activated at relatively polarized membrane potential. They are widespread in a variety of tissue types and are likely associated with repetitive firing and pace-making activities in excitable cells. The high voltage-activated channels of the L, N, P/Q and R types are distinct in location and pharmacology. The L-type channels are associated mainly, although not exclusively, with the cardiovascular system and can be found in some neurons. In neurons the L-type channels are triggered post-synaptically by membrane depolarisation, permitting initiation of calcium-dependent signalling (Mori *et al.*, 1996; Pringle, 2004; Triggle, 2006) The N, P/Q and R types are primarily associated with neurons and can be found pre-synaptically. These channels mediate the release of neurotransmitters such as glutamate (Mori *et al.*, 1996; Pringle, 2004; Triggle, 2006).

2.1.4.1 L-Type calcium channels

L-type calcium channels are distributed across the cardiovascular system, nonvascular smooth muscle, secretory tissue and neurons. All L-type calcium channels share a common pharmacological profile, with a high sensitivity to several classes of drugs that have been used as selective L-type channel blockers, including diltiazem, the prototypical benzothiazepine; nimodipine, the prototypical 1,4-dihydropyridine and verapamil, the prototypical phenylalkylamine (Janis *et al.*, 1987; Hockerman, 1997; Triggle, 2003).

These three classes of Ca²⁺ channel blockers show significant differences in their selectivity to the L-type calcium channel. Verapamil and diltiazem have been described as being essentially non-selective and the 1,4-dihydropyridines as being selective. This fact may primarily be attributed to dissimilar topographic localizations of binding sites for these chemical classes on the α_1 subunit of the L-type channel. However, these drugs also exhibit state-dependent interactions with the ion channel. Thus, drug binding can occur in either the resting, open or the inactive state (Triggle, 2006). The chemical structure and physicochemical properties of these drugs, such as polarity and charge, control the access to the receptor site. Polar and charged drugs may access the channel through a polar and hydrophilic pathway, including the channel pore, while non-polar drugs may access their binding sites through membrane-delineated pathways (Triggle, 2006). State-dependent interactions have been reported to influence the observed cardiac effect for diltiazem, verapamil and nifedipine (Timin, 2004). Diltiazem and verapamil both exhibit frequency-dependent interactions with drug potency increasing with increasing frequency of depolarizing stimulus, while the potency of nifedipine increased with increasing levels of maintained depolarization (Triggle, 2006).

2.2 DRUGS USED IN THE TREATMENT OF NEURODEGENERATIVE DISORDERS

2.2.1 L-TYPE CALCIUM CHANNEL BLOCKERS

As previously discussed the neuronal L-type calcium channels are a major drug target for preventing excessive and potentially damaging or lethal influx of calcium into neuronal cells. The focus thus far, have mainly been on L-type calcium channel blockers in cardiac smooth muscle and their significant role in the treatment of cardiovascular diseases such as arrhythmia, hypertension, congestive heart failure, etc. (Mori *et al.*, 1996). However, numerous studies have demonstrated L-type calcium channel antagonists to be neuroprotective (Kobayashi & Mori, 1998; Pizzi *et al.*, 2002). In recent years it has become abundantly clear that L-type calcium channel blockers have an important role to play in the treatment of neurodegenerative diseases and two mechanisms were proposed for the possible neuroprotection provided by these compounds. First, an improvement of cerebral blood circulation, and second, a direct inhibition of neuronal calcium channels (Kobayashi & Mori, 1998) can be argued as neuroprotective mechanisms for these compounds.

L-type calcium channels all share a common pharmacological profile, with a high sensitivity assigned to several classes of these drugs that have been used as selective L-type calcium channel blockers (Hockerman *et al.*, 1997). Fleckenstein, (1977) first described the pharmacological actions of verapamil and other phenylalkylamines. They used the term “Ca²⁺ antagonist” to initially classify these compounds, which was later changed to “Ca²⁺ channel blockers” as their mechanism of action became better understood. Because there are no significant structural differences between L-type calcium channels located in the cardiac smooth muscle, vascular smooth muscle or neuronal cells, compounds that are active on the L-type calcium channels in the cardiac and vascular smooth muscle can also be used on neuronal L-type calcium channels. The three main classes of selective L-type calcium channel blockers currently available for clinical use are the phenylalkylamines, the benzothiazepines, and the dihydropyridines (Mori *et al.*, 1996; Hockerman *et al.*, 1997). These drugs

bind to three separate receptor sites on L-type calcium channels, which are allosterically linked, but these details will not be reviewed for the purpose of this study. Verapamil, desmethoxyverapamil and methoxyverapamil are three compounds within the phenylalkylamine class that have been extensively studied. Verapamil however, is the prototype phenylalkylamine and is the only drug of this class that is currently in clinical use (Hockerman *et al.*, 1997). In this study, we used verapamil as a reference compound for evaluating L-type calcium channel antagonistic activity for a series of test compounds.

Diltiazem, clentiazem, (+)-cis-azidodiltiazem, SQ32,910 and benziazem are some of the compounds studied within the benzothiazepine class. Diltiazem is the prototype and only drug within this class that is currently in clinical use (Hockerman *et al.*, 1997). Nimodipine, nifedipine, nitrendipine, amlodipine and nicardipine are some of the compounds studied within the dihydropyridine class (Hockerman *et al.*, 1997; Kobayashi & Mori, 1998). Due to the extensive use of nimodipine in literature as an effective L-type calcium channel blocker, we chose it as a second reference compound for evaluating the L-type calcium channel antagonistic activity for a series of test compounds (Hockerman *et al.*, 1997; Horn & Limburg, 2001).

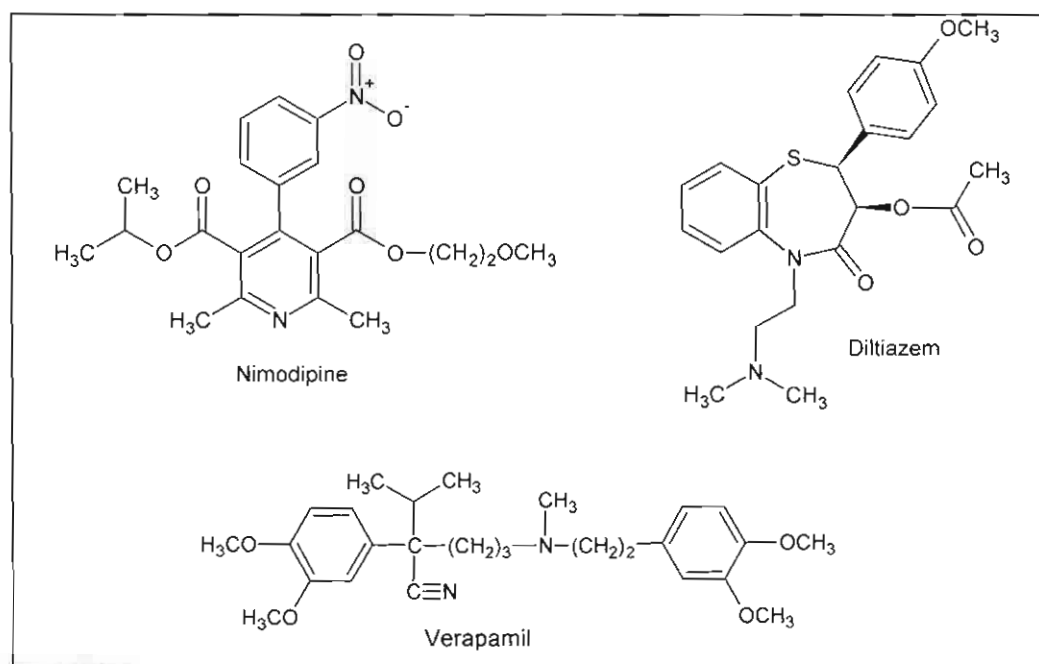


Figure 2.4: Molecular structures of prototypical Ca^{2+} antagonists.

2.2.2 NMDA RECEPTOR ANTAGONISTS

Drug candidates that prevent excessive activation of the NMDAR, termed NMDA receptor antagonists, reduce the potentially damaging and lethal influx of calcium into neurons via this channel. NMDAR antagonists are used to treat neurodegenerative disorders. Many NMDAR antagonists previously evaluated in human clinical trials, such as high-affinity competitive and noncompetitive NMDAR channel blockers, either prevented glutamate from binding to the NMDAR, or blocked the NMDAR channel for a longer period of time than was considered safe (Fig. 2.5). While they protected neurons from excitotoxicity, these antagonists also prevented normal signal communication and interfered with essential functioning. This led to the development of the low-affinity uncompetitive NMDAR antagonists such as amantadine and its dimethyl derivate, memantine, which modulate the NMDAR channel, rather than blocking it completely. These compounds remain in the channel long enough to reduce excessive calcium influx, but do not block calcium flow completely, thus permitting normal functioning. Memantine thus exhibits the characteristics desirable for a potentially safe and effective therapeutic agent (Neurobiological Technologies, Inc. 2002).

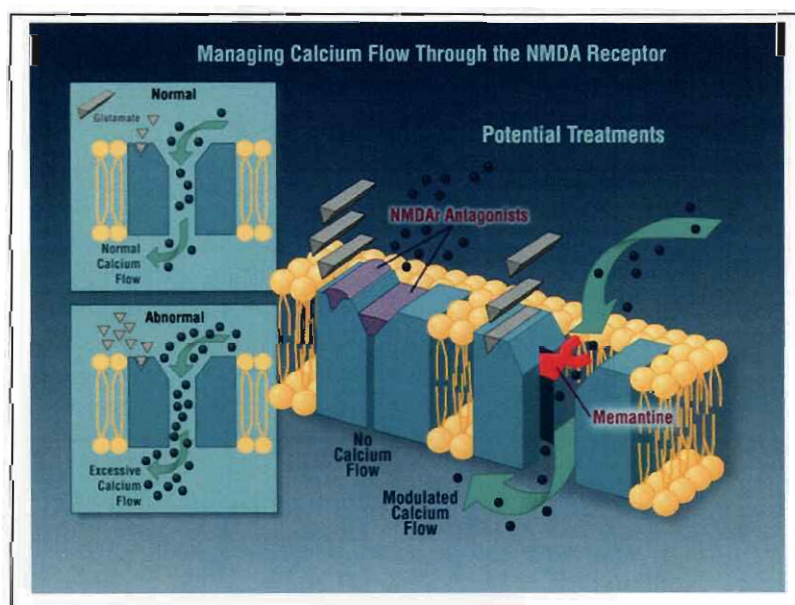


Figure 2.5: Different mechanisms for regulating calcium flux through the NMDA receptor (credit: Neurobiological Technologies, Inc. 2002).

2.2.2.1 Noncompetitive and uncompetitive NMDA receptor antagonists

High and low-affinity noncompetitive and uncompetitive antagonists exert their effect by binding to the PCP binding site in the open state of the receptor operated ion channel. These antagonists do not compete with endogenous ligands (glutamate or glycine) and exert their effect by direct blockade of the calcium flux through the NMDA receptor operated ion channel. Noncompetitive antagonists including PCP (phencyclidine), ketamine, MK-801 (dizocilpine) are lipophilic compounds that can effectively penetrate the CNS and block the NMDAR channel with a very high-affinity. Unfortunately, these compounds exhibit behavioural side effects that limit their eventual usefulness. This is in part due to their high-affinity block that results in these drugs being trapped within the channel and discontinuation of normal neuronal calcium flux (Malone *et al.*, 1993). In contrast, the low-affinity uncompetitive channel blockers including amantadine and memantine function in a use dependent manner and do not display behavioural side effects. This is due to the low-affinity uncompetitive binding kinetics that only blocks the NMDAR channel during excessive calcium flux and do not remain within the channel during normal neuronal calcium flux (Parsons & Quack, 1999).

In a study by Kroemer *et al.*, (1998) the authors evaluated the activity of a set of molecules at the PCP binding site to determine the structural requirements for uncompetitive inhibition. Phencyclidine (PCP) was used as reference compound to develop a pharmacophore model and two main interactions were proposed: a hydrogen bond and a hydrophobic interaction (Fig. 2.6). MK-801, amantadine and memantine (Fig. 2.7) also showed favourable inhibition constants and were superimposed on the PCP derived pharmacophore to validate the model, and yielded good fittings. The first point of interaction was determined to be a hydrogen bond with the protonated amine which is represented by three points: the nitrogen (“donor atom”), a positive partial charge at the hydrogen (“positive”), and the putative interaction site at the receptor (“acceptor site”). The second point of interaction was determined to be located at the position of the cyclohexyl moiety of PCP and suggested a hydrophobic interaction. It was also noted that a third point of interaction increased binding affinity compared to other compounds. The third point of

interaction was determined to be steric interaction with an aromatic ring, which indicated another hydrophobic interaction with the receptor. The authors also stated that the Quantitative Structure-Activity Relationship (QSAR) analysis was mainly dominated by steric descriptors and that the molecules should not be too bulky. The critical diameter was determined, by Sobolevsky *et al.* (1999), to be approximately 17Å for the NMDA channel pore.

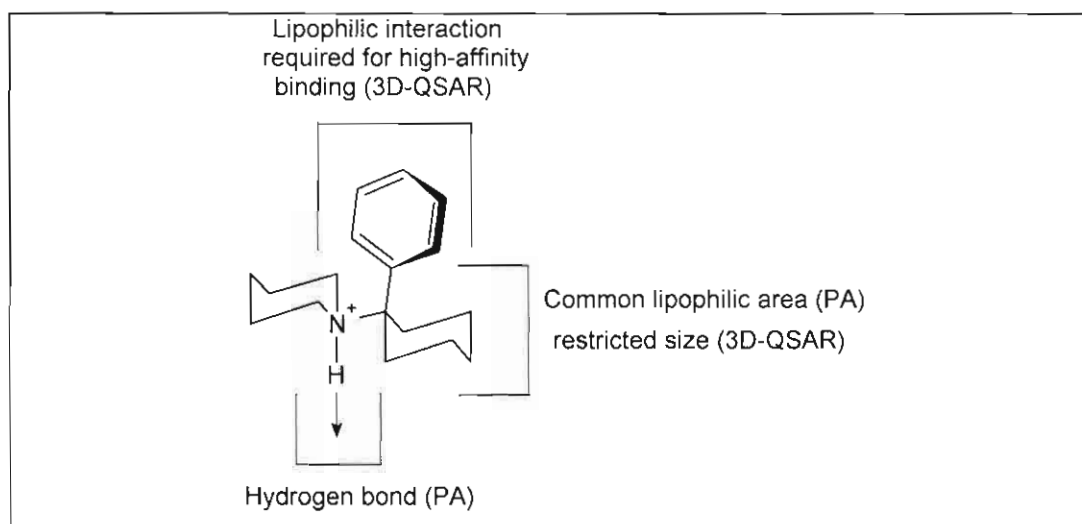


Figure 2.6: Combination of the results of the pharmacophore analysis (PA) and the 3D-QSAR, indicating the main structural requirements for PCP binding site blockers (Kroemer *et al.*, 1998).

Literature reports also suggested NMDA activity for several other interesting structures related to those tested by Kroemer *et al.*, (1998). What is interesting to note is that several of these structures included tricyclic ring structures similar to the triquinane structure we are investigating in this study. Malone *et al.*, (1993) synthesised a series of 4a-phenanthreneamines (PD 33352 & PD 134365), of which PD 134365 showed a favourable pharmacological profile as an NMDAR antagonist. Desimipramine is known as a noradrenaline receptor inhibitor, but also showed activity as an NMDAR antagonist, with binding to the PCP binding site (Kornhuber & Weller, 1997). Amantadine and its derivative memantine (the only clinically used

NMDA receptor antagonist) are also ligands for the sigma receptor (Kornhuber & Weller, 1997).

Ifendopril has a different mechanism of action from other open channel blockers: it binds on the NR2B-subunit of the NMDA receptor and is reported to protect neurons without severe side effects (Kemp & McKernan, 2002). The structural similarities of tricyclic ring systems like MK-801, carbamazepine, desimipramine, PD 33352 and PD 134365 - all with favourable pharmacological profiles and more rigid structures than PCP - stimulated our interest in the triquinylamines and their possible antagonistic activity on the NMDAR.

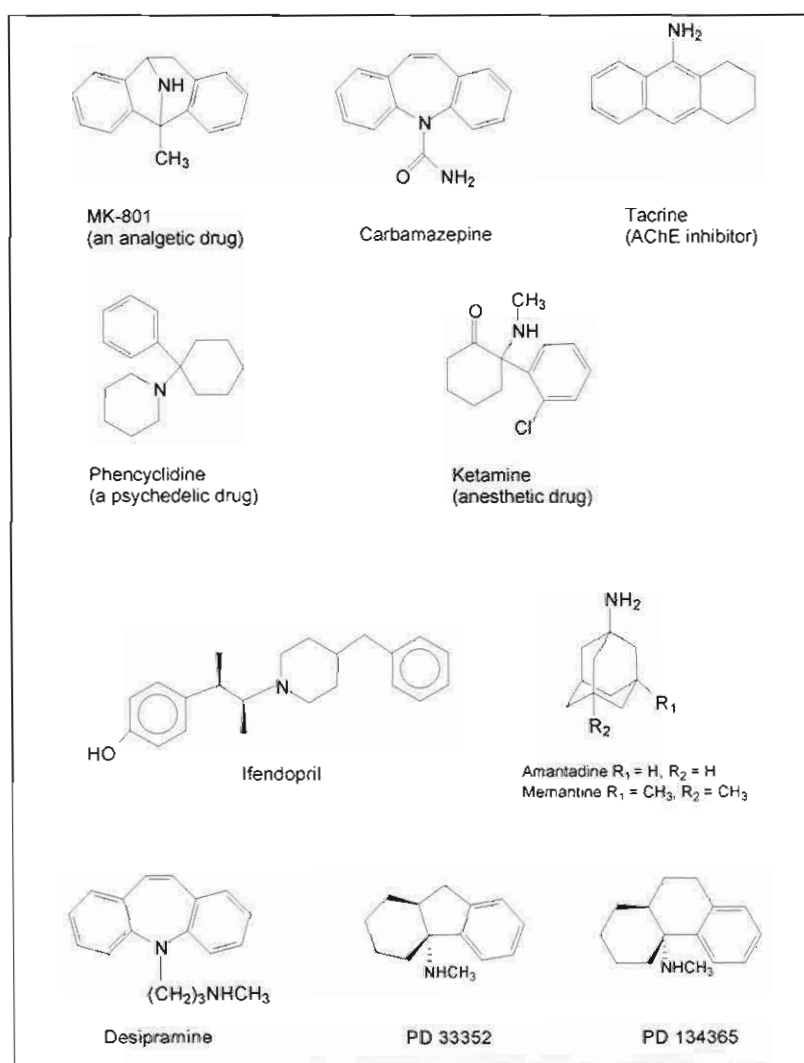


Figure 2.7: Noncompetitive and uncompetitive NMDA receptor antagonists

2.2.3 POLYCYCLIC COMPOUNDS

2.2.3.1 Adamantane Amines

Attention was first drawn to the pharmacology of the polycyclic cage compounds by the findings that amantadine or 1-amino-adamantane (**1**) had antiviral activity against the influenza virus. A congener of amantadine, rimantadine (**3**) [1-(1-aminoethyl)adamantane] and a dimethyl derivate (**2**) memantine (1-amino-3,5-dimethyladamantane) also displayed antiviral activity (Davies *et al.*, 1964).

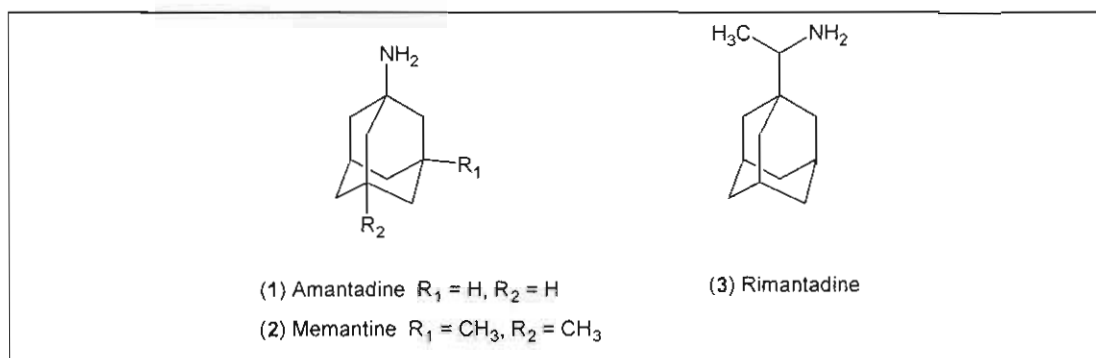


Figure 2.8: Low-affinity uncompetitive NMDAR antagonists.

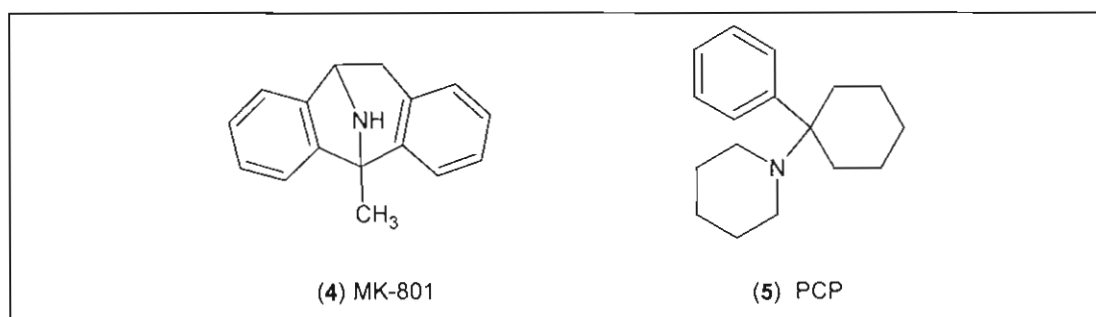


Figure 2.9: High-affinity noncompetitive NMDAR antagonists.

The antiparkinsonian activity of amantadine (**1**) was first discovered by chance when it was observed that patients with Parkinson's disease treated with amantadine for influenza, showed unexpected improvement of symptoms (Schwab *et al.*, 1972). Amantadine (**1**) and its derivative memantine (**2**) are low-affinity uncompetitive NMDAR antagonists and are clinically better tolerated than high-affinity noncompetitive NMDAR antagonists like PCP (**5**) and MK-801 (**4**) (Parsons *et al.*, 1999). As previously discussed, MK-801 (**4**) and PCP (**5**) block the channel completely, thus not allowing normal calcium flow. Because compounds like MK-801 (**4**) have a high affinity for the binding site they can also be trapped when the channel closes. This block is difficult to reverse and exhibits a long duration of action that leads to the adverse CNS effects seen with the high affinity channel blockers. Memantine (**2**), however, modulate the receptor channel, rather than blocking it completely. It remains in the channel long enough to reduce excessive calcium influx but does not block calcium flow completely, thus permitting normal functioning. Because of its low affinity, memantine (**2**) is speculated to leave the receptor site before the channel closes (Parsons *et al.*, 1999; Chen & Lipton, 2006).

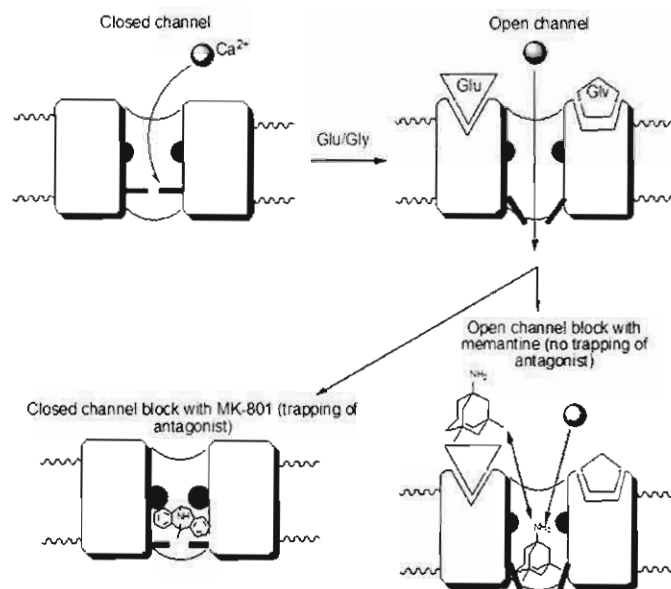


Figure 2.10: Concept of open and closed-channel NMDA receptor block with memantine and MK-801 (Rogawski & Wenk, 2003).

2.2.3.2 Pentacycloundecylamines

Cookson *et al.*, (1958) first synthesised the pentacyclic diketone (9) that formed the substrate for the synthesis of several subsequent derivatives. The pentacycloundecylamines are derived from Cookson's diketone (9) (pentacyclo[5.4.0.0^{2,6}.0^{3,10}.0^{5,9}]undecane-8,11-dione), the so-called "bird cage" compound, obtained from the intramolecular [2 + 2] photocyclization of the Diels-Alder adduct (8) of *p*-benzoquinone (6) and cyclopentadiene (7) (Cookson *et al.*, 1958).

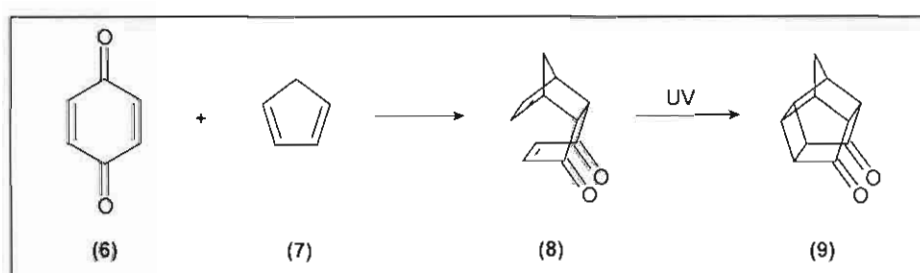


Figure 2.11: Synthesis of Cookson's diketone (Cookson *et al.*, 1958)

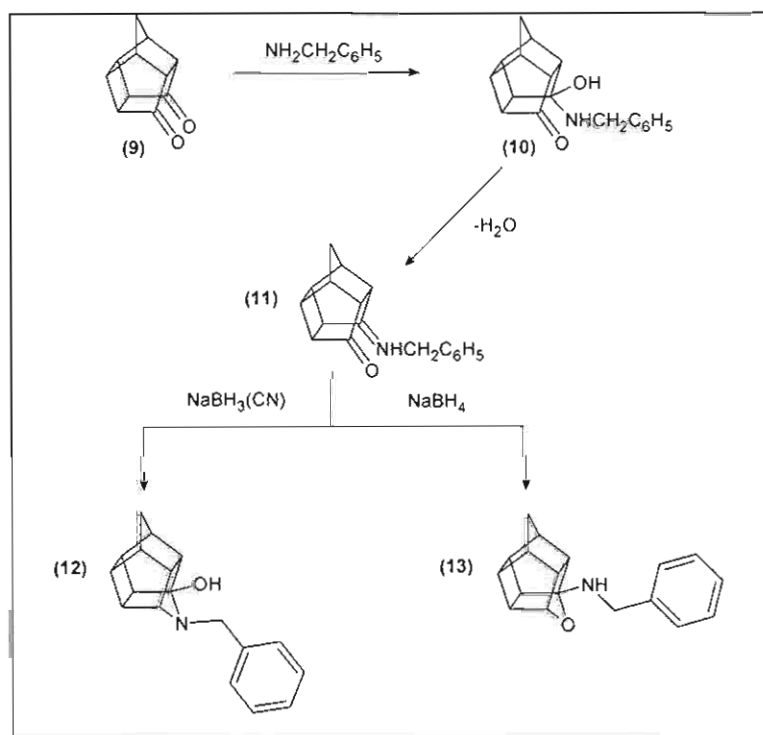


Figure 2.12: Synthetic route of NGP1-01 (13) and aza-cage compound (12).

The development of NGP1-01 (**13**), our current lead compound, evolved from pentacyclo[5.4.0.0^{2,6}.0^{3,10}.0^{5,9}]undecane-8,11-dione (**9**) and was first prepared by Sasaki *et al.*, (1974). This compound however, was not pharmacologically characterised until 1986 when the group of Van der Schyf (Van der Schyf *et al.*, 1986) characterised and patented its action as calcium channel antagonist. Initial investigations with NGP1-01 (**13**) were based on electrophysiological experiments in isolated guinea-pig papillary muscle and sheep Purkinje fibres. The structure of NGP1-01 (**13**) was initially incorrectly assigned by Sasaki *et al.*, (1974) as the aza derivative, 3-hydroxy-4-benzyl-azahexacyclo[5.4.1.0^{2,6}.0^{3,10}.0^{5,9}.0^{8,11}]dodecane. Marchand *et al.*, (1988) and Van der Schyf *et al.*, (1989) nearly simultaneously and independently assigned the structure of NGP1-01 correctly as the oxa derivative, 8-benzylamino-8,11-oxapentacyclo[5.4.0.0^{2,6}.0^{3,10}.0^{5,9}]undecane (**13**) by NMR spectroscopy and X-ray crystallography, respectively. Marchand *et al.*, (1988) then proceeded to synthesize the aza-compound (**12**) by means of reduction of the intermediate imine (**11**) with sodium cyanoborohydride (Fig. 2.12).

Further investigations were carried out to explain the mechanism of calcium channel blocking for the pentacycloundecanes in cardiac myocytes (Van der Walt *et al.*, 1988). NGP1-01 (**13**) was described as being a frequency- and voltage-dependent calcium channel blocker, suggesting open channel block. The activity reported in this study correlated with those of the then widely used dihydropyridine calcium channel blockers.

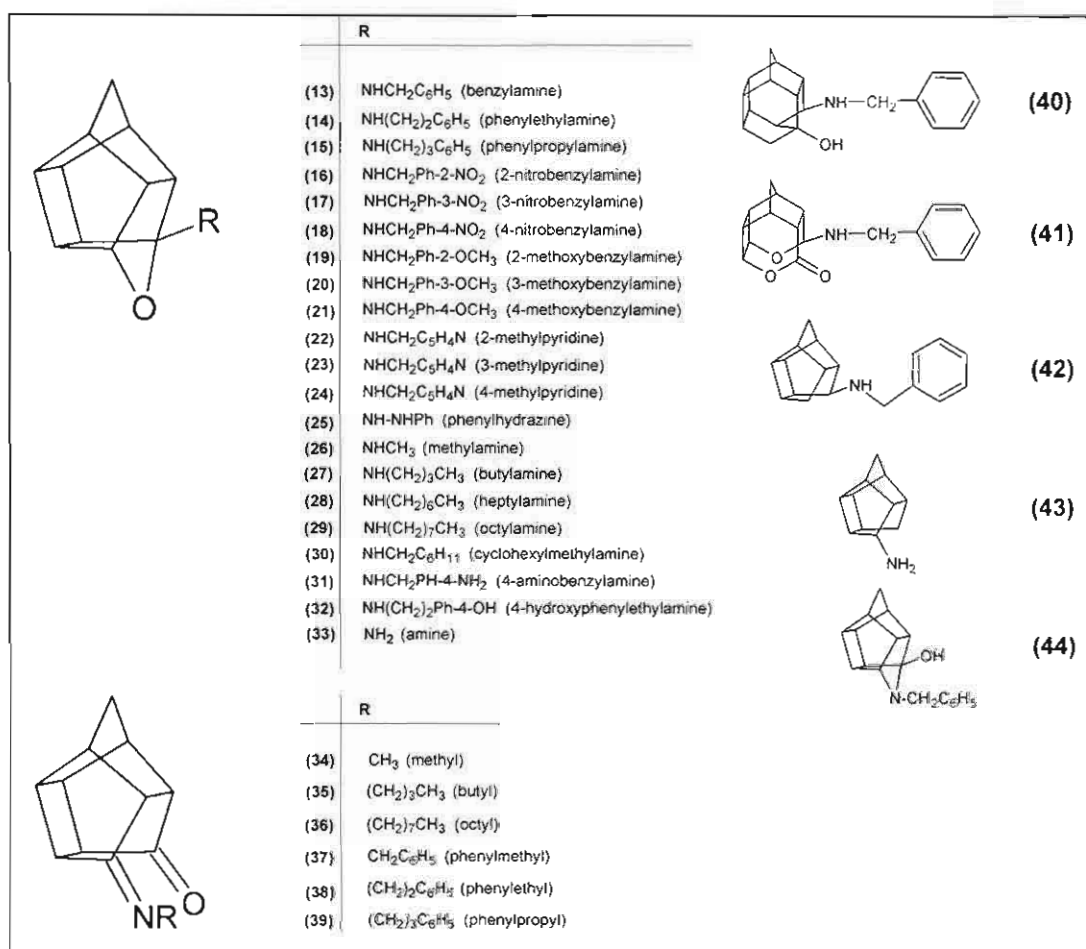


Figure 2.13: Composite of the polycyclic cage compounds synthesized since 1974 (see literature for details).

It was postulated that the pentacycloundecane skeleton served only as a bulk contributor to the activity of NGP1-01 (**13**) and related compounds, with the activity situated primarily in the amino side chain moiety (Van der Schyf *et al.*, 1986). Based on this argument Liebenberg *et al.*, (1996) synthesised *N*-benzyl-3,11-azatricyclo[6.3.0.0^{2,6}]undecane (**45**) and *N*-octyl-3,11-azatricyclo[6.3.0.0^{2,6}]undecane (**46**), two triquinane aza-bridgehead compounds, by thermal [2 + 2] cycloreversion from pentacyclo[5.4.0.0^{2,6}.0^{3,10}.0^{5,9}]undecane-8,11-dione (**9**). These compounds were evaluated on electrically stimulated guinea pig papillary muscle to evaluate their suppressant activity of calcium mediated action potential and chronotropy. Both compounds tested were found to be active and the authors concluded that opening of the “cage” moiety of the hydrocarbon polycycle did not diminish the calcium channel

activity or the chronotropic effects. This study also revealed some structure activity relationships with the benzylamine (aromatic) derivative (45) being more active than its aliphatic (octylamine) counterpart (46).

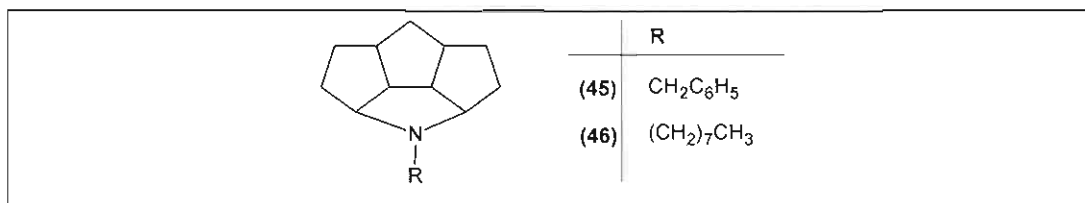


Figure 2.14: Triquinylamine derivatives synthesised by Liebenberg *et al.*, (1996).

Malan *et al.*, (2000) also used NGP1-01 (13) as lead compound and synthesised several derivatives by modifying the side chain (Fig. 2.15). This included nitrobenzylamines (16-18), methoxybenzylamines (19-21), methyl pyridines (22-24) and phenylhydrazine (25) derivatives. The polycyclic skeleton, 8,11-oxapentacyclo[5.4.0.0^{2,6}.0^{3,10}.0^{5,9}]undecane was also substituted with 3-hydroxyhexacyclo[6.5.0.0^{3,7}.0^{4,12}.0^{5,10}.0^{9,13}]tridecane (40), 8,13-dioxapentacyclo[6.5.0.0^{2,6}.0^{5,10}.0^{3,11}]tridecane-9-one (41), and pentacyclo[5.4.0.0^{2,6}.0^{3,10}.0^{5,9}]undecane (42) to evaluate the effect of the polycyclic cage size on activity.

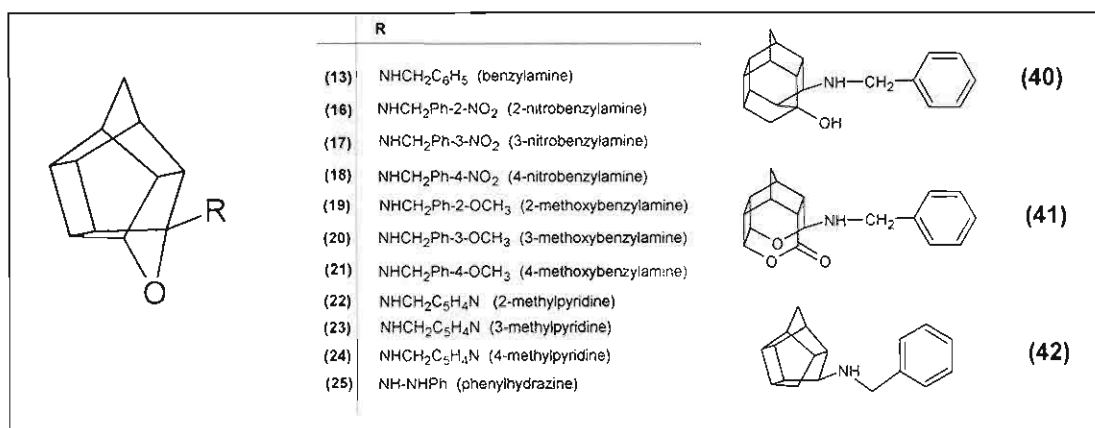


Figure 2.15: Compounds synthesised by Malan *et al.*, (2000).

Whole cell voltage clamping on guinea-pig ventricular myocytes was used to examine the L-type calcium channel blocking effects for this set of compounds. Structure-activity Relationship (SAR) studies found that the activity of this series of calcium channel blockers appeared to be dominated by geometric (e.g. surface area and volume) or steric constraints rather than by electronic considerations (e.g. molar refractivity and polarisability). However, the data also indicated that the electronic characteristics should be accounted for, even if the electronic characteristics exerted a lesser influence on the activity and/or affinity of these compounds. These conclusions were drawn from findings that inhibition of calcium current was more pronounced with aromatic substitution where substitution occurred in the *ortho* (**16**, **19** & **22**) or *meta* (**17**, **20**, **23**) positions; while the activity for *para* (**18**, **21**, **24**) substituted compounds more closely followed that of the "unsubstituted" NGP1-01 (**13**). The activities for the methoxy compounds (**19-21**) were reported to be slightly higher than for the corresponding nitro compounds (**16-18**), while replacement of the aromatic benzylamine (**13**) with phenylhydrazine (**25**) and aminomethylpyridine (**22-24**) led to a distinct decrease in activity. Improved inhibition of the calcium current was also observed for compounds where the polycyclic "cages" were enlarged (**40**, **41**). Removal of the endocyclic ether bond resulted in a compound (**42**) with activity similar to that of NGP1-01 (**13**). The study also indicated that the lowest activity was observed for compounds (**22-25**) in which the aromatic side chain tends to fold back onto the polycyclic cage. Incidentally these compounds also had the lowest calculated minimum energy (Malan *et al.*, 2000).

Liebenberg *et al.*, (2000) describes the structure activity relationships of several aromatic and aliphatic imino-keto and amino-ether derivatives of NGP1-01 (**13**) on calcium channels using electrically stimulated guinea-pig papillary muscle. The study indicated compounds with aromatic side-chains (**13**, **15**, **37-39**) all to be active as opposed to aliphatic compounds (**26-29**, **34**, **35**) with methyl or butyl side-chains, which were all inactive. However, it was found that aliphatic compounds with octyl side chains (**36**) were as active as their aromatic counterparts. The study concluded that bulky substituents were essential for calcium channel activity with an increase in lipophilicity showing greater activity. Activity of these compounds also improved with increased chain length between the polycyclic cage and the aromatic moiety.

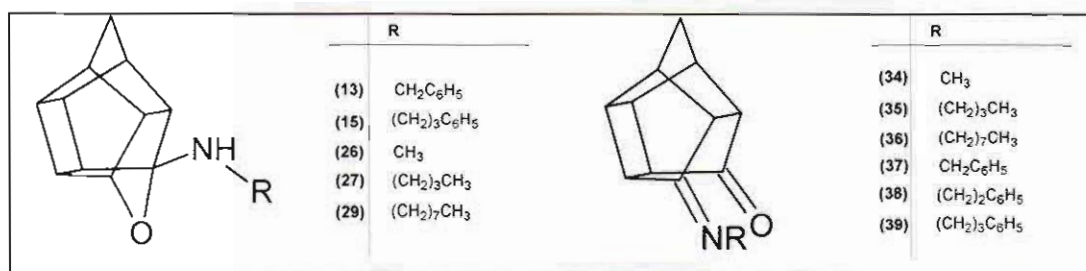


Figure 2.16: Polycyclic amine derivatives synthesised by Liebenberg *et al.*, (2000).

The neuroprotective activity of the polycyclic cage amine, memantine (**2**), prompted interest in the possible neuroprotective abilities of the pentacycloundecylamines. As part of the ongoing investigation into the therapeutic potential for these compounds, a study by Geldenhuys *et al.*, (2003) led to the screening, for neuroprotective activity, of a series of pentacycloundecylamines (Fig. 2.17) with NGP1-01 (**13**) as lead compound, in the 1-methyl-4-phenyl-1,2,3,6-tetrahydropyridine (MPTP) parkinsonian mouse model. It was postulated that these compounds exert their action by attenuation of the NMDA receptor as well as direct blocking of neuronal L-type calcium channels.

It was found that only the phenylethyl derivative (**14**) attenuated MPTP-induced striatal dopamine depletion. The two known NMDA antagonists, MK-801 (**4**) and memantine (**2**), also failed to provide significant neuroprotection under these experimental conditions. It was thus postulated that the MPTP parkinsonian mouse model might be inadequate to screen mechanistically for neuroprotection based on NMDA receptor antagonism. However, the pentacycloundecanes could not be dismissed as being devoid of any neuroprotective activity due to the similarity in the activity profile of these compounds and the known NMDA receptor antagonists, as well as their structural similarities with memantine (**2**) and MK-801 (**4**). The latter aspect was indicated by favourable root mean square fitting onto the PCP-ligand shown in molecular modelling studies. These relationships thus warranted re-evaluation of the pentacycloundecanes as NMDA receptor antagonists (Geldenhuys *et al.*, 2003).

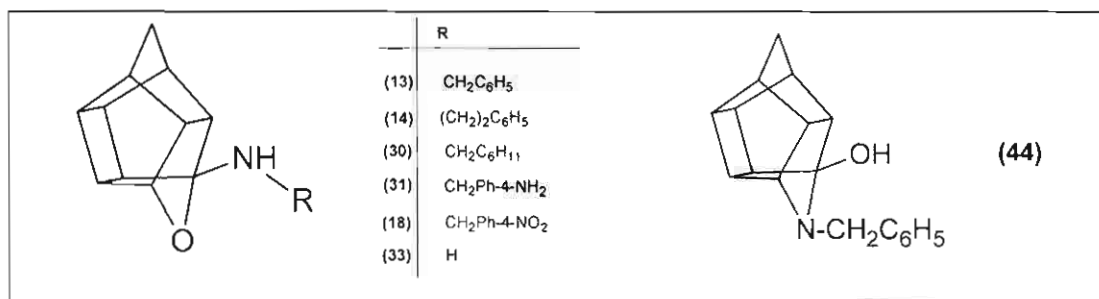


Figure 2.17: Pentacycloundecanes synthesised by Geldenhuys *et al.*, (2003).

Zah *et al.*, (2003) studied the blood-brain barrier permeability of the polycyclic cage compounds (Fig. 2.18). For activity in the central nervous system (CNS), it is not only important that compounds should have pharmacological activity within the CNS, but should also show sufficient blood-brain barrier permeability. The study by Zah *et al.*, (2003) investigated the ability of the pentacycloundecylamines to cross the blood-brain barrier and reported that optimal permeability is usually found for compounds with a log BB value $\{\log BB = \log([\text{brain}]/[\text{blood}])\}$, in the range of 0.3. Larger values indicate highly permeable drugs, and values smaller than -1.0 indicate poor permeability. It was found that all studied polycyclic cage compounds exhibit log BB values that range between -0.5 and 0.43 and accordingly, penetrate the CNS sufficiently to exert a meaningful pharmacological effect. A model, by which the blood - brain barrier permeability of the cage compounds could be predicted, was also developed. According to the experimental data, Zah *et al.*, (2003) suggested that the polycyclic compounds show a high likelihood to penetrate the CNS, and that the main mode of entry into the CNS is by passive diffusion.

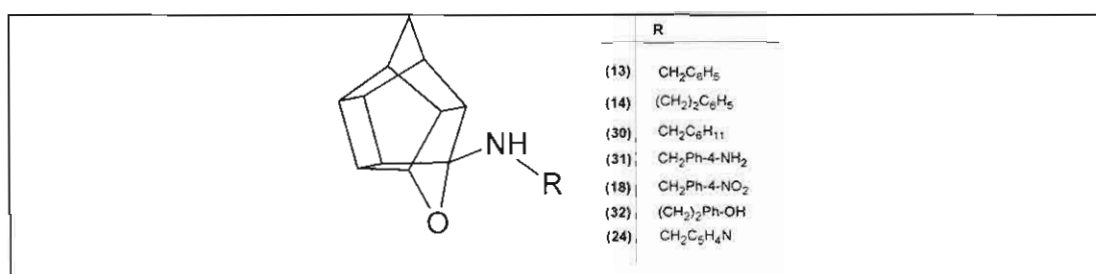


Figure 2.18: Pentacycloundecanes synthesised by Zah *et al.*, (2003).

In a further attempt to establish the mechanism through which the pentacycloundecylamines exercise their pharmacological action in the central nervous system Grobler *et al.*, (2006) evaluated the effect of a series of polycyclic amine derivatives with NGP1-01 (**13**) as lead compound (Fig. 2.19), on membrane potential. As mentioned earlier, the activation state of both the NMDAR channel and L-type calcium channels is regulated through changes in membrane potential (Green & Greenamyre, 1996). In this study, the fluorescent potentiometric probe tetramethylrhodamine methyl ester (TMRM) was used in conjunction with laser scanning confocal microscopy to evaluate the influence of pentacycloundecane derivatives (Fig. 2.19) on the transmembrane potential in an SH-SY5Y neuroblastoma cell line. The test compounds caused an overall reduction in KCl-induced membrane depolarisation with the benzylamine derivative (**13**) showing significant inhibition. The 4-methylpyridine (**24**) and methyl derivatives (**26**) also caused significant reductions in depolarization although not statistically significant. These results indicated that some structure activity relationships associated with cyclic unsaturated substitution (**13**) on the pentacycloundecane template is important for activity, which correlated with the QSAR study done by Kroemer *et al.*, (1998). From this study it could also be inferred that the introduction of hydrogen bonding through a heterocyclic moiety (**24**), and a decrease in molecular volume (**26**) led to an increase in the effect on membrane potential.

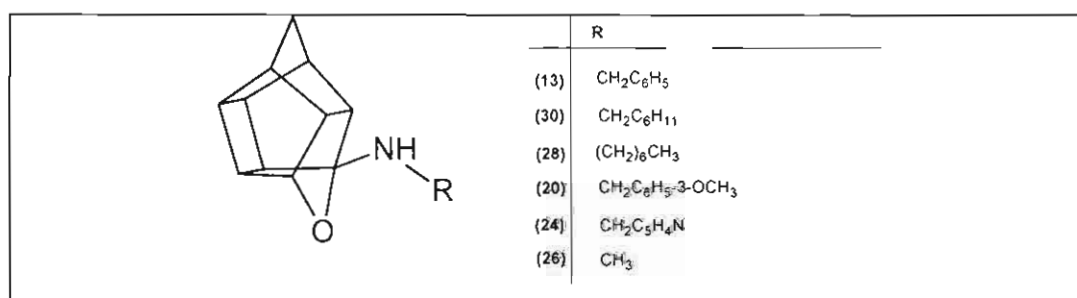


Figure 2.19: Pentacycloundecylamines synthesised by Grobler *et al.*, (2006).

Prompted by the interest in neuroprotective agents with multiple mechanisms of action, NGP1-01 (**13**) was tested on the L-type calcium channels and NMDA receptor channels by Kiewert *et al.*, (2006). To evaluate this possible multimodal action of

NGP1-01 (**13**), the calcium flux through both the L-type calcium channel and NMDA receptor channel was measured utilising fluorescent microscopy with fura-2/AM as fluorescent probe. NGP1-01 (**13**) blocked depolarisation-induced calcium flux through the L-type calcium channel with a potency comparable to that of nimodipine or diltiazem. NGP1-01 (**13**) also blocked the NMDA-induced calcium flux through the NMDA receptor channel with potency slightly lower than that of memantine (**2**). This study also confirmed that NGP1-01 (**13**) is brain permeable: it is a requirement that any neuroprotective agent should be sufficiently brain-permeable to be active *in vivo*. To evaluate the permeability, *in vivo*-microdialysis was used to monitor choline release during NMDA infusion as a measure of excitotoxic membrane breakdown. Both NGP1-01 (**13**) and memantine (**2**) were showed to be sufficiently brain-permeable with NGP1-01 (**13**) being slightly less potent than memantine (**2**). However, both compounds showed a highly significant (memantine, $p < 0.001$; NGP1-01, $p < 0.002$) reduction of NMDA-induced choline release. The authors established NGP1-01 (**13**) to be a promising lead structure for a new class of neuroprotective agents with a dual mechanism of action (Kiewert *et al.*, 2006).

After Kiewert *et al.*, (2006) established the NMDAR channel blocking activity for NGP1-01 (**13**) a study was done by Geldenhuys *et al.*, (2006) to further investigate the NMDAR channel blocking activity for a series of structurally related polycyclic cage compounds (Fig. 20). The series selected for this study was very similar to the series of polycyclic cage compounds evaluated for L-type calcium channel activity by Malan *et al.*, (2000), thus allowing for direct comparison between the activities of these compounds on both channel types. Ligand-stimulated $^{45}\text{Ca}^{2+}$ influx into synaptoneuroosomes was utilised to measure NMDAR channel block for this series of compounds. Dose-response curves were performed on the most active compounds to determine IC_{50} , Hill slopes, and goodness of fit or r^2 values. In order to gain insight into the site of interaction inside the NMDA channel, radioligand binding studies were done with either [^3H]MK-801 or [^3H]TCP to measure the displacement of these blockers by the selected series of polycyclic cage compounds. The study reported MK-801 (**4**, tested as reference compound) to be the most potent antagonist (IC_{50} ca. $1\mu\text{M}$) of NMDA/Gly-specific $^{45}\text{Ca}^{2+}$ uptake, followed by memantine (**2**) (IC_{50} ca. 3

μM) and then amantadine (**1**). Of the pentacycloundecanes tested, **13**, **14**, **16**, **17**, **20**, **40**, and **43** showed the best overall inhibition and of these, three compounds (**13**, **14** and **43**) were selected for further evaluation in the radio-ligand binding study with [^3H]MK-801 and [^3H]TCP. The binding studies indicated that these compounds do not bind to the MK-801 (**4**) binding site and bind only weakly to the TCP binding site. The study concluded that although these compounds showed inhibition of NMDA/Gly mediated calcium flux they interact with a unique binding site in the NMDA receptor/ion channel complex, different to that reported for MK-801 (**4**) or PCP (**5**) (Geldenhuis *et al.*, 2006).

The structure-activity relationships for the pentacycloundecanes tested in this study were again dominated by geometric factors, with a small influence of electronic effects. Similar to the study done by Kroemer *et al.*, (1998) the bulky polycyclic cage moiety was found to be essential for interaction with the NMDA receptor and compounds were also found to be limited by molecular size (compounds **40** and **41**), with a decrease in activity observed for an increase in molecular size. When compound (**13**) was compared to (**43**), an increase in potency was observed for (**13**) which suggest that the phenyl ring increased the interaction with the NMDA receptor. Kroemer *et al.*, (1998) also indicated a second point of hydrophobic interaction to be essential for high-affinity binding. In this study, it was also observed that an increase in chain length, compound **14** compared to **13**, led to a dramatic decrease in potency. In general, lower potencies were observed for compounds with aromatic substitution and the authors suggested that the moieties might be too bulky and that steric hindrance caused the attenuated affinity. Amongst the compounds with aromatic substitution, it was observed that *meta*-substituted compounds (**17** and **20**) displayed higher activity than *para*-substituted compounds (**18** and **21**). This correlated with the earlier findings of Malan *et al.*, (2000). Electronic effects had a slight impact with a higher potency observed for the electron donating methoxy moiety (**19-21**) as opposed to the electron withdrawing effect of the nitro group (**16-18**). The authors suggested that the donation of electrons made the phenyl ring more lipophilic and would increase the affinity for an aromatic π - π or hydrophobic interaction (Geldenhuis *et al.*, 2006).

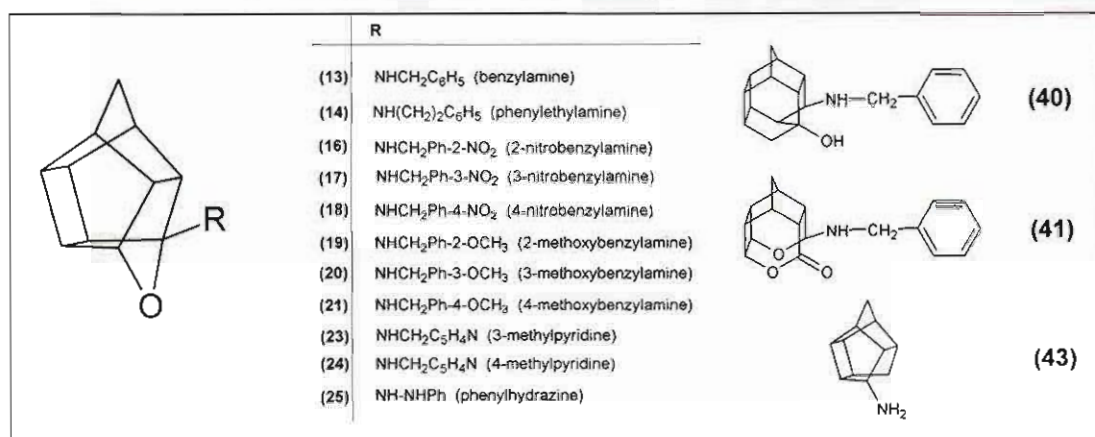


Figure 2.20: Polycyclic cage compounds synthesised by Geldenhuys *et al.*, (2006).

2.2.3.3 Triquinylamines

2.2.3.3.1 Natural triquinanes

Coriolin (**48**) and its precursor hirsutene (**47**) are both natural triquinanes. Coriolin was first isolated in 1969 by Umezawa from fermentation broths of a culture of the Basidiomycete *Coriolus consors*. The structure thereof was established in 1971 and confirmed by X-ray crystallographic studies in 1974. Thus, it became clear that coriolin is a member of the hirsutaniod sesquiterpene group of compounds, of which hirsutic acid and hirsutene (**47**) are also members. Both the unusual biological activity (enhancing cell immunity) and the unique tricyclo 5-5-5-fused ring, *cis,anti,cis* – tricyclo[6.3.0.0^{2,6}]undecane system, have attracted widespread interest (Tutsuta *et al.*, 1981).

This high level of interest had been stimulated and sustained by the discovery (from plant, marine and fungal sources) of many new and interesting compounds containing polycyclopentanoid carbon skeletons. From the polyquinanes, two stereoisomeric C₁₁-triquinanes (Fig. 2.21) are important, the *cis,syn,cis*-isomer (**49**) and *cis,anti,cis*-isomer (**50**) (Mehta *et al.*, 1981).

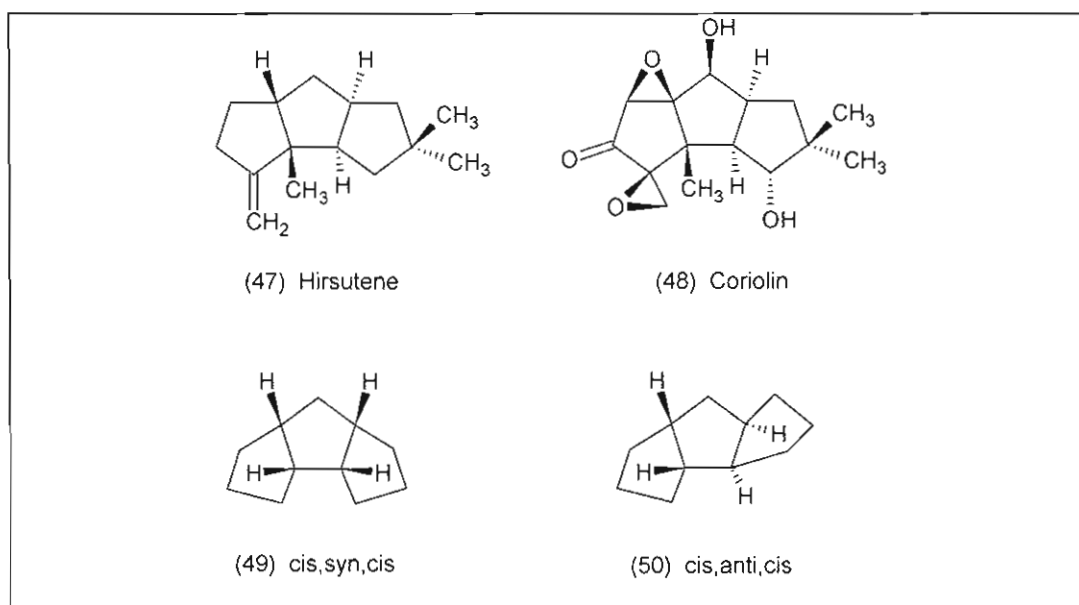


Figure 2.21: Natural triquinanes and their stereoisomeric conformation (Mehta *et al.*, 1981).

2.2.3.3.2 Synthesis of the triquinanes

Mehta *et al.*, (1981) first described the synthesis of the triquinane from Cookson's diketone. Using the polycyclic cage compounds as starting point gave these authors access to the triquinane system by means of thermal fragmentation as also described in Liebenberg *et al.*, (1996).

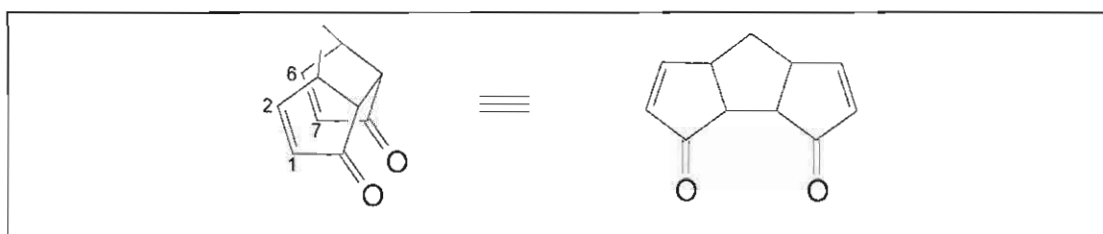


Figure 2.22: Product of thermal fragmentation.

To further investigate the hypothesis that the pentacycloundecane skeleton may serve only as a bulk contributor for the biological activity of NGP1-01 (**13**), Liebenberg *et al.* (1996), synthesised thermal ring-opened derivatives of NGP1-01 (**13**) to obtain the *cis.syn,cis* triquinylamine system derived from the pentacycloundecane moiety (Fig. 2.23). Both triquinylamine compounds showed suppression of the calcium action potential (AP) in guinea-pig papillary muscle, with the aromatic derivative (**45**) capable of completely suppressing the AP while the aliphatic derivative (**46**) suppressed the AP by approximately 50%. These two compounds were also able to slow heart rate. It was thus concluded that ring opening of the cage moiety of NGP1-01 (**13**) did not diminish its calcium channel activity or chronotropic effects. This is an important concept in justifying further investigation of the triquinylamines, for to our knowledge no studies have been carried out on the triquinylamines in order to determine their activity as blockers of calcium channels in the CNS, including the L-type calcium channels and/or NMDA receptors channels.

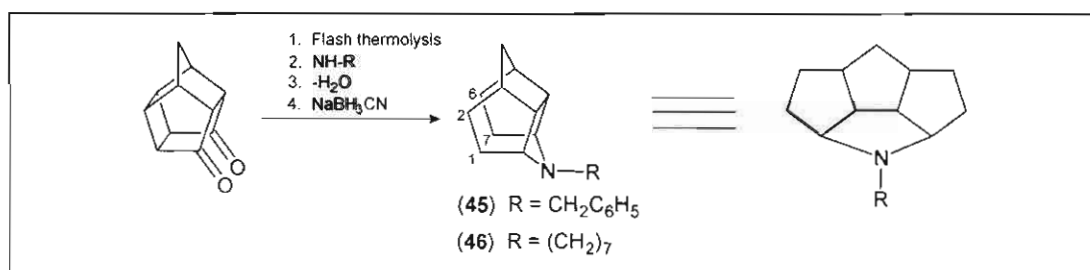


Figure 2.23: The synthesis of triquinylamine derivatives (Liebenberg *et al.*, 1996).

In a quest for a simple, general method for the synthesis of tricyclo[6.3.0.0^{2,6}]undecanes (triquinanes), Mehta's team conceived a novel two-step photo-thermal sequence. The method described by Mehta *et al.*, (1981) utilised Cookson's diketone, pentacyclo[5.4.0.0^{2,6}.0^{3,10}.0^{5,9}]undecane-8-11-dione (**9**) that was synthesised by photochemical $\pi_s^2 + \pi_s^2$ cycloaddition of the Diels-Alder adduct (**8**), which may be obtained from the reaction between 1,3-cyclopentadiene and *p*-benzoquinone. Regiospecific thermal fragmentation of the saturated four-member ring

(9) was used to form the stereospecific *cis,syn,cis*-triquinane system (51) (Liebenberg *et al.*, 1996 & Mehta *et al.*, 1981).

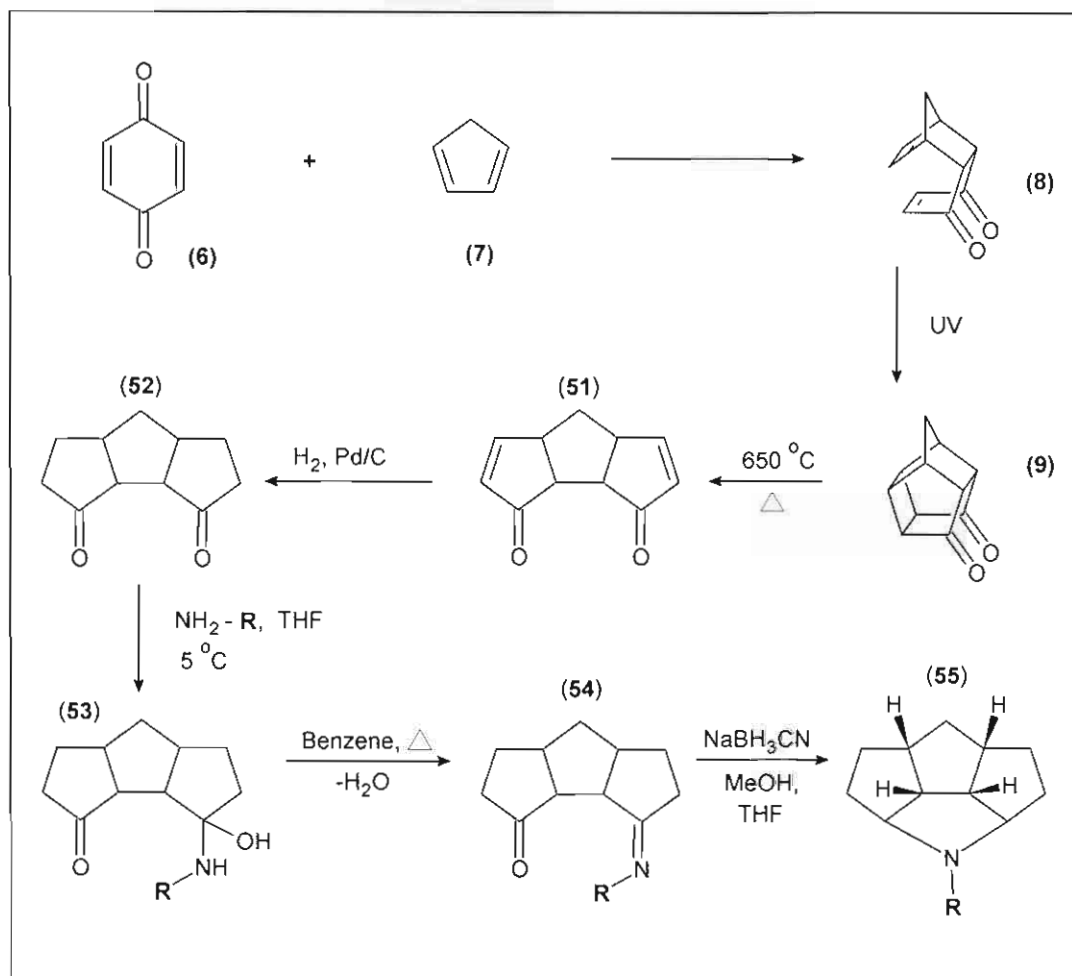


Figure 2.24: The synthesis of *N*-3,11-azatricyclo[6.3.0.0^{2,6}]undecane (55).

Flash thermolysis or flash vacuum pyrolysis was used to perform the thermal fragmentation. The method and conditions of flash thermolysis is thoroughly described by Liebenberg *et al.*, (1996) as well as others (Mehta *et al.*, 1981; Venter, 1988; Brown, 1980). The product of thermolysis, tricycloundecane-3,11-dione (51) was catalytically hydrogenated over 10% Pd-C catalyst to yield the symmetric

saturated dione **52**. Treatment of **52** with a primary amine in THF renders the mono imine intermediate (**53**) which was reduced with NaBH_3CN to obtain, through a transannular reaction and ring closure, compound **55** (Liebenberg *et al.*, 1996). The mechanism by which the amination and transannular cyclisation takes place is illustrated in (Fig. 2.25).

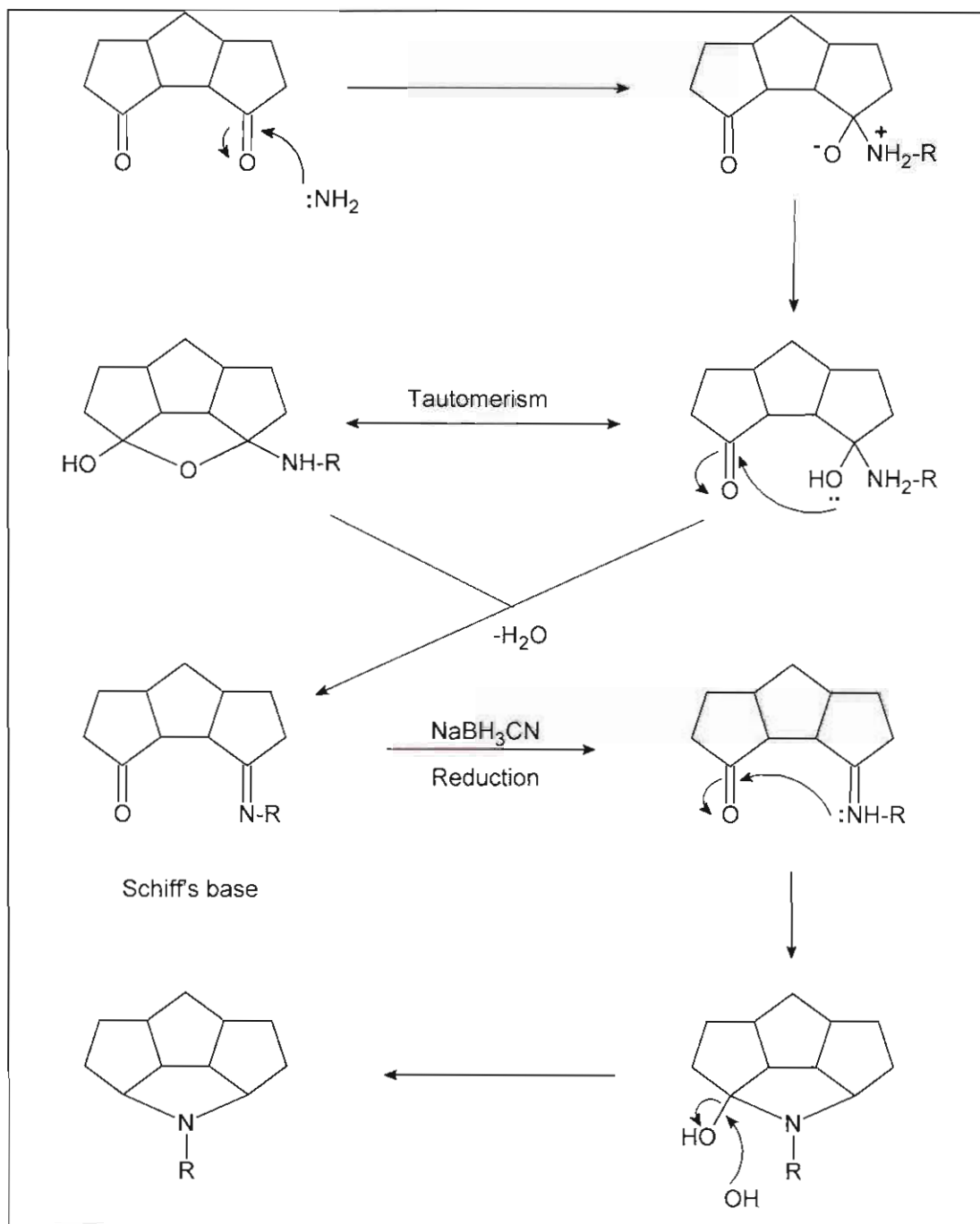


Figure 2.25: Mechanism for amination and transannular cyclisation (adapted from Swanepoel, 1991).

2.3 SCREENING TECHNIQUES FOR EVALUATING L-TYPE CALCIUM CHANNEL ACTIVITY OF THE TRIQUINYLAMINES

Unlike the pentacycloundecanes for which the calcium channel blocking activity have been extensively studied, both peripheral and in the CNS (Van der Walt *et al.*, 1988; Van der Schyf *et al.*, 1986; Malan *et al.*, 1996; Malan *et al.*, 2000; Liebenberg *et al.*, 2000; Geldenhuys *et al.*, 2003; Kiewert *et al.*, 2006 & Geldenhuys *et al.*, 2006), the triquinanes have thus far just been evaluated for calcium channel activity peripherally on the L-type calcium channel (Liebenberg *et al.*, 1996)

In the study done by Liebenberg *et al.*, (1996) as previously discussed (section 2.2.3.2) two triquinane derivatives were prepared and electrophysiologically tested. In this study, we will continue the biological evaluation of the triquinanes in neuronal cells by utilizing fluorescent microscopy to measure calcium influx through the L-type calcium channel after KCl-induced depolarisation in the N₂α mouse neuroblastoma cell line. To measure the activity on the NMDAR channel we will utilize radioligand binding studies to evaluate the displacement of [³H]MK-801 from murine synaptoneurosome in the presence and absence of the triquinylamine derivatives. The radioligand binding studies will evaluate whether these compounds compete with MK-801 for the PCP binding site to establish their mechanism of action on the NMDA receptor.

2.3.1 FLUORESCENT MICROSCOPY

Being able to measure [Ca²⁺]_i is crucial in the evaluation of deregulated calcium homeostasis. Currently the most popular method for measuring [Ca²⁺]_i in mammalian cells is to monitor the fluorescence of a calcium indicator. Several instruments and techniques can be utilized to measure the fluorescent changes of calcium indicators. Some examples are: multiparameter digitized video microscopy, confocal laser

scanning microscopy, two-photon excitation laser scanning microscopy, pulsed-laser imaging for rapid Ca^{2+} gradients, time-resolved fluorescence lifetime imaging microscopy, photomultiplier tube and flow cytometry (Takahashi *et al.*, 1999). The use of fluorescent microscopy in conjunction with fluorescent calcium indicators is common practice. However, obtaining these systems are very expensive and the choice of instrument will most likely depend on what is already available. Therefore it is very important to choose the right fluorescent Ca^{2+} indicator to produce the desired result with the available instrumentation and experimental conditions.

There are several different types of fluorescent calcium indicators, and it is important to select the most suitable probe for a given experiment. These indicators can be divided into various groups based on several different criteria. One way would be to divide them into two groups based on whether they are ratiometric or nonratiometric indicators, another would be to divide them into groups based on their excitation wavelength. The ratiometric indicators include indo-1, fura-2, mag-fura-2; whereas the nonratiometric indicators include fluo-3, the calcium green class, rhodamine-2 and quin-2. The use of ratiometric indicators allows for correction of differences of path length and accessible volume in three-dimensional specimens (Takahashi *et al.*, 1999).

Several other criteria also need to be taken into consideration when choosing the most suitable indicator for experimental setup (Takahashi *et al.*, 1999). Some of these criteria are:

- The excitation/emission spectra for the fluorescent indicator. It is important to match the absorption spectra [e.g., ultraviolet (UV) or visible wavelength (blue, green, and red)] of the indicator with the output (available wavelengths) of the excitation lights source (laser) in the system.
- The method for incorporating the indicator into the cell depends on the chemical form of the indicator. Calcium indicators are provided commercially in various forms such as salts (acid), esters, and dextran conjugates, rendering the indicator permeable or impermeable to the cell. Thus, the chemical form also needs to be taken into consideration.

- The indicator's Ca^{2+} -binding affinity, which is reflected in the dissociation constant (K_d) is a very important consideration. The K_d value of the indicator will determine the point at which the indicator will become saturated. Although high affinity (low K_d) Ca^{2+} indicators may emit brighter fluorescence, they may also buffer intracellular Ca^{2+} . More important, errors can occur because the high-affinity Ca^{2+} indicator becomes saturated at relatively low $[\text{Ca}^{2+}]$. The low-affinity (high K_d) Ca^{2+} indicators however, can be used to measure $[\text{Ca}^{2+}]$ of much higher proportions without becoming saturated. The low-affinity calcium indicators can also be used to measure rapid changes in $[\text{Ca}^{2+}]$. Because of their low affinity for Ca^{2+} , the kinetics of the reactions are rapid enough to analyze Ca^{2+} alterations with high temporal resolution.

For the accurate measurement of elevated intracellular free calcium concentration $[\text{Ca}^{2+}]_i$, an indicator with low calcium affinity and high selectivity is required. The high-affinity calcium indicators such as Fura-2 and Indo-1 ($K_d \sim 0.22 \mu\text{M}$ and $0.25 \mu\text{M}$ respectively, Grynkiewicz *et al.*, 1985) are limited in their useful detection range for calcium concentrations above 1-2 μM . Low-affinity calcium indicators such as Calcium-Green-5N and Calcium-Orange-5N do not undergo shifts in their emission or excitation wavelengths, which precludes the use of ratiometric measurement techniques (Hyrc *et al.*, 2000).

In a study by Stout and Reynolds, (1999) two high-affinity calcium indicators (Fura-2 and Fluo-3) were compared with two low-affinity calcium indicators (Mag-fura-2 and Calcium Green-5N) by measuring glutamate-stimulated increases in $[\text{Ca}^{2+}]_i$ in cultured rat forebrain neurons. The results suggested that the high-affinity calcium indicators underestimate the increase in $[\text{Ca}^{2+}]_i$ induced by excitotoxic glutamate stimuli and that these responses are greater than have previously been reported. Thus the high-affinity Ca^{2+} indicator Fura-2 have failed to establish a correlation between the magnitude of the stimulation-induced increases in $[\text{Ca}^{2+}]_i$ and subsequent toxicity (Stout & Reynolds, 1999). **This is** due to the fact that high-affinity calcium indicators becomes saturated at relatively low $[\text{Ca}^{2+}]_i$ causing errors (Takahashi *et al.*, 1999).

Based on these studies we selected Mag-Fura-2 for measuring the $[Ca^{2+}]_i$ in our study. Although Mag-Fura-2/AM was initially developed as indicator to monitor the cytosolic Mg^{2+} concentration, it can successfully be used as a Ca^{2+} indicator, because the Mg^{2+} reaction time during depolarisation is two to three orders of magnitude slower and smaller than the Ca^{2+} reaction time (Takahashi *et al.*, 1999). Another reason why we selected Mag-Fura-2 as indicator is based on the fact that it is a ratiometric probe. The use of ratiometric indicators allows for correction of differences of path length and accessible volume in three-dimensional specimens. The ratio signal for a ratiometric indicator is also not dependent on dye concentration. Therefore, since dye leakage and photobleaching leads to loss of indicator during an experiment, the ratiometric indicator will give a more stable measurement of $[Ca^{2+}]_i$. Ratiometric measurements also produce an additional increase in sensitivity (Simpson, 1999). We also decided to use the acetoxymethyl ester (AM) form of Mag-Fura-2 that is cell permeable. This will allow for direct cell loading for the AM form of the indicator can passively diffuse across the cell membranes and, once inside the cell, esterase cleave the AM group leading to a cell impermeable indicator. This has a second advantage because rendering the indicator cell impermeable after it entered the cell will minimise dye leakage (Simpson, 1999; Takahashi *et al.*, 1999).

2.4 SCREENING TECHNIQUES FOR EVALUATING NMDAR CHANNEL ACTIVITY OF THE TRIQUINYLAMINES.

As previously described (section 2.2.2), both noncompetitive and uncompetitive NMDAR antagonists bind to the PCP binding site within the NMDAR channel. A very popular and highly effective technique to determine the site of interaction for specific compounds inside the NMDAR channel is by means of radio ligand binding studies with either $[^3H]MK-801$ or $[^3H]TCP$ to measure the displacement of these blockers by the series of test compounds. This technique assesses whether the test compound interacts with the same binding site as reported in literature for MK-801 and TCP (Vignon *et al.*, 1983; Woodruff *et al.*, 1987).

Radio ligand binding studies was done for the pentacycloundecylamines by the group of Geldenhuys *et al.*, (2006). The investigators used both [³H]MK-801 and [³H]TCP as radio ligands and unlabeled MK-801 as reference compound to determine the non-specific binding. The study was conducted in synaptoneurosomes prepared from the whole brains of male ICR mice (Harlan) and calcium flux through the NMDAR channel was initiated by the addition of (100 μM) Glutamate and (100 μM) Glycine. Surprisingly the study indicated that although the pentacycloundecylamines showed inhibition of the NMDA/Gly mediated calcium flux, they interact with a unique binding site, different to that reported for MK-801 and PCP. Since the triquinylamines are structurally related to the pentacycloundecylamines and we wanted to allow for direct comparison with the pentacycloundecylamines, we conducted radio ligand binding studies similar to that described by Geldenhuys *et al.*, (2006). This will allow us to asses whether the triquinylamines have activity as NMDAR channel blocker and if they interact with the same binding site as MK-801 or PCP.

CHAPTER 3

SELECTION AND SYNTHESIS OF RELEVANT COMPOUNDS

3.1 INTRODUCTION

Chemical structures were selected in order to obtain a meaningful series of triquinylamine compounds that would allow for direct comparison with pentacycloundecane compounds which, in earlier studies, were discovered to be calcium channel blockers on both the NMDA receptor and L-type calcium channel. NGP1-01 was used as a lead compound as it has been extensively studied for its dual mechanistic action on both these channels (Van der Schyf *et al.*, 2006). Earlier postulations suggested that the pentacycloundecane skeleton may serve only as a bulk contributor to the activity of NGP1-01 and related polycyclic cage compounds, Liebenberg *et al.*, (1996) and Malan *et al.*, (2000). In order to further investigate the validity of this thesis; we synthesised a series of thermal ring-opened derivatives of the pentacycloundecane moiety. Malan *et al.*, (1998 and 2000) evaluated the structure-activity relationships of different aromatic amine side chains on the pentacycloundecane skeleton based on their activity as L-type calcium channel blockers. Later, Geldenhuys *et al.*, (2006) continued the work by Malan and co-workers by evaluating the structure-activity relationships on the NMDA receptor for the same selection of compounds. In a study by Kroemer *et al.*, (1998) the activity for a set of molecules were evaluated at the PCP binding site to determine the structural requirements for uncompetitive NMDAR block. From the proposed pharmacophore several structure activity relationships could be determined (see section 2.2.1.1). With a few exceptions, the side chains selected for the triquinylamines synthesised in the current study were based on the findings by these earlier studies.

The benzylamine side chain was selected for compound **LB-1** to allow comparison with NGP1-01, the extensively studied lead compound. The cyclohexylmethylamine

side chain was included in the current study (compound **LB-2**) to contrast aromatic ring substitution with aliphatic ring substitution. This substitution was also designed to evaluate the lipophilic interaction suggested by Kroemer *et al.*, (1998) to be necessary for high-affinity binding to the PCP site. The heptylamino substituent was introduced as a moiety with significant flexibility but with a volume comparable to that of the cyclohexylmethylamino moiety.

The 3-methoxybenzylamine side chain was selected (compound **LB-3**) to evaluate electronic effects on varying aromatic ring substitution patterns. It is well established that the methoxy group can be either electron-donating or electron-withdrawing, depending on the position of the group's substitution on an aromatic ring system. In the benzyl system, when a methoxy group is attached to the *meta* position, the electronegativity of the oxygen atom results in an inductive effect with significant electron-withdrawing properties. In this regard, positive sigma (σ) values in the region of 0.12 have been reported (Hansch *et al.*, 1991, 1995). In the *para* position, however, only a relatively small inductive effect would be expected. Further attenuating this small inductive effect is an electron-donating resonance effect that occurs for the methoxy group substituted in the *para* position. These two factors combined result in an overall electron-donating effect for *para*-substituted methoxy groups with a negative σ value in the region of ~ -0.27 (Hansch *et al.*, 1991 & 1995). Perhaps associated with these electronic effects, it has been reported by Malan *et al.*, (2000) that substitution with a methoxy group in the *ortho* or *meta* positions, compared with the *para* position, showed an increase in calcium blocking activity at the L-type calcium channel. The same effects were observed by Geldenhuys *et al.*, (2006) were the authors suggested that the donation of electrons made the phenyl ring more lipophilic and would increase the aromatic π - π interaction and affinity for the PCP binding site as described by Kroemer *et al.*, (1998).

The 3-phenylpropylamine side chain of compound **LB-4** was selected to evaluate the effect of increasing chain length and consequential increasing separation of the polycyclic moiety and the aromatic ring, compared to **LB-1**. This compound would give an indication of the available space or volume for interaction within the channel or receptor, referring specifically to the length of the channel or receptor. An increase

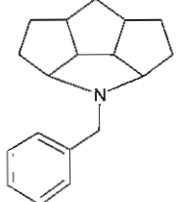
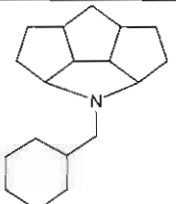
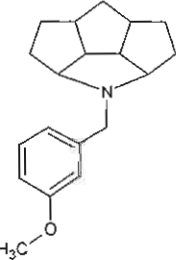
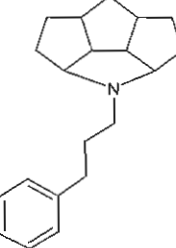
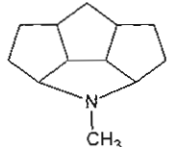
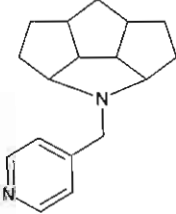
in chain length might also increase the free energy of hydrophobic interaction for a blocker with the NMDA channel (Sobolevsky *et al.*, 1999). In a study done by Geldenhuys *et al.*, (2006) it was observed that an increase in chain length from benzylamine to phenylethylamine leads to a decrease in activity on the NMDA channel. However Liebenberg *et al.*, (2000) found that the activity on the L-type calcium channels increased with an increase in chain length between the polycyclic cage and the aromatic moiety. The methyl side chain on compound **LB-5** was selected to evaluate the necessity of aromatic substitution, compared to compound **LB-1**, as well as the effect of chain length with aliphatic substitution when compared to compound **LB-2**. As mentioned for **LB-2** it has been reported by Kroemer *et al.*, (1998) that a second hydrophobic interaction is necessary for high-affinity binding with the NMDA receptor channel. Geldenhuys *et al.*, (2006) confirmed that removal of the aromatic substituents diminished the activity on the NMDA receptor channel. It has also been reported by Liebenberg *et al.*, (2000) that compounds with aliphatic short chain length substituents were inactive on the L-type calcium channel. However, in this study it was observed that aliphatic substituted compounds with octyl side chains were as active as their aromatic counterparts.

The pyridine side chain on compound **LB-6** was selected to evaluate the effect of hydrogen bonding introduced by the presence of a hetero atom in the aromatic moiety. By evaluating this compound the effects of hydrogen bonding can be compared to the normal hydrophobic interactions of the phenyl ring. It was also observed that the pyridine ring tends to fold back onto the polycyclic cage and through-space influences of the aromatic ring on the cage moiety can accordingly be evaluated (Malan *et al.*, 2000). Pyridine is an aromatic six-membered heterocycle with a π electron structure similar to that of benzene with six p orbitals, each containing one π electron, perpendicular to the plane of the ring. However, the nitrogen lone-pair electrons are contained in a sp^2 orbital in the plane of the ring and are not involved with the aromatic π system (McMurry, 1996). Thus the pyridine ring still retains its aromaticity, while the lone-pair of electrons allow for hydrogen bonding. Although the pyridine ring still retains aromaticity, it is much more hydrophilic than benzene with many more electrophilic elements. The study by Kroemer *et al.*, (1998) indicated that a possible second site for hydrogen bonding might exist in the region of a second

Selection and synthesis of relevant compounds

site that allows for hydrophobic interaction. The author commented that although steric descriptors are dominant, electrostatic interactions should not be disregarded.

Table 3.1: Structures selected for synthesis and evaluation

LB-1		N-benzyl-3,11-azatricyclo[6.3.0.0^{2,6}]undecane
LB-2		N-cyclohexylmethyl-3,11-azatricyclo[6.3.0.0^{2,6}]undecane
LB-3		N-(3-methoxybenzyl)-3,11-azatricyclo[6.3.0.0^{2,6}]undecane
LB-4		N-(phenylpropyl)-3,11-azatricyclo[6.3.0.0^{2,6}]undecane
LB-5		N-methyl-3,11-azatricyclo[6.3.0.0^{2,6}]undecane
LB-6		N-(pyridin-4-ylmethyl)-3,11-azatricyclo[6.3.0.0^{2,6}]undecane

3.2 GENERAL APPROACH

Reagents were obtained from Sigma-Aldrich (U.K. & U.S.A.), Merck (Germany), D.H. chemicals (U.K.), Acros Organics (U.S.A.), Fluka (Switzerland & U.S.A.) and Saarchem (South Africa). Reaction and elution solvents were purchased from commercial sources in South Africa. Column chromatography was performed using either conventional glass columns packed with silica gel, 60 Å pore size, mesh 70 – 230, purchased from Separations (South Africa) or by flash chromatography utilizing the Versa Flash station with VersaPak columns, silica cartridge 40 × 75 mm, purchased for Supelco (Pretoria, South Africa). Preparative thin-layer chromatography was performed on pre-coated silica gel glass plates, 60 Å pore size, diameter 20 × 20 cm and layer thickness 2 mm with fluorescent indicator for 245 nm, purchased from Separations (South Africa), and also on C-18 preparative chromatography glass plates, 60 Å pore size, diameter 20 × 20 cm and layer thickness 0.25 mm, purchased from Whatman Chemical Separation Inc (U.S.A.).

Differential scanning calorimetry (DSC) thermograms were recorded with a Shimadzu DSC-50 instrument (Shimadzu, Kyoto, Japan). The measurement conditions were as follows: sample weight, approximately 2 mg; sample holder, aluminium crimp cell; gas flow, nitrogen at 35 ml/min; heating rate, 10 °C per minute. Melting points (mp) were measured using a Gallenkamp melting point apparatus and infrared (IR) spectra were recorded on a Nicolet 470 FT-IR spectrophotometer. Mass spectra (MS) were recorded using a VG 7070E mass spectrometer. Nuclear magnetic resonance (NMR) spectra were acquired on a Varian Gemini 300 with ¹H spectra recorded at a frequency of 300.075 MHz and ¹³C spectra at 75.462 MHz. Chemical shifts are reported in parts per million (ppm) relative to the internal standard, tetramethylsilane (TMS). The following abbreviations were used to indicate multiplicities of the respective signals: s, singlet; bs, broad singlet; d, doublet; t, triplet; q, quartet; m, multiplet.

ABBREVIATIONS

DSC	differential scanning calorimetry
FVP	flash vacuum pyrolysis
IR	infrared spectroscopy
Mp	melting point
MS	mass spectrometry
NMDA	N-methyl-D-aspartate
NMR	nuclear magnetic resonance spectroscopy
ppm	parts per million
THF	tetrahydrofuran
TLC	thin-layer chromatography
TMS	tetramethylsilane

3.3 SYNTHESIS OVERVIEW

The synthesis pathway used in this study is shown in Figure 3.1. Pentacyclo[5.4.0.0^{2,6}.0^{3,10}.0^{5,9}]undecane-8-11-dione also called Cookson's "bird cage" compound (**9**) was synthesised by photocyclisation of the Diels-Alder adduct (**8**) obtained from the reaction of 1,3-cyclopentadiene (**6**) with p-benzoquinone (**7**). Thermal fragmentation of the saturated four-membered ring (**9**) was used to form the *cis,syn,cis*-triquinane system, tricyclo[6.3.0.0^{2,6}]undecane-4,9-diene-3,11-dione, (**51**). The thermal fragmentation was performed through flash thermolysis or flash vacuum pyrolysis (FVP) and was carried out in a quartz vigreux column connected to a substrate tube and a vacuum line provided with a liquid nitrogen cold trap. We designed a tube furnace to heat the quartz column in which the thermal fragmentation took place. The temperature was measured with a thermocouple and regulated with a Shinko Ramp/Soak Auto tune PID controller. The substrate is contained in a borosilicate glass tube, heated with commercially available heating tape wound around a copper tube for even heat distribution. The product is trapped in a specially

designed freeze fall cooled with liquid nitrogen. The entire apparatus is evacuated to ca. 1 torr by a high-capacity, rotary vane oil pump.

Sublimation of (**9**) into the delivery tube was achieved at 150 °C, vacuum 1 torr. The substrate slowly travelled through the quartz column, which was heated to a temperature of 650 °C, vacuum 1 torr. The condensate was deposited in the freeze fall and yielded tricyclo[6.3.0.0^{2,6}]undecane-4,9-diene-3,11-dione (**51**). The product of thermolysis (**51**) was hydrogenated over 10% Pd-C catalyst to yield tricyclo[6.3.0.0^{2,6}]undecane-3,11-dione (**52**). Treatment of **52** with a primary amine in THF rendered the carbinolamine intermediate (**53**), which was dehydrated under Dean-Stark conditions in dry benzene to give the imine (**54**). Subsequent reduction in anhydrous methanol and tetrahydrofuran (THF) using NaBH₃CN facilitated ring closure through a transannular reaction and resulted in the formation of the aza compound (**55**) as a light brown oil (Liebenberg *et al.*, 1996; Mehta *et al.*, 1981). Purification was achieved with consecutive sequences of column chromatography, flash column chromatography and/or preparative thin-layer chromatography.

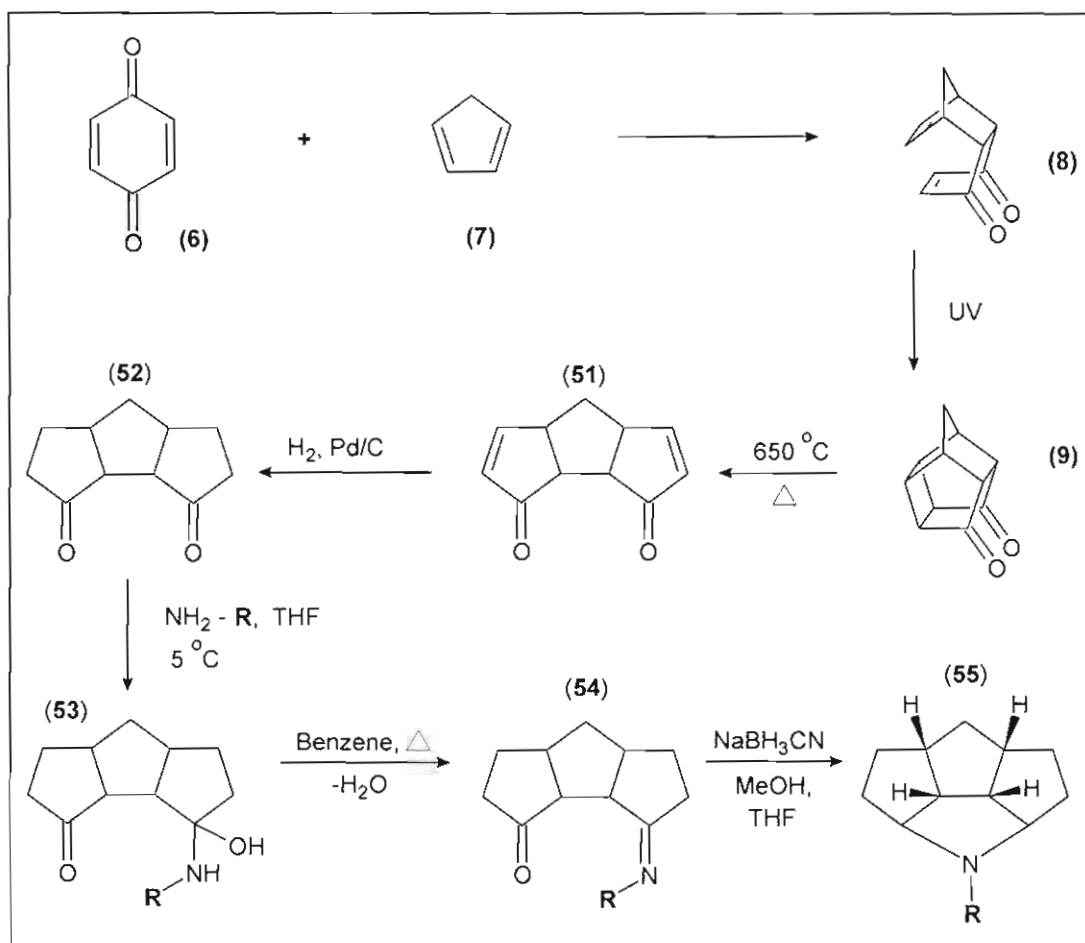


Figure 3.1: Reaction scheme for the synthesis of the triquinylamines.

3.4 DEVELOPMENT OF PYROLYSIS APPARATUS

In the current project we had to develop custom made flash vacuum pyrolysis equipment specific to our needs since similar equipment could not be found commercially. Tube furnaces available commercially were unaffordable and not suited to our requirements. In addition, flash vacuum pyrolysis apparatus reported in the literature were not described in sufficient detail to allow us to build an apparatus by following assembly directions. We therefore adapted the design of our pyrolysis apparatus based on descriptions detailed in papers published by McNab (2004) and Brown (1980).

Selection and synthesis of relevant compounds

Our first objective was to plan the general route of the synthesis and the path that the compound would travel through the apparatus. In order to achieve sublimation we required a tube that could be heated to 150 °C, connected to a closed system that could be evacuated to 1 torr. Pentacyclo[5.4.0.0^{2,6}.0^{3,10}.0^{5,9}]undecane-8-11-dione (**9**) would be placed in the sublimation tube and from there, once sublimated, travel through the connecting tube that must be heated to a high temperature of 650 °C in order to achieve thermal fragmentation. Quartz was used for the connecting tube because of the high temperatures tolerated by this substance without undergoing deformation under low vacuum. The substrate tube however, was made out of borosilicate glass as it was only required to tolerate temperatures up to 150 °C. We also decided that the connecting tube should be a vigreux column to afford a bigger surface area, thus requiring a shorter transit time and preventing decomposition of the organic molecules, with subsequent formation of secondary products and tars. To trap the formed compound, it had to travel through a liquid nitrogen cold trap. A second cold trap was added to ensure that no solids enter the vacuum pump. Figure 3.2 and 3.3 shows the entire system and different components of the glass apparatus.

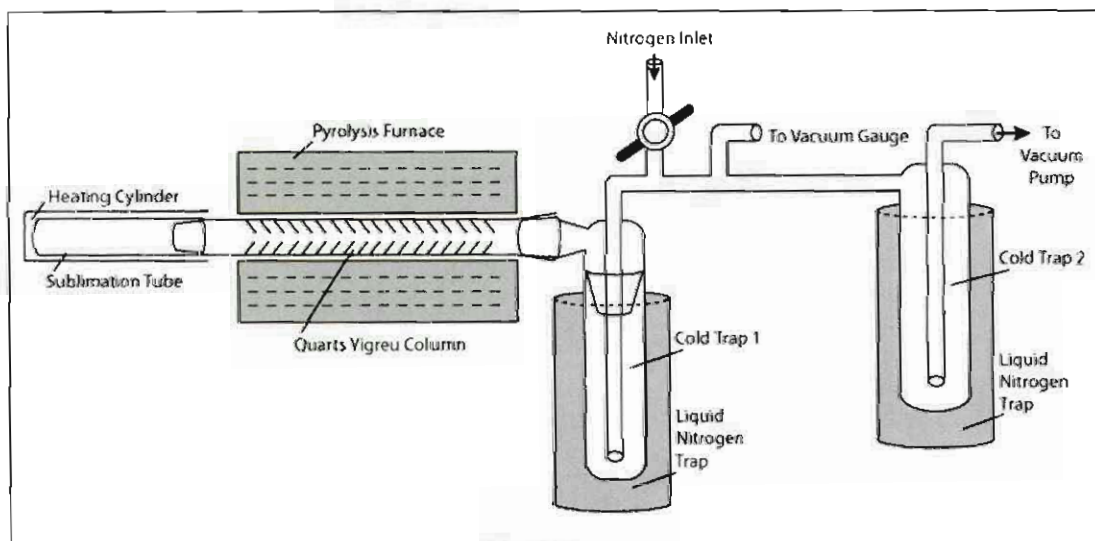


Figure 3.2: Schematic of apparatus for flash vacuum pyrolysis (FVP)

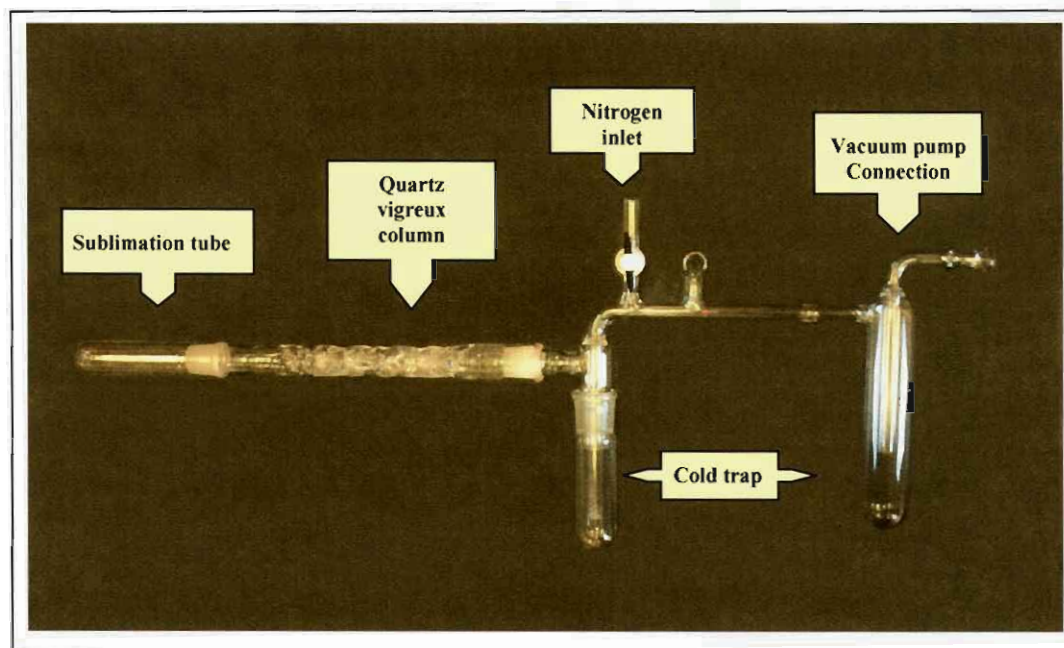


Figure 3.3: Components of the glass apparatus.

The remaining units of the apparatus were designed around individual synthetic pathway requirements. As stated earlier, to achieve sublimation we required heating of the sublimation tube to 150 °C. This was accomplished with silicone heating tape purchased from Hi-Tech Elements (South Africa). A copper cylinder was constructed to fit snugly over the sublimation tube to facilitate even heat distribution. Heating tape was then wound around the copper cylinder to provide heating to a temperature necessary for sublimation (Fig. 3.4). The heating tape was also wound around a portion of the glass connection just distal to the furnace to allow the compound to migrate through to the cold trap, preventing the formation of precipitation that tended to block the connecting joint with the cold trap. The temperature of the heating tape was measured with a K-type thermocouple, purchased from Wika (South Africa), placed between the glass tube and the heating tape and controlled with Shinko ($1/16$ DIN, JCD Series) digital indicating PID controllers purchased from Wika (South Africa). Figure 3.4 also illustrates the furnace into which the quartz vigreux column is inserted.

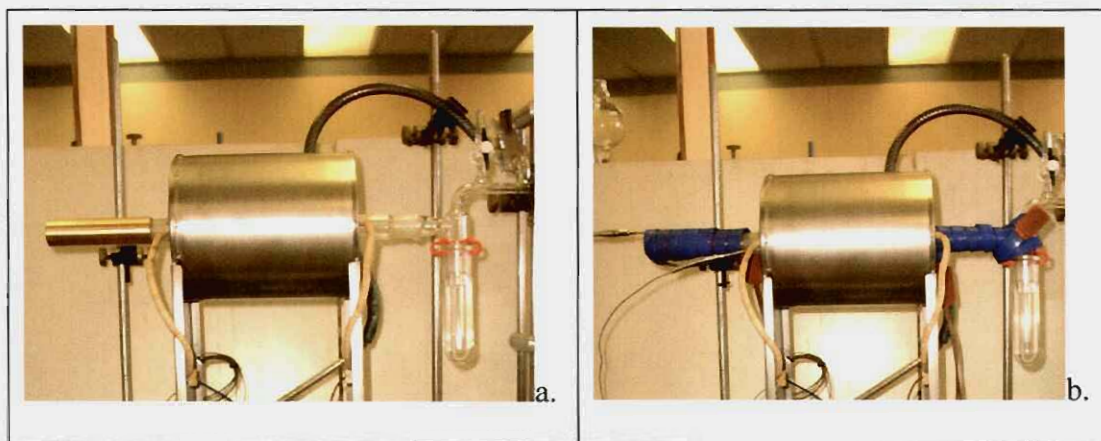


Figure 3.4: Glass tubing and the furnace; (a) shows the copper cylinder, and (b) shows the placement of the heating tape proximal and distal to the furnace.

To obtain temperatures exceeding $650\text{ }^{\circ}\text{C}$ a type of material had to be selected for the furnace tube that could withstand extremely high temperatures, not expand too much thereby breaking the quartz column, and also be machineable. We chose soapstone (also known as steatite); a material soft enough to be machineable and once baked, becomes hard and durable like ceramic. During the machining process the soapstone was formed into a hollow cylinder ($200\text{ mm length} \times 60\text{ mm diameter}$, outer volume 302.18 cm^3 , inner volume 108.79 cm^3), through which the quartz vigreux column could be placed. A screw-thread was cut into the outside wall of the cylinder. In order to obtain a maximum temperature of $800\text{ }^{\circ}\text{C}$, nichrome wire 15.5 m with a resistance of $\sim 96.8\text{ ohms}$ (resistance 6.3 ohms/m) was used as heating element. The wire was wound around the cylinder, following the grooves of the screw-thread. The grooves cut into the outer wall of the cylinder were 1 mm thick and 1.5 mm apart and functioned to prevent wire contact and thus a short-circuit. Cylinders (Fig. 3.5-d) were also constructed from soapstone and slid over the wire for insulation and protection. Finally, before winding the wire onto the tube furnace, all the soapstone components were baked in a furnace, under slowly increasing heat to $1000\text{ }^{\circ}\text{C}$, and then allowed to cool down slowly and incrementally to avoid the stone from cracking.

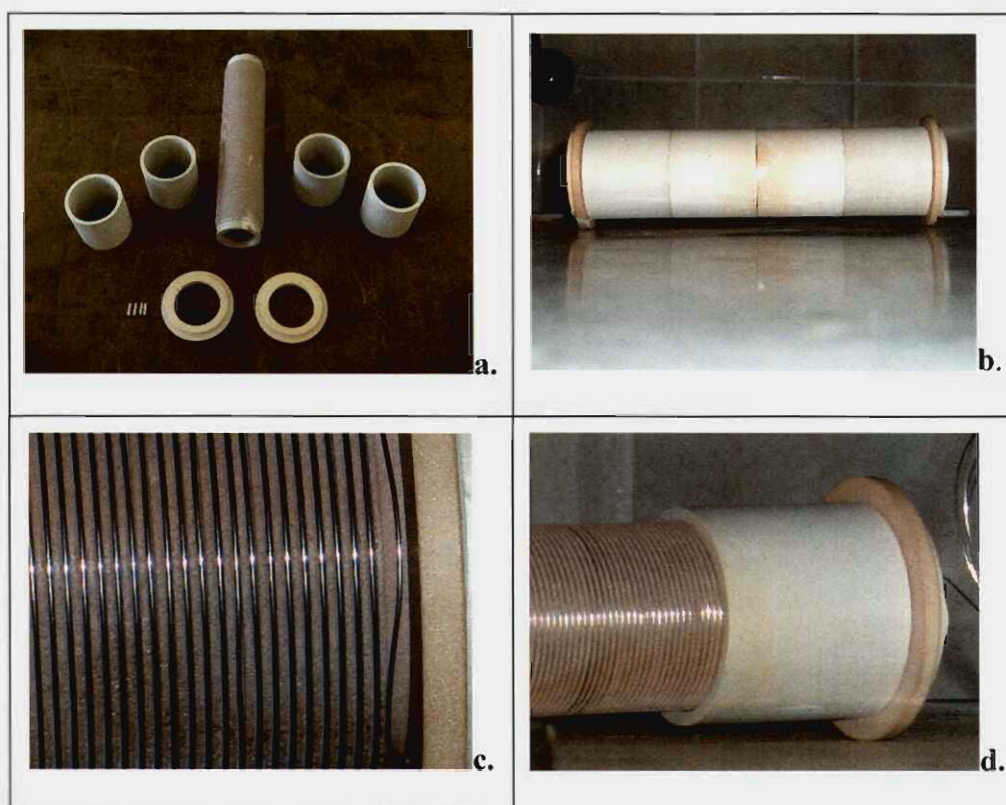


Figure 3.5: The tube furnace where (a) shows all the components, (b) shows the full assembly, (c) illustrates the grooves in which the wire is placed and (d) illustrates the cylinders covering the wire.

In order to better insulate and protect the tube furnace it was wrapped in glass wool and placed inside a stainless steel casing. Shinko ($\frac{1}{4}$ DIN, JCD Series) digital indicating, ramp/soak, auto tune PID controllers purchased from Wika (South Africa) were used to regulate the heating of the furnace. These controllers enabled us to regulate the furnace rate of heating, the maximum temperature setting and the time to remain at maximum temperature setting after which the furnace will automatically switch off and cool down at normal convection rate. The temperature was measured with a thermocouple placed in a hole drilled through the length of the inner tube. The end of the thermocouple reached into the centre of the tube (heating zone) where the furnace was at its hottest. Studies were done to evaluate the heat loss over the length of the tube and also to establish a safe rate at which to heat the furnace. It was found that there was a $150\text{ }^{\circ}\text{C}$ difference between the centre and the furthest point, but that it still provided adequate contact time to achieve thermal fragmentation. We also found

Selection and synthesis of relevant compounds

that it was safest to heat the furnace over a period of 60 min to prevent it from expanding too rapidly and cracking.

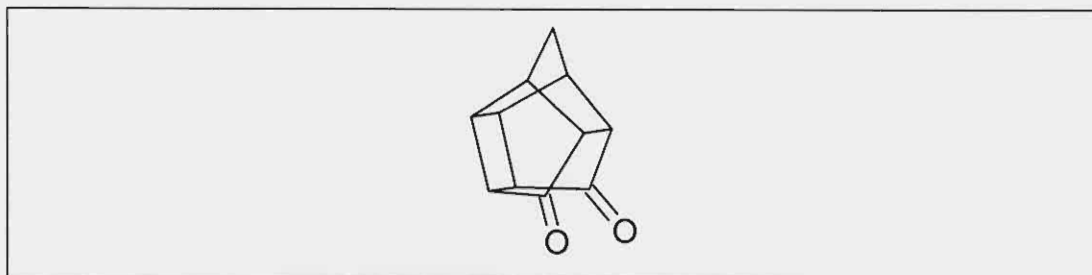
The cold trap, based on a description of the design of McNab (2004), was designed with two cold fingers that fit into separate flasks containing liquid nitrogen. The function of these cold traps is to collect the emerging vapours from the furnace. Literature suggested that the cold trap needed to be situated as close as possible (less than 10 cm) to the furnace to minimise decomposition of the unstable pyrolysate. In our design the first cold finger can be taken apart to allow easy access to the product. The function of the second cold finger is to prevent any vapour condensate that was not trapped by the first cold finger from entering the vacuum pump. We also included two connections on the cold trap, a nitrogen inlet and a connection to the vacuum gauge. Figure 3.6 illustrates the full assembly of the flash vacuum apparatus. The entire system was evacuated to 1 torr using a two stage ILVAC, rotary vane oil vacuum pump (Model PK 2 DC, rated pumping speed 2 m³/h) purchased from Air & Vacuum technologies (South Africa).



Figure 3.6: Full assembly of apparatus for flash vacuum pyrolysis.

3.5 SYNTHESIS

3.5.1 PENTACYCLO[5.4.0.0^{2,6}.0^{3,10}.0^{5,9}]UNDECANE-8,11-DIONE



CHEMICALS AND REAGENTS

1,4-Benzoquinone , 98% (C ₆ H ₄ O ₂)	(108.1 g/mol)
Cyclopentadiene (66.1 g/mol) , monomerised from dicyclopentadiene (C ₅ H ₆)	(132.2 g/mol)

SYNTHETIC PROCEDURE

p-Benzoquinone (10 g, 0.0925 mol) was dissolved in dry Benzene (100 ml) and oxidized with MnO₂ (± 50 mg) under reflux for 1 hour. An excess of activated charcoal was added and the mixture was refluxed for an additional 15 min. The hot solution was then vacuum-filtered through Celite® to produce a dark amber coloured solution. Recrystallisation of the oxidized 1,4-benzoquinone was prevented by immediately filtering 100 ml of warm benzene through the same system. The mixture was placed on an external ice bath and cooled down to ± 5 °C before slowly adding the freshly monomerised cyclopentadiene stoichiometrically (6.972 ml, 0.0925 mol). The photo labile reaction mixture was removed from the ice bath, protected from light and stirred overnight at room temperature. The reaction was monitored by TLC and presumed complete when all p-benzoquinone was used. If not complete, additional cyclopentadiene was added while monitoring the reaction on TLC-plates until complete. The reaction mixture was treated with activated charcoal, filtered through Celite®, solvents removed *in vacuo* and allowed to fully evaporate in a dark fume cupboard to afford the Diels-Alder adduct as yellow crystals. Recrystallisation

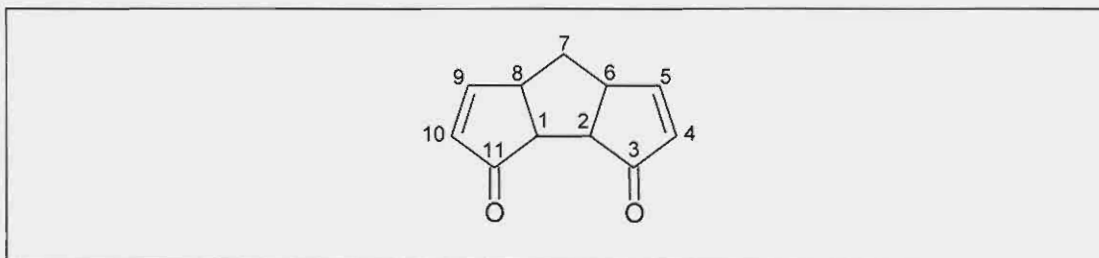
Selection and synthesis of relevant compounds

from petroleum ether resulted in the formation of bright yellow needle-like crystals. The Diels-Alder adduct was dissolved in acetone (± 4 g in 100 ml) and irradiated for approximately six hour with a 1000 W medium pressure mercury UV lamp (Phillips HPA 1000/20). Decolouration of the solution from dark yellow to light yellow/almost transparent confirmed that cyclisation of the adduct was completed. The solvent was subsequently removed *in vacuo* as a light yellow residue.

PURIFICATION

The resulting light yellow residue was purified by Soxhlett extraction in cyclohexane to produce the diketone as a waxy white precipitate (Yield: 10.0610 g, 0.0578 mol, 62.44 %). The data obtained from physical characterisation of this compound correlate with the physical characteristics of the pentacyclo[5.4.0.0^{2,6}.0^{3,10}.0^{5,9}]undecane-8,11-dione (174.196 g/mol) described by Cookson *et al.*, (1958) and therefore, no spectral data for this compound are presented in this dissertation.

3.5.2 TRICYCLO[6.3.0.0^{2,6}]UNDECANE-4,9-DIENE-3,11-DIONE (Triq-1)



CHEMICALS AND REAGENTS

Pentacyclo[5.4.0.0^{2,6}.0^{3,10}.0^{5,9}]undecane-8,11-dione, (C₁₁H₁₀O₂) (174.196 g/mol)

SYNTHETIC PROCEDURE

We found, also reported in literature Brown, 1980; that optimal yield was achieved when the starting compound was sublimated using small samples of starting

compound (9) spread as a thin film over the entire inner surface of the sublimation tube. Pentacyclo[5.4.0.0^{2,6}.0^{3,10}.0^{5,9}]undecane-8,11-dione (1g, 0.006 g/mol) was dissolved in a minimal amount of dichloromethane and spread over the surface of the sublimation tube using a heat gun to evaporate the dichloromethane while turning the sublimation tube over the heat source in a fume hood. The sublimation tube was connected to the vigreux column by interspersing Teflon joint tape in preference to silicone grease due to the instability of the latter at very high temperatures. Nitrogen was flushed through the system with the vacuum pump turned on. The nitrogen inlet was closed and the whole apparatus evacuated to 1 torr by a high-capacity, rotary vane oil pump. Sublimation was achieved by sliding the copper cylinder with wounded heating tape, as previously described, over the sublimation tube and heating the sublimation tube to 150 °C under a 1 torr vacuum. The substrate slowly migrated through the quartz column which was preheated to a temperature of 650 °C. The condensate that yielded the tricyclo[6.3.0.0^{2,6}]undecane-4,9-diene-3,11-dione was deposited as white waxy crystals mixed with black tar in the freeze fall cooled with liquid nitrogen. The pyrolysis was carried out at a throughput rate of 45 minutes and repeated several times. We found it necessary to remove the condensate after every 5 grams pyrolysed to prevent it from blocking the inlet to the freeze fall.

PURIFICATION

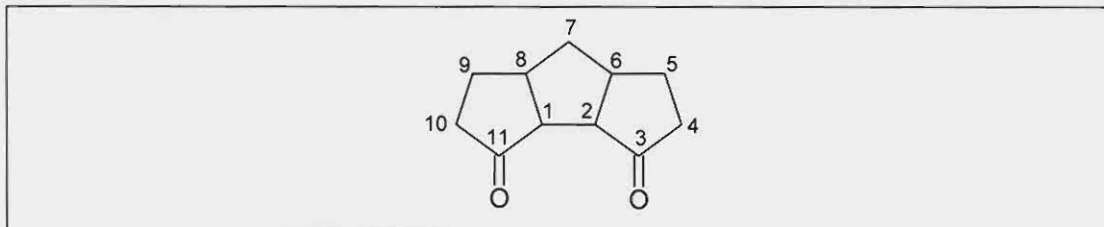
The condensate from the freeze fall was purified by recrystallisation in cyclohexane to produce the tricyclo[6.3.0.0^{2,6}]undecane-4,9-diene-3,11-dione as white needle-like crystals (Yield: 0.798 g, 0.00458 mol for every 1 g pyrolysed, 79.758 %).

PHYSICAL DATA

C₁₁H₁₀O₂; **m.p.** DSC (Spectrum 1) 97.23 °C; **IR (KBr)** ν_{\max} (Spectrum 3): 3315, 1720, 1639 cm⁻¹; **MS** (EI, 70 eV) m/z (Spectrum 9): 174 (M⁺), 146, 131, 117, 91, 66, 39, 28; **¹H NMR** (300 MHz, CDCl₃) δ_{H} (spectrum 14): 7.510 – 7.300 (m, 2H, H-5, 9), 6.170 – 5.500 (m, 2H, H-4, 10), 3.670 – 3.350 (m, 2H, H-6, 8), 3.280 – 3.030 (m, 2H, H-1, 2), 2.450 – 2.100 (m, 1H, H-7b), 2.060 - 1.750 (m, 1H, H-7a); **¹³C NMR** (75 MHz, CDCl₃) δ_{C} (Spectrum 21, 22): 207.350 (s, 2C, C-3, 11), 165.933 (d,

2C, C-4, 10), 133.348 (d, 2C, C-5, 9), 53.046 (d, 2C, C-1, 2), 50.293 (d, 2C, C-6, 8), 31.364 (t, 1C, C-7).

3.5.3 TRICYCLO[6.3.0.0^{2,6}]UNDECANE-3,11-DIONE (Triq-2)



CHEMICALS AND REAGENTS

Tricyclo[6.3.0.0^{2,6}]undecane-4,9-diene-3,11-dione, (C₁₁H₁₀O₂) (178.228 g/mol)

10% Pd-C, (106.42 g/mol)

SYNTHETIC PROCEDURE

Tricyclo[6.3.0.0^{2,6}]undecane-4,9-diene-3,11-dione (3.09g, 0.0177 mol) was dissolved in 500 ml of dry ethyl acetate and reduction was done with 10% Pd-C (300 mg) at a pressure of 2 atm (H₂) for 40 minutes. The catalyst was removed by filtration through Celite[®] and the solvent was removed *in vacuo*.

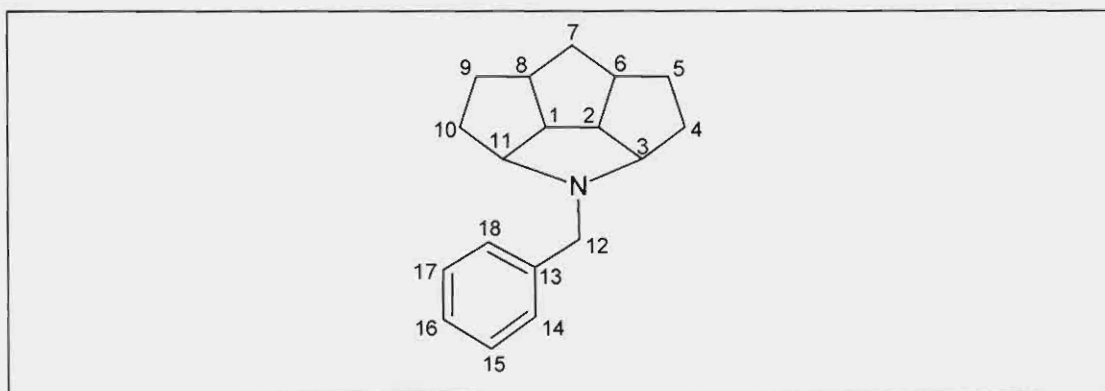
PURIFICATION

Recrystallisation from cyclohexane produced the tricyclo[6.3.0.0^{2,6}]undecane-3,11-dione as needle-like white/colourless crystals (Yield: 3.01 g, 0.0169 mol, 95.42%). Physical characterisation for this product correlates with the literature characterizations reported by Liebenberg (1989) and Mehta *et al.*, (1981).

PHYSICAL DATA

C₁₁H₁₄O₂; **m.p.** DSC (Spectrum 2) 95.82 °C; **IR (KBr)** ν_{\max} (Spectrum 4): 2944, 1736, 1417 cm^{-1} ; **MS** (EI, 70 eV) m/z (Spectrum 10): 178 (M^+), 122, 96, 79, 66, 55, 39, 28; **¹H NMR** (300 MHz, CDCl₃) δ_{H} (spectrum 15): 2.970 – 2.697 (m, 4H, H-1, 2, 6, 8), 2.492 – 2.122 (m, 5H, H-4a, 4b, 7b, 10a, 10b), 2.115 – 1.935 (m, 2H, H-5b, 9b), 1.720 – 1.535 (m, 2H, H-5a, 9a), 1.304 – 1.098 (m, 1H, H-7a); **¹³C NMR** (75 MHz, CDCl₃) δ_{C} (Spectrum 23, 24): 218.587 (s, 2C, C-3, 11), 55.973 (d, 2C, C-1, 2), 43.440 (d, 2C, C-6, 8), 38.538 (t, 1C, C-7), 37.023 (t, 2C, C-4, 10), 26.011 (t, 2C, C-5, 9).

3.5.4 N-BENZYL-3,11-AZATRICYCLO[6.3.0.0^{2,6}]UNDECANE (LB-1)



CHEMICALS AND REAGENTS

Tricyclo[6.3.0.0^{2,6}]undecane-3,11-dione , (C ₁₁ H ₁₄ O ₂)	(178.23 g/mol)
Benzylamine , 99% (C ₇ H ₉ N)	(107.16 g/mol)
NaBH₃CN	(62.84 g/mol)

SYNTHETIC PROCEDURE

Tricyclo[6.3.0.0^{2,6}]undecane-3,11-dione (2.0838 g, 0.0117 mol) was dissolved in anhydrous tetrahydrofuran (THF; 30 ml) and cooled down to 5 °C on an external ice bath. Benzylamine (1.333 g, 0.0124 mol) was slowly added stoichiometrically while

Selection and synthesis of relevant compounds

the mixture was stirred for approximately 6 hours at low temperature. The reaction was constantly monitored on TLC. The reaction was then stirred at room temperature for an additional 35 hours while continuously monitoring on TLC. After 35 hours the reaction was still not completed but was terminated at this step to proceed to the next. The carbinolamine did not precipitate as described in other literature reports and the reaction mixture had a light brownish colour. The solvent was removed *in vacuo* to yield a dark yellow oil. This product was dehydrated under Dean Stark conditions for approximately 1 hour using 40 ml anhydrous benzene. Benzene was removed *in vacuo* to produce the Schiff base (3-benzyliminotricyclo[6.3.0.0^{2,6}]undecane-11-one) in the form of a yellow/brown oil. The resulting oil was dissolved in anhydrous methanol (20 ml) and anhydrous THF (75 ml). Reduction was carried out by adding NaBH₃CN (0.8 g, 0.0127 mol) in molar excess and stirring overnight (18 hours) at room temperature. The solvents were removed and the resulting yellow/brown oil was suspended in approximately 50 ml of distilled water in a separation funnel. The product was extracted with dichloromethane (4 × 20 ml) and the combined dichloromethane fractions were washed with distilled water (2 × 50 ml). The organic phase was dried over anhydrous CaSO₄ and filtered. Subsequent *in vacuo* removal of the solvent resulted in the formation of a yellow/brown oil which was purified with consecutive column chromatography sequences (Yield 0.393 g, 0.002 mol, 13.27 %).

PURIFICATION

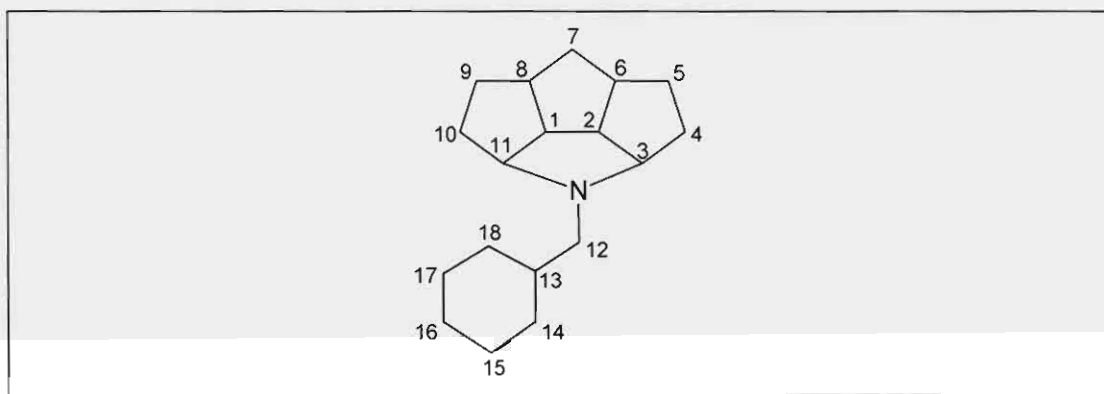
Purification of the product mixture was accomplished with consecutive column and flash column chromatography sequences. The first purification step utilized a mobile phase consisting of petroleum ether: ethyl acetate: ethanol in a 5:4:2 ratio. Fractions were collected and analyzed by NMR and MS to ascertain fraction content and purity. Fractions containing the desired compound were identified and underwent further purification in cases where by-products were present. A second purification step was done by flash column chromatography (n-hexane: ethyl acetate: dichloromethane in a 3:1:1 ratio), and the product mixture eluted at 4 ml/min. Again, fractions were analyzed with NMR and MS as detailed above. A third purification step was needed and this was achieved by column chromatography (petroleum ether: diethyl ether in a 5:1 ratio) at lowered temperature (5 °C). NMR and MS analyses

confirmed the purity of the compound, which had the following spectral characteristics:

PHYSICAL DATA

C₁₈H₂₃N; **IR (KBr)** ν_{\max} (Spectrum 5): 2944, 1458 cm^{-1} ; **MS** (EI, 70 eV) m/z (Spectrum 11): 253 (M^+), 224, 170, 162, 91, 65, 28; **¹H NMR** (300 MHz, CDCl₃) δ_{H} (spectrum 16): 7.396 – 7.094 (m, 5H, H-14, 15, 16, 17, 18), 3.769 – 3.565 (s, 2H, H-12a, 12b), 3.272 – 3.048 (m, 2H, H-3, 11), 2.882 – 2.687 (m, 2H, H-1, 2), 2.599 – 2.346 (m, 2H, H-6, 8), 2.004 – 1.467 (m, 8H, H-4a, 4b, 5a, 5b, 9a, 9b, 10a, 10b), 1.372 – 1.156 (m, 2H, H-7a, 7b); **¹³C NMR** (75 MHz, CDCl₃) δ_{C} (Spectrum 25, 26): 141.032 (s, 1C, C-13), 128.725 (d, 2C, C-14, 18), 127.842 (d, 2C, C-15, 17), 126.413 (d, 1C, C-16), 73.555 (d, 2C, C-3, 11), 58.523 (t, 1C, C-12), 54.470 (d, 2C, C-1, 2), 47.331 (d, 2C, C-6, 8), 37.463 (t, 1C, C-7), 34.495 (t, 2C, C-4, 10), 32.739 (t, 2C, C-5, 9).

3.5.5 N-CYCLOHEXYLMETHYL-3,11-AZATRICYCLO[6.3.0.0^{2,6}]-UNDECANE (LB-2)



CHEMICALS AND REAGENTS

Tricyclo[6.3.0.0 ^{2,6}]undecane-3,11-dione, (C ₁₁ H ₁₄ O ₂)	(178.23 g/mol)
Cyclohexylmethylamine, 98% (C ₇ H ₁₅ N)	(113.20 g/mol)
NaBH ₃ CN	(62.84 g/mol)

SYNTHETIC PROCEDURE

Tricyclo[6.3.0.0^{2,6}]undecane-3,11-dione (2.721 g, 0.0153 mol) was dissolved in anhydrous tetrahydrofuran (THF; 30 ml) and cooled down to 5 °C on an external ice bath. Cyclohexylmethylamine (1.7304 g, 0.0153 mol) was slowly added stoichiometrically while the mixture was stirred for approximately 6 hours at lowered temperatures. The reaction was constantly monitored on TLC and after 6 hours was still not completed. The reaction was then stirred at room temperature for an additional 41 hours while continuously monitoring on TLC. After 41 hours the reaction was heated for 2 hours under reflux. Evaluation on TLC showed that reaction was still not complete, but was stopped at this point to proceed to the next step. The carbinolamine did not precipitate and the reaction mixture had a light brown colour. Removing the solvent *in vacuo* resulted in a light brown oil. This product was dehydrated under Dean Stark conditions for approximately 1 hour using 100 ml anhydrous benzene. Benzene was removed *in vacuo* to produce the Schiff base (3-cyclohexylmethyliminotricyclo[6.3.0.0^{2,6}]undecane-11-one) in the form of a light brown oil. The resulting oil was dissolved in anhydrous methanol (20 ml) and anhydrous THF (75 ml). Reduction was carried out by adding NaBH₃CN (1 g, 0.0159 mol) in about 3× molar excess and stirring overnight (18 hours) at room temperature. The solvents were removed and the resulting light brown oil was suspended in approximately 50 ml of distilled water in a separation funnel. The product was extracted with dichloromethane (4 × 20 ml) and the combined dichloromethane fractions were washed with distilled water (2 × 50 ml). The organic phase was dried over anhydrous CaSO₄ and filtered. Subsequent *in vacuo* removal of the solvent resulted in the formation of a light brown oil which was purified with consecutive column chromatography sequences (Yield 0.106 g, 0.0004 mol, 2.67 %).

PURIFICATION

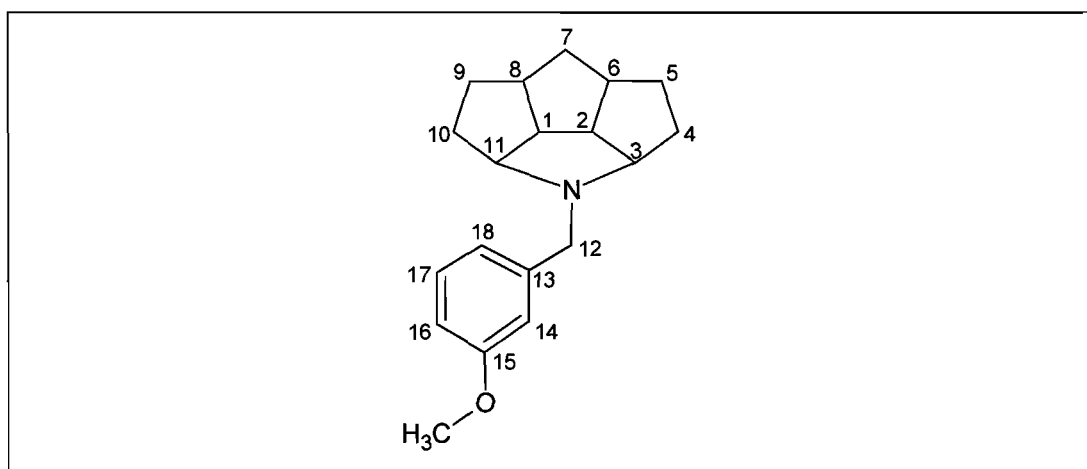
Purification of the product mixture was accomplished with consecutive column chromatography sequences. The first purification step utilized a mobile phase consisting of petroleum ether: chloroform: ethyl acetate in a 1:1:1 ratio. Fractions

were collected and analyzed by NMR and MS to ascertain fraction content and purity. Fractions containing the desired compound were identified and underwent further purification in cases where by-products were present. A second purification step was done by column chromatography (petroleum ether: tetrahydrofuran in a 5:1 ratio) at lowered temperature (5 °C). NMR and MS analyses confirmed the purity of the compound, which had the following spectral characteristics:

PHYSICAL DATA

$C_{18}H_{29}N$; IR (KBr) ν_{max} (In progress). 1H NMR (300 MHz, $CDCl_3$) δ_H (Spectrum 17): 3.652 – 3.370 (t, 2H, H-3, 11), 3.252 – 2.999 (t, 2H, H-1, 2), 2.950 – 2.638 (m, 2H, H-12a, 12b), 2.521 – 2.248 (m, 2H, H- 6, 8), 2.219 - 1.602 (m, 19H, H-4a, 4b, 5a, 5b, 9a, 9b, 10a, 10b, 13, 14a, 14b, 15a, 15b, 16a, 16b, 17a, 17b, 18a, 18b), 1.600 – 1.470 (m, 2H, H – 7a, 7b); ^{13}C NMR (75 MHz, $CDCl_3$) δ_C (Spectrum 27, 28): 63.077 (d, 2C, C-3, 11), 60.443 (d, 2C, C-1, 2), 47.398 (d, 2C, C-6, 8), 45.879 (d, 1C, C-13), 40.390 (t, 1C, C-12), 40.384 (t, 2C, C-15, 17), 39.509 (t, C, C-16), 37.222 (t, 2C, C-14, 18), 32.357 (t, 2C, C-4, 10), 32.134 (t, 2C, C-5, 9), 26.913 (t, 1C, C - 7).

3.5.6 N-(3-METHOXYBENZYL)-3,11-AZATRICYCLO[6.3.0.0^{2,6}]-UNDECANE (LB-3)



CHEMICALS AND REAGENTS

Tricyclo[6.3.0.0 ^{2,6}]undecane-3,11-dione, (C ₁₁ H ₁₄ O ₂)	(178.23 g/mol)
3-Methoxybenzylamine, 98% (C ₈ H ₁₁ NO)	(137.18 g/mol)
NaBH ₃ CN	(62.84 g/mol)

SYNTHETIC PROCEDURE

Tricyclo[6.3.0.0^{2,6}]undecane-3,11-dione (3.01 g, 0.0169 mol) was dissolved in anhydrous tetrahydrofuran (THF; 50 ml) and cooled down to 5 °C on an external ice bath. 3-Methoxybenzylamine (2.32 g, 0.0169 mol) was slowly added stoichiometrically while the mixture was stirred for approximately 6 hours at lowered temperature. Reaction was constantly monitored on TLC. The reaction was then stirred at room temperature for an additional 48 hours while continuously monitoring on TLC. After 48 hours the reaction was still not completed. Molecular sieves were added to the reaction mixture in an attempt to shift the reaction equilibrium and it was stirred for an additional 24 hours at room temperature. Evaluation on TLC showed that reaction was still not complete and the reaction was stopped at this point. The molecular sieves were filtered off and the solvent was removed *in vacuo* to yield a red/brown oil. This product was dehydrated under Dean Stark conditions for approximately 3 hour using 100 ml anhydrous benzene. Benzene was removed *in vacuo* to produce the Schiff base (3-methoxybenzyliminotricyclo[6.3.0.0^{2,6}]undecane-11-one) in the form of a red/brown oil. The resulting oil was dissolved in anhydrous methanol (20 ml) and anhydrous THF (80 ml). Reduction was carried out by adding NaBH₃CN (4 g, 0.0637 mol) in about 3× molar excess and stirring overnight (18 hours) at room temperature. The solvents were removed and the resulting red/brown oil was suspended in approximately 100 ml of distilled water in a separation funnel. The product was extracted with dichloromethane (4 × 50 ml) and the combined dichloromethane fractions were washed with distilled water (2 × 100 ml). The organic phase was dried over anhydrous CaSO₄ and filtered. Subsequent *in vacuo* removal of the solvent resulted in the formation of a red/brown oil which was purified with consecutive column chromatography sequences (Yield 0.4523 g, 0.002 mol, 9.46 %).

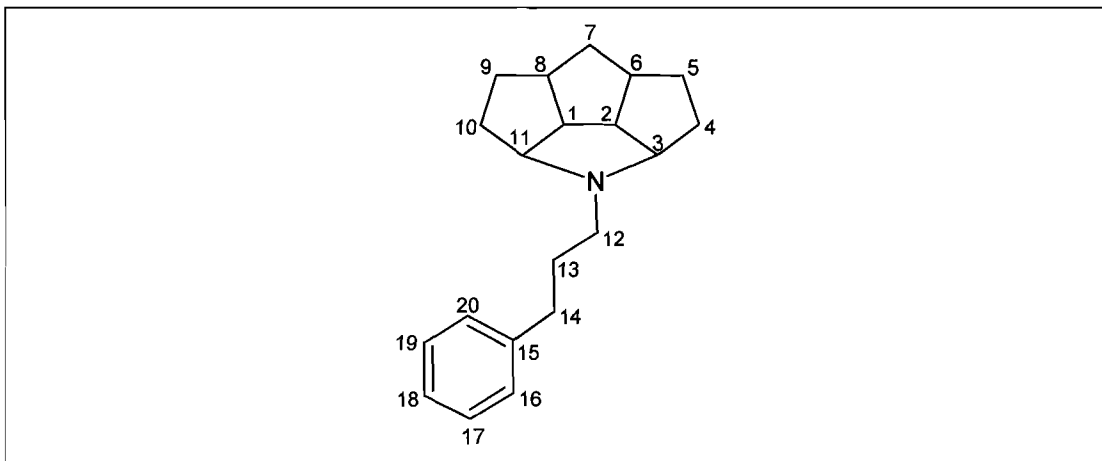
PURIFICATION

Purification of the product mixture was accomplished with consecutive column chromatography sequences. The first purification step utilized a mobile phase consisting of petroleum ether: chloroform: ethyl acetate in a 10:6:1 ratio. Fractions were collected and analyzed by NMR and MS to ascertain fraction content and purity. Fractions containing the desired compound were identified and underwent further purification in cases where by-products were present. A second purification step was needed and this was achieved by column chromatography [petroleum ether: tetrahydrofuran (THF) in a 5:1 ratio] at lowered temperature (5 °C). NMR and MS analyses confirmed the purity of the compound, which had the following spectral characteristics:

PHYSICAL DATA

C₁₉H₂₅NO; **IR (KBr)** ν_{\max} (Spectrum 6): 3424, 2944, 1611, 1270 cm^{-1} ; **MS** (EI, 70 eV) m/z (Spectrum 12): 283 (M^+), 254, 220, 205, 162, 122, 91, 57, 28; **¹H NMR** (300 MHz, CDCl₃) δ_{H} (Spectrum 18): 7.23 – 7.055 (t, 1H, H-17), 6.926-6.820 (m, 2H, H-14, 18), 6.800 – 6.577 (dd, 1H, H-16), 3.925 – 3.739 (s, 3H, OCH₃), 3.694 – 3.568 (s, 2H, H-12a, 12b), 3.301 – 3.048 (q, 2H, H-3, 11), 2.882-2.658 (m, 2H, H-1, 2), 2.619 – 2.346 (m, 2H, H-6, 8), 2.004 – 1.468 (m, 8H, H-4a, 4b, 5a, 5b, 9a, 9b, 10a, 10b), 1.344 – 1.156 (m, 2H, H-7a, 7b); **¹³C NMR** (75 MHz, CDCl₃) δ_{C} (Spectrum 29, 30): 159,383 (s, 1C, C-15), 142.990 (s, 1C, C-13), 128.748 (d, 1C, C-17), 120.923 (d, 1C, C-18), 114.052 (d, 1C, C-14), 111,933 (d, 1C, C-16), 73,731 (d, 2C, C-3, 11), 58.558 (t, 1C, C-12), 55.104 (q, 1C, OCH₃), 54.492 (d, 2C, C-1, 2), 47.342 (d, 2C, C-6, 8), 37.453 (t, 1C, C-7), 34.511 (t, 2C, C-4, 10), 32.787 (t, 2C, 5, 9).

3.5.7 N-(3-PHENYLPROPYL)-3,11-AZATRICYCLO[6.3.0.0^{2,6}]UNDECANE (LB-4)



CHEMICALS AND REAGENTS

Tricyclo[6.3.0.0 ^{2,6}]undecane-3,11-dione, (C ₁₁ H ₁₄ O ₂)	(178.23 g/mol)
3-Phenylpropylamine, 99% (C ₉ H ₁₃ N)	(135.21 g/mol)
NaBH ₃ CN	(62.84 g/mol)

SYNTHETIC PROCEDURE

Tricyclo[6.3.0.0^{2,6}]undecane-3,11-dione (3.44 g, 0.0193 mol) was dissolved in anhydrous tetrahydrofuran (THF; 50 ml) and cooled down to 5 °C on an external ice bath. Phenylpropylamine (2.613 g, 0.0193 mol) was slowly added stoichiometrically while the mixture was stirred for approximately 6 hours at reduced temperature. The reaction was stirred at room temperature for an additional 48 hours while continuously monitoring on TLC. After 48 hours the reaction was still not completed. The reaction pH was lowered to 6.29 from pH 9.41 with glacial acetic acid in an effort to obtain optimum reaction rate (McMurry, 1996). The reaction was then stirred at room temperature for a further 12 hours. TLC showed that reaction was still not complete but was stopped at this point to proceed to the next step. An extraction was done with dichloromethane and distilled water to remove the acid and any protonated amine present. Removal of the solvent *in vacuo* resulted in a dark brown oil. This product was dehydrated under Dean Stark conditions for approximately 3 hour using 100 ml anhydrous benzene. Benzene was removed *in vacuo* to produce the Schiff base

(3-phenylpropyliminotricyclo[6.3.0.0^{2,6}]undecane-11-one) in the form of a dark brown oil. The resulting oil was dissolved in anhydrous methanol (20 ml) and anhydrous THF (80 ml). Reduction was carried out by adding NaBH₃CN (4 g, 0.0637 mol) in about 3× molar excess and stirring overnight (18 hours) at room temperature. The solvents were removed and the resulting dark brown oil was suspended in approximately 50 ml of distilled water in separation funnel. The product was extracted with dichloromethane (4 × 50 ml) and the combined dichloromethane fractions were washed with distilled water (2 × 100 ml). The organic phase was dried over anhydrous CaSO₄ and filtered. Subsequent *in vacuo* removal of the solvent resulted in the formation of a dark brown oil which was purified with consecutive column and preparative plate chromatography sequences (Yield 0.1871 g, 0.0007 mol, 3.44 %).

PURIFICATION

Purification of the product mixture was accomplished with consecutive column, flash column and preparative plate chromatography sequences. The first purification step utilized a mobile phase consisting of ethyl acetate: ethanol in a 9:1 ratio. Fractions were collected and analyzed by NMR and MS to ascertain fraction content and purity. Fractions containing the desired compound were identified and underwent further purification in cases where by-products were present. A second purification step was performed by flash column chromatography (petroleum ether: diethyl ether in a 3:1 ratio) at lowered temperatures (5 °C), and the product mixture eluted at 4 ml/min. Again, fractions were analyzed with NMR and MS as detailed above. The third purification step was achieved by column chromatography at lowered temperature (5 °C), with mobile phase dichloromethane. Again, fractions were analyzed as above. A fourth purification step was needed and this was achieved by preparative thin-layer chromatography utilizing dichloromethane: petroleum ether in a 9:1 ratio as mobile phase. NMR and MS analyses assessed the purity of the compound and although the compound was found not to be completely pure we decided to utilise the semi-pure product obtained since further attempts at

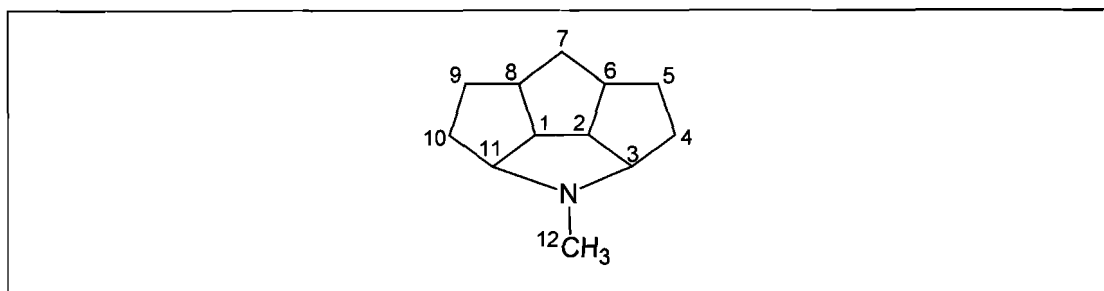
Selection and synthesis of relevant compounds

purifications were unsuccessful and spectral data did not improve. The compound had the following spectral characteristics:

PHYSICAL DATA

$C_{20}H_{27}N$; IR (KBr) ν_{max} (Spectrum 7): 2944, 1444 cm^{-1} ; MS (EI, 70 eV) m/z (In progress). 1H NMR (300 MHz, $CDCl_3$) δ_H (Spectrum 19): 7.367 – 7.077 (m, 5H, H-15, 16, 17, 18, 19, 20), 3.404-3.270 (m, 2H, H-1, 2), 3.254 – 3.138 (t, 2H, H-3, 11), 3.012 – 2.427 (m, 6H, H-6, 8, 13a, 13b, 14a, 14b), 2.194 – 2.056 (m, 2H, H-12a, 12b), 1.991 – 1.623 (m, 8H, H-4a, 4b, 5a,5b, 9a, 9b, 10a, 10b), 1.556-1.388 (m, 2H, H-7a, 7b). ^{13}C NMR (75 MHz, $CDCl_3$) δ_C (Spectrum 31, 32): 141,904 (s, 1C, C-15), 128.341 (d, 2C, C-16, 20), 125.807 (d, 2C, C-17, 19), 73.113 (d, 1C, C-18), 61,731 (d, 2C, C-3, 11), 53,553 (d, 2C, C-1, 2), 51.054 (t, 1C, C-12), 47.105 (d, 2C, C-6, 8), 40.261 (t, 1C, C-14), 37.071 (t, 1C, C-7), 34.350 (t, 1C, C-13), 33.826 (t, 2C, C-4, 10), 32.616 (t, 2C, C-5, 9).

3.5.8 N-METHYL-3,11-AZATRICYCLO[6.3.0.0^{2,6}]UNDECANE (LB-5)



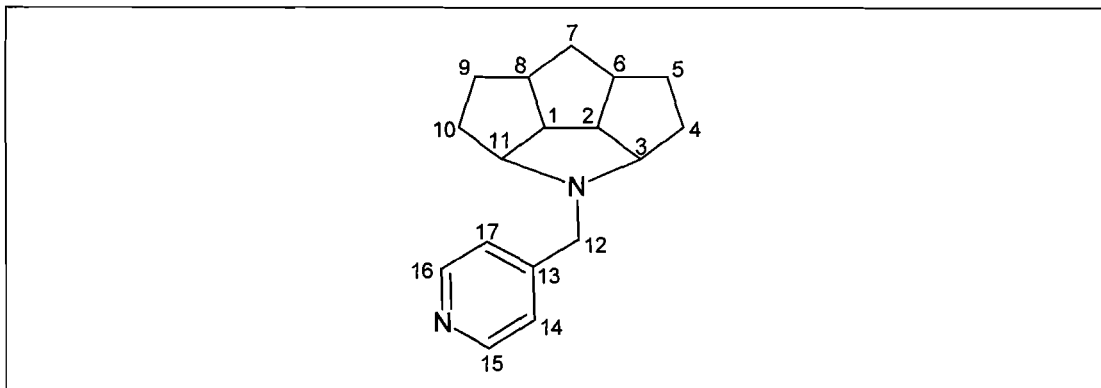
CHEMICALS AND REAGENTS

Tricyclo[6.3.0.0 ^{2,6}]undecane-3,11-dione, ($C_{11}H_{14}O_2$)	(178.23 g/mol)
Methylamine, 33% in absolute ethyl alcohol (CH_5N)	(31.06 g/mol)
$NaBH_3CN$	(62.84 g/mol)

SYNTHETIC PROCEDURE

Tricyclo[6.3.0.0^{2,6}]undecane-3,11-dione (3.89 g, 0.0219 mol) was dissolved in anhydrous tetrahydrofuran (THF; 70 ml) and cooled down to 5 °C on an external ice bath. Methylamine (1.555 g, 0.0219 mol) was slowly added in a stoichiometric amount while the mixture was stirred for approximately 6 hours at lowered temperatures. The reaction flask was closed tightly for methyl amine is very volatile with its point of flight at -18 °C. Reaction was continuously monitored on TLC and after 6 hours the reaction was still not completed as the unreacted tricyclo[6.3.0.0^{2,6}]undecane-3,11-dione was still present in reaction mixture. Molecular sieves were added and the reaction was stirred at room temperature for an additional 19 hours while continuously monitoring on TLC. The reaction required heating under reflux for an additional 45 hours. The reflux condenser was connected to a low temperature circulating bath that was set to 5 °C because of the volatility of methylamine. After 45 hours, evaluation on TLC showed that reaction was still not complete and was stopped at this point to proceed to the next step. The carbinolamine did not precipitate and reaction mixture had a light brown colour. Removing the solvent *in vacuo* yielded a light brown oil. This product was dehydrated under Dean Stark conditions for approximately 3 hour using 100 ml anhydrous benzene. Benzene was removed *in vacuo* to produce the Schiff base (3-methyliminotricyclo[6.3.0.0^{2,6}]undecane-11-one) in the form of a light yellow oil. The resulting oil was dissolved in anhydrous methanol (20 ml) and anhydrous THF (80 ml). Reduction was carried out by adding NaBH₃CN (4.2 g, 0.067 mol) in molar excess and stirring overnight (18 hours) at room temperature. The solvents were removed and the resulting light yellow oil was suspended in approximately 100 ml of distilled water in a separation funnel. The product was extracted with dichloromethane (4 × 50 ml) and the combined dichloromethane fractions were washed with distilled water (2 × 100 ml). The organic phase was dried over anhydrous CaSO₄ and filtered. Subsequent *in vacuo* removal of the solvent resulted in the formation of a light yellow oil. Isolation of the compound was not successful. Section 3.7 investigates this observation by using computational chemistry.

3.5.9 N-(1-PIPERIDINYL)-3,11-AZATRICYCLO[6.3.0.0^{2,6}]UNDECANE
(LB-6)



CHEMICALS AND REAGENTS

Tricyclo[6.3.0.0 ^{2,6}]undecane-3,11-dione, (C ₁₁ H ₁₄ O ₂)	(178.23 g/mol)
Pyridinylamine, 95% (C ₆ H ₈ N ₂)	(108.14 g/mol)
NaBH ₃ CN	(62.84 g/mol)

SYNTHETIC PROCEDURE

Tricyclo[6.3.0.0^{2,6}]undecane-3,11-dione (3.87 g, 0.0217 mol) was dissolved in anhydrous tetrahydrofuran (THF; 70 ml) and cooled down to 5 °C on an external ice bath. Pyridinylamine (2.351 g, 0.0217 mol) was slowly added stoichiometrically while the mixture was stirred for approximately 6 hours at lowered temperature. The reaction was monitored on TLC. Molecular sieves were added in an attempt to shift the reaction equilibrium. The reaction was stirred at room temperature for an additional 18 hours and then heated for 45 hours under reflux. Evaluation on TLC showed that reaction was still not complete and was stopped to proceed to the next step. The carbinolamine did not precipitate and the reaction mixture had a light brown colour. The molecular sieves were filtered off and solvent was removed *in vacuo* to yield a light brown oil. This product was dehydrated under Dean Stark conditions for approximately 3 hour using 100 ml anhydrous benzene. Benzene was removed *in vacuo* to produce the Schiff base (3-piperidinyliminotricyclo[6.3.0.0^{2,6}]undecane-11-one) in the form of a dark brown oil. The resulting oil was dissolved in anhydrous

Selection and synthesis of relevant compounds

methanol (20 ml) and anhydrous THF (80 ml). Reduction was carried out by adding NaBH₃CN (4.099 g, 0.065 mol) in molar excess and stirring overnight (18 hours) at room temperature. The solvents were removed and the resulting dark brown oil was suspended in approximately 100 ml of distilled water in separation funnel. The product was extracted with dichloromethane (4 × 50 ml) and the combined dichloromethane fractions were washed with distilled water (2 × 100 ml). The organic phase was dried over anhydrous CaSO₄ and filtered. Subsequent *in vacuo* removal of the solvent resulted in the formation of a dark red/brown oil which was purified with consecutive column chromatography sequences (Yield 0.22 g, 0.00009 mol, 0.40 %).

PURIFICATION

Purification of the product mixture was accomplished with consecutive column and preparative thin-layer chromatography sequences. The first purification step utilized a mobile phase diethyl ether. Fractions were collected and analyzed by NMR and MS to ascertain fraction content and purity. Fractions containing the desired compound were identified and underwent further purification in cases where by-products were present. A second purification step was done by preparative thin-layer chromatography utilizing ethyl acetate as mobile phase. Again, fractions were analyzed with NMR and MS as detailed above. A third purification step was needed and this was achieved by preparative thin-layer chromatography with C-18 absorbent layer for further separation could not be achieved on silica. Methanol: acetonitrile in a 2:1 ratio were utilized as mobile phase. NMR and MS analyses assessed the purity of the compound and although the compound was found not to be completely pure we decided to utilise the semi-pure product obtained since further attempts at purifications were unsuccessful and spectral data did not improve. The compound had the following spectral characteristics:

PHYSICAL DATA

C₁₇H₂₂N₂; IR (KBr) ν_{\max} (Spectrum 8): 3389, 2944, 1611 cm⁻¹; MS (EI, 70 eV) *m/z* (Spectrum 13): 254 (M⁺), 225, 180, 162, 120, 91, 67, 41, 28; ¹H NMR (300 MHz,

CDCl₃) δ_{H} (Spectrum 20): 8.732 – 7.065 (dd, 4H, H-14, 15, 16, 17), 3.740-3.516 (s, 2H, H-12), 3.231 – 3.120 (m, 2H, H-3, 11), 2.861 – 2.674 (m, 2H, H-1, 2), 2.663 – 2.400 (m, 2H, H-6, 8), 2.123 – 1.611 (m, 8H, H-4a, 4b, 5a, 5b, 9a, 9b, 10a, 10b), 1.565-1.405 (m, 2H, H-7a, 7b); ^{13}C NMR (75 MHz, CDCl₃) δ_{C} (Spectrum 33, 34): 151,000 (s, 1C, C-13), 149.401 (d, 2C, C-15, 16), 122.800 (d, 2C, C-14, 17), 74.327 (d, 2C, C-3, 11), 58.053 (t, 1C, C-12), 54.566 (d, 2C, C-1, 2), 47,275 (d, 2C, C-6, 8), 37,358 (t, 1C, C-7), 34.574 (t, 2C, C-4, 10), 32.697 (t, 2C, C-5, 9).

3.6 CONCLUSION

Synthesis of all the compounds resulted in very low ultimate yields, varying between 0.4% and 13.27%. These low yields could result from the inability to complete any of the reactions, formation of various possible by-products during the synthetic procedure as well as inadequate purification of product mixture during column chromatography. We found the purification process to be exceptionally difficult because of the by-products that formed during the reaction. Purification was further complicated owing to the products being oils and not crystalline. Yields could be improved through optimisation of synthetic procedures and purification techniques.

3.7 COMPUTATIONAL STUDY

3.7.1 PROBLEM STATEMENT

Reductive amination of ketones is an important synthetic route for the preparation of bioactive molecules in medicinal chemistry (Godoy-Alcantar *et al.*, 2005). In its simplest form, condensation of a ketone with an amine leads to the formation of an imine, which can be reduced by the addition of a diversity of hydride reducing agents (Marchand *et al.*, 1988) to yield a corresponding azatetraquinane.

Selection and synthesis of relevant compounds

During our synthetic efforts, we discovered that we were unable to isolate a methylamine derivative *N*-methyl-3,11-azatricyclo[6.3.0.0^{2,6}]undecane (Fig. 3.7, **61**), yet the synthesis of the comparable benzylamine derivative *N*-benzyl-3,11-azatricyclo[6.3.0.0^{2,6}]undecane (Fig. 3.7, **60**) proceeded in a facile way through reductive amination. We therefore initiated a computational study in an effort to explain the apparent selectivity in the formation of products derived from the reductive amination of triquinanes with benzylamine, compared with methylamine.

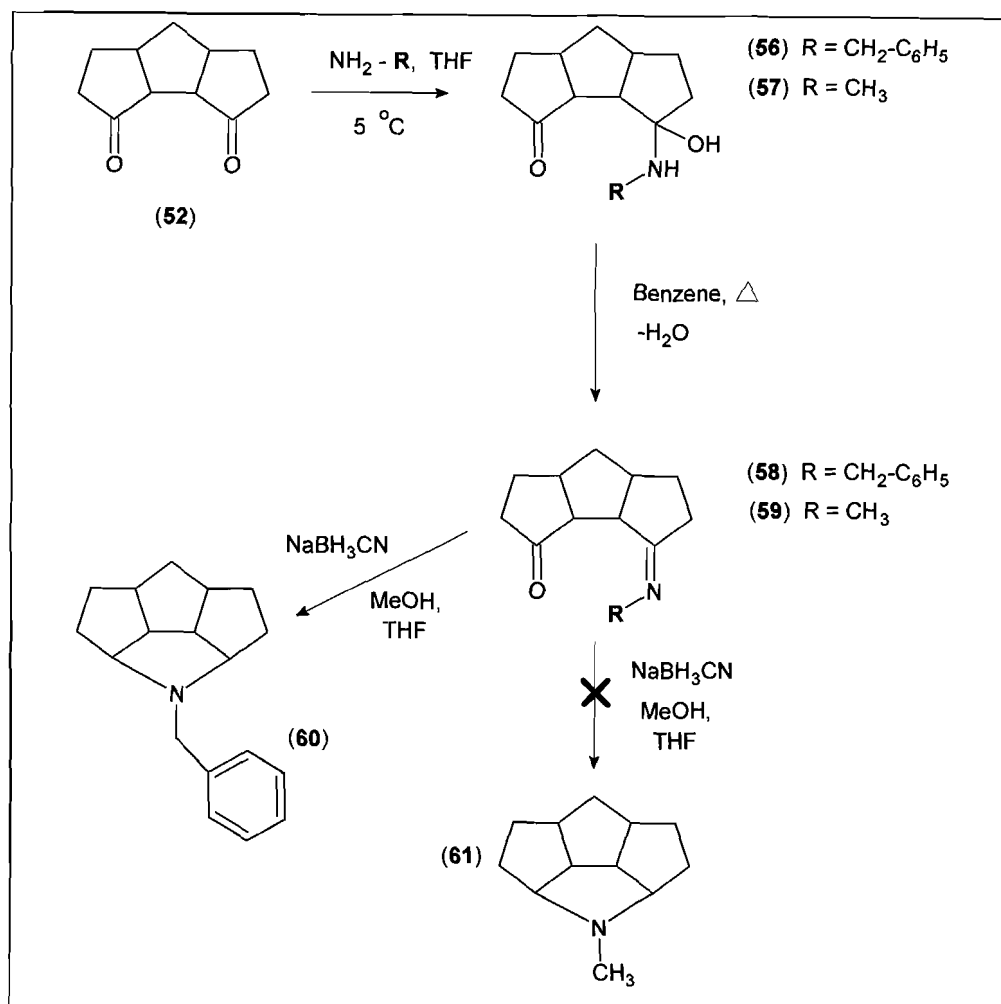


Figure 3.7: Reductive amination of the *cis-syn-cis* triquinyl-dione system described in the text.

Figure 3.7 shows the synthetic route to prepare the molecules of interest. Amination of carbonyl carbon on the triquinane (**52**) initially leads to the formation of the

Selection and synthesis of relevant compounds

triquinolamines (**56**, **57**). Dehydration under Dean-Stark conditions, leads to the formation of the monoimine intermediates (**58**, **59**) which are then reduced and cyclised in one step with sodium cyanoborohydride to yield the expected corresponding aza-triquinylamines (**60**, **61**).

3.7.2 COMPUTATIONAL CALCULATIONS

Ab initio and semi-empirical calculations were performed using the SPARTAN '04 program (Wavefunction Inc., 18401 Von Karman Avenue, Suite 370 Irvine, CA 92612). Semi-empirical calculations were carried out *in vacuo* with AM1, while the *ab initio* Hartree-Fock calculations were performed using the 6-31G* basis set, with density functional theory (DFT) theory applied with the B3LYP functional and 6-31G* basis sets.

3.7.3 RESULTS

The starting triquinane as well as the intermediate structures were geometry optimized using semi-empirical AM1, and with *ab initio* level HF 6-31G* as well as DFT B3LYP/6-31G*. The resulting energies (kcal/mol) are shown in table 3.2.

Table 3.2: Calculated energies (kcal/mol) for the compounds shown in figure 3.7.

Compound	AM1	HF	DFT
52	-92.55	-360466	-362728
Benzylamine	19.37	-203789	-205136
Methylamine	-7.38	-59745	-60148
56	-74.27	-564255	-567868
57	-100.87	-420211	-398217
58	-14.84	-516545	-519908
59	-42.60	-372502	-374920
60	9.13	-470301	-473466
61	-19.48	-326257	-328479

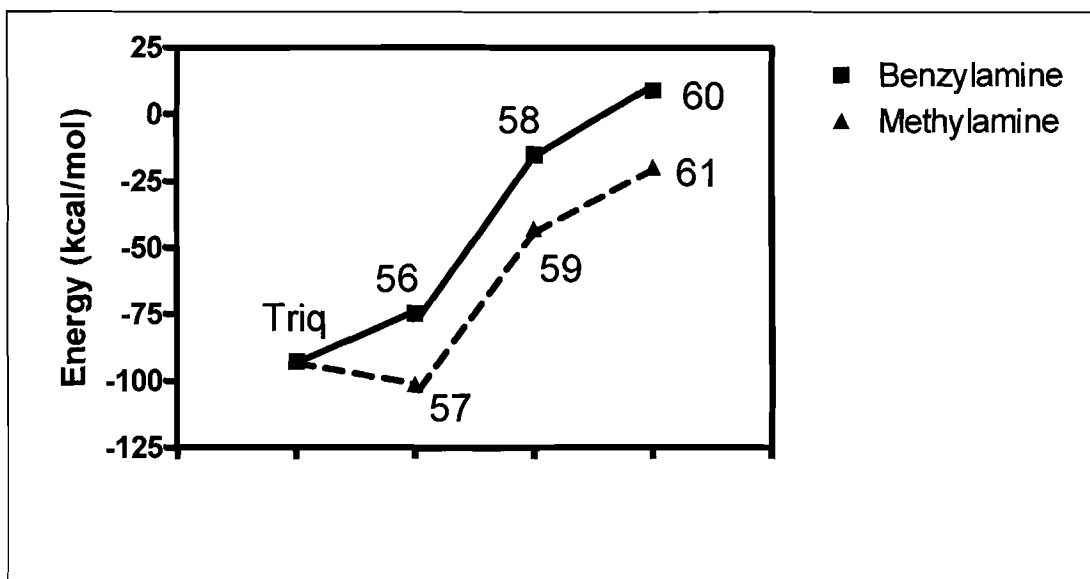


Figure 3.8: Energy profile of the reaction between benzylamine-triquinane (**56** and **58**) and methylamine-triquinane (**57** and **59**). Semi-empirical AM1 calculations were used. Compound numbers refer those listed in figure 3.7, and energies to those listed in table 3.2, Triq = triquinane.

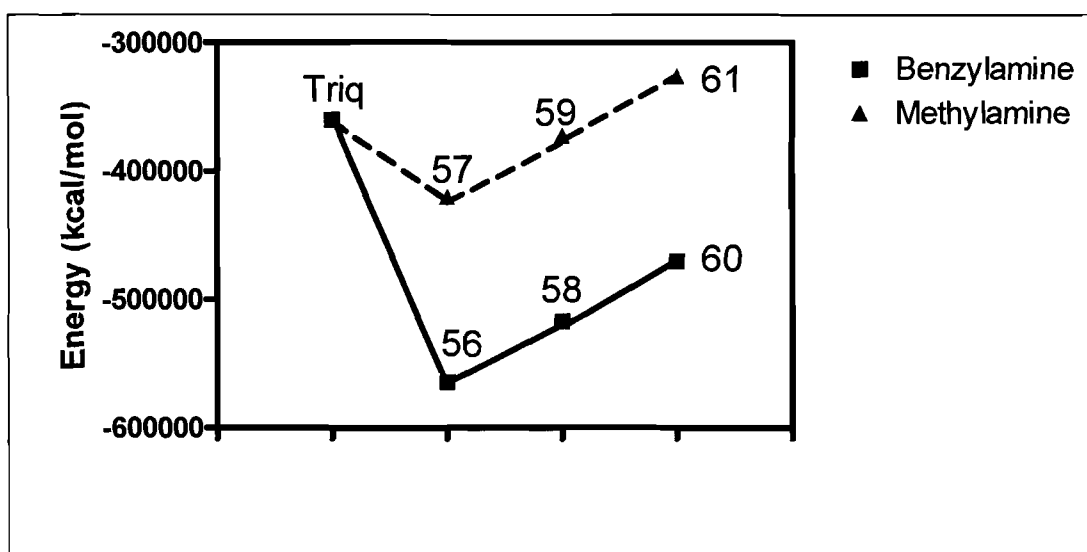


Figure 3.9: Energy profile of the reaction between benzylamine-triquinane (**56** and **58**) and methylamine-triquinane (**57** and **59**). HF 6-31G* calculations were used. Compound numbers refer those listed in figure 3.7, and energies to those listed in table 3.2, Triq = triquinane.

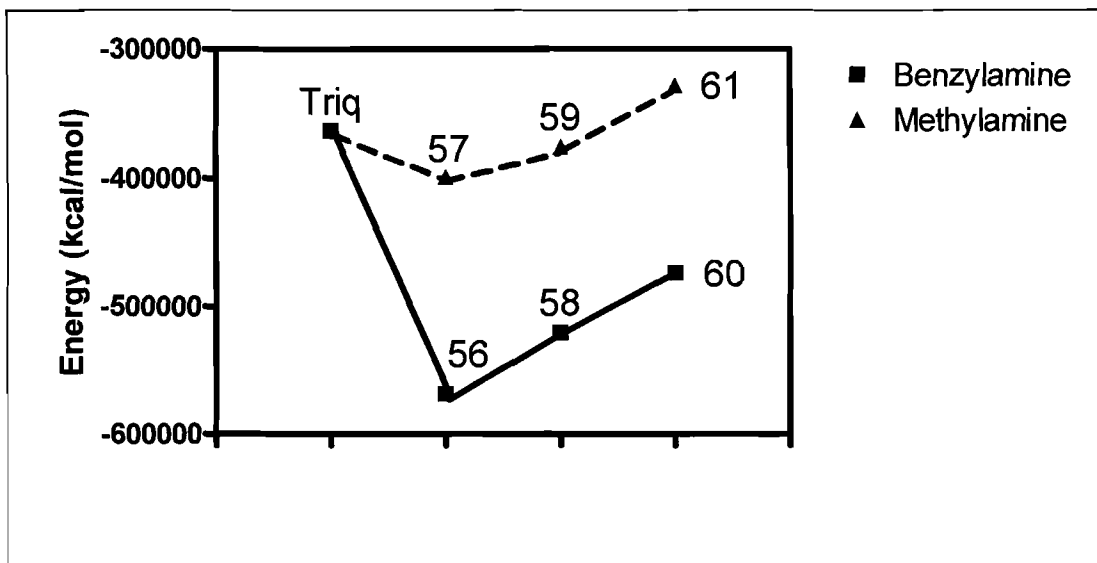


Figure 3.10: Energy profile of the reaction of benzylamine-triquinane (**56** and **58**) and methylamine-triquinane (**57** and **59**). DFT BLYP/6-31G* calculations were used. Compound numbers refer those listed in figure 3.7, and energies to those listed in table 3.2, Triq = triquinane.

As can be seen from the energy profiles of the reaction (Fig. 3.8-3.10), AM1 calculations predicted the formation of **61** to be favoured over **60**. In contrast, both *ab initio* approaches suggest that the formation of **60** will be favoured experimentally. Both HF and DFT calculations showed a much lower energy for the benzylamine reaction than for the methylamine reaction. In both cases, the energy of **60** is lower by approximately 100,000 kcal/mol compared with the energy of the starting triquinane (**52**), while in contrast, the end product **61** has a slightly higher energy than the starting triquinane (**52**), as seen in figure 3.9 (HF) and figure 3.10 (DFT). This may account for the absence of formation of **61** in our syntheses. The ΔE for the formation of **57** is calculated to be 0.435 kcal/mol, while for **59** the ΔE is 0.835 kcal/mol, suggesting that higher activation energy is required for the formation of **59** compared with **57**.

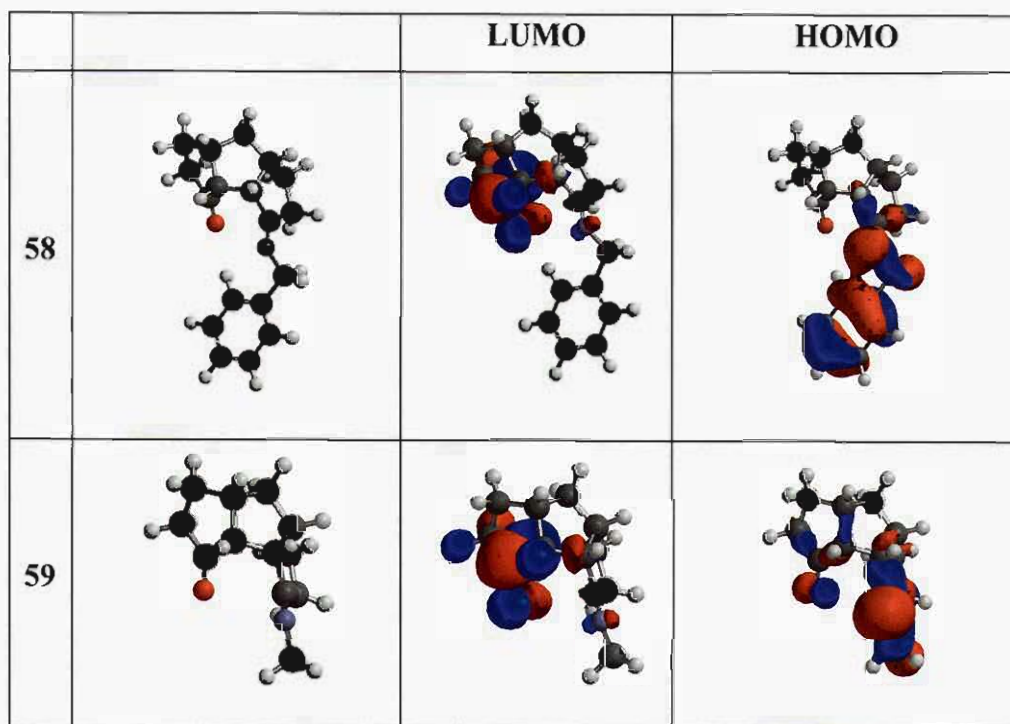


Figure 3.11: HOMO and LUMO orbitals for compounds **58** and **59**, calculated with DFT.

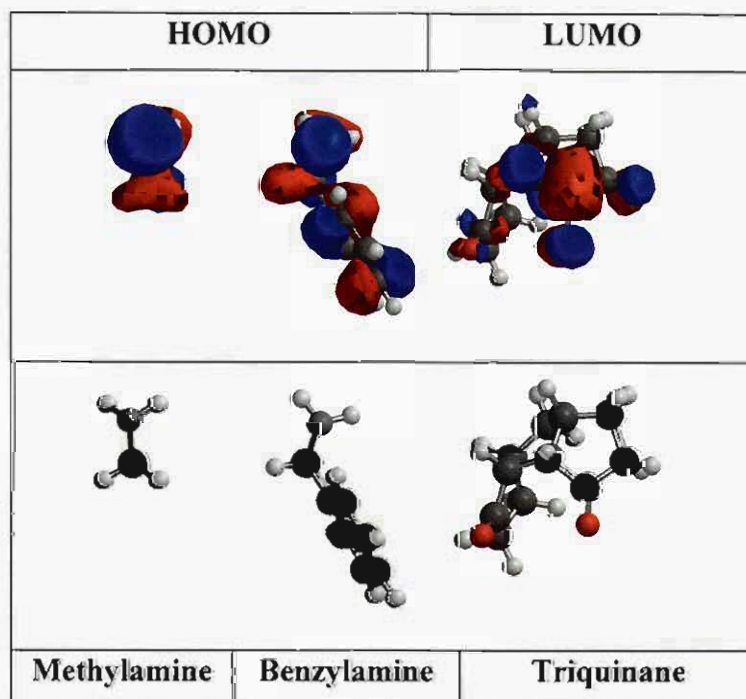


Figure 3.12: HOMO and LUMO orbitals for the starting compounds used in the reductive amination, calculated with DFT.

Frontier molecular orbital theory (FMO) has been shown to be a helpful tool in understanding chemical reactions (Silva *et al.*, 2003). The DFT level of theory has been found to give satisfactory results in pericyclic reactions, as well as Diels-Alder reactions and was therefore chosen for the FMO evaluations (Silva *et al.*, 2003). However, the amination reaction between the respective amines and a carbonyl group of the triquinane dione, cannot be satisfactorily explained by FMO. As seen in figure 3.11, both amines shown have HOMO orbitals that are capable of interacting with the LUMO orbital in the triquinane. In the benzylamine case, however, the HOMO orbital may be able to interact more effectively with a LUMO orbital. This slight advantage may not offer a sufficient argument to explain the formation of the more stable **56** instead of **57**. On the other hand, inspection of the HOMO and LUMO orbitals of **58** and **59** respectively (Fig. 3.12), shows that a small HOMO orbital is located on the carbonylic oxygen of **59**, while none is seen in **58**. Since the measure of the potential strength of a covalent bond is dependent on the difference between HOMO and LUMO energies (Godoy-Alcantar *et al.*, 2005), the lower energy for the formation of **60**, and not **61**, may in part be explained by the HOMO and LUMO locations on the intermediates **58** and **59**.

3.7.4 CONCLUSIONS

This computational study was initiated to investigate the experimental formation of N-benzyl-3,11-azatricyclo[6.3.0.0^{2,6}]undecane (**60**) in preference to that of the methyl derivative (**61**), which could not be isolated. Semi-empirical calculations at the AM1 level incorrectly predicted the formation of **61** as opposed to **60**, while *ab initio* HF calculations and DFT correctly predicted the preference of formation of **60** with a significantly lower energy assigned than for **61**. FMO analysis suggests that a stronger HOMO-LUMO overlap may occur for **58** than for **59**, which may further account for the preferential formation of **60** over **61**. These findings may be useful in optimizing the reductive amination of triquinanes derivatives as pharmacologically interesting molecules and present possibilities for future studies.

CHAPTER 4

BIOLOGICAL EVALUATION

SUMMARY

The fluorescent ratiometric indicator, Mag-Fura-2/AM, and a real-time fluorescence microscope system were used to evaluate the influence of the test compounds on calcium homeostasis *via* VGCC in the N₂α mouse neuroblastoma cell line. Radioligand binding studies were also performed to evaluate the displacement of [³H]MK-801 from murine synaptoneurosomes in the presence and absence of the triquinylamine derivatives. The radioligand binding studies evaluate whether these compounds compete with MK-801 for the PCP binding site to establish their mechanism of action on the NMDA receptor.

ABBREVIATIONS

AM	Acetoxymethyl ester
ANOVA	Analysis of variance
BSA	Bovine serum albumin
CNS	Central nervous system
DMEM	Dulbecco's modified eagle's medium
DMSO	Dimethylsulphoxide
HBSS	Hanks balanced salt solution
HEPES	<i>N</i> -2-Hydroxyethylpiperazine- <i>N'</i> -2-ethanesulphonic acid
Mag-Fura-2/AM	2-[5-[2-[(acetyloxy)methoxy]-2-oxoethoxy]-6-[bis[2-[(acetyloxy)methoxy]-2-oxoethyl]amino]-2-benzofuranyl]- (acetyloxy)methyl ester
MK-801	Dizocilpine
NMDA	N-methyl-D-aspartate

PCP	Phencyclidine
ROI	Region of interest
SEM	Standard error of mean
TCP	N-(1-[2-thienyl]cyclohexyl)3,4-piperidine
VGCC	Voltage gated calcium channels
UV	Ultra-violet

4.1 EVALUATION OF CALCIUM HOMEOSTASIS

4.1.1 INTRODUCTION

The ratiometric fluorescent probe, Mag-Fura-2/AM, was selected for this study. This fluorescent indicator belongs to the low Ca^{2+} affinity class of Ca^{2+} indicators which are particularly useful for Ca^{2+} measurements because of their high K_d values. For example, these indicators are used for measurements of rapid changes of $[\text{Ca}^{2+}]$ as well as measuring very high Ca^{2+} levels in internal compartments. Although Mag-Fura-2/AM was initially developed as an indicator to monitor the cytosolic Mg^{2+} concentration, it can also successfully be used as a Ca^{2+} indicator, for the reason that the Mg^{2+} reaction during depolarisation is two to three orders of magnitude slower and smaller than the Ca^{2+} reaction (Takahashi *et al.*, 1999). Mag-Fura-2/AM is a UV-excited Ca^{2+} indicator that allows ratiometric measurement. This indicator undergoes a shift in absorption rather than the emission peak. The maximal absorption peaks are 335 and 363 nm at maximal and minimal $[\text{Ca}^{2+}]$, respectively, and the emission peak of both Ca^{2+} -bound and Ca^{2+} -free forms is 500 nm. For ratiometric measurements, excitation at 340 and 380 nm is usually preferred, because the absorption peak of Ca^{2+} -free Mag-Fura-2/AM is quite close to its isosbestic point, and the Ca^{2+} -free form emits more than the Ca^{2+} -bound form when excited by wavelengths longer than 370 nm (Grynkiewicz *et al.*, 1985). Cells, pre-treated with Mag-fura-2/AM and our test compounds, were exposed to a 140 mM KCl solution in order to induce membrane depolarisation and changes in the calcium flux were visualised employing fluorescence microscopy.

In order to support the hypothesis that the pentacycloundecane skeleton serves only as a bulk contributor for the biological activity of these polycyclic classes of compounds (Liebenberg, 2000 and Malan, 2000), two pentacycloundecanes (**H2** and **H3**, figure 4.1) with similar structures were tested in addition to the triquinylamines to allow for direct comparison. NGP1-01, also a pentacycloundecylamine, was included in this study as a reference compound due to the fact that this compound has been extensively studied and established as a voltage gated calcium channel blocker by Van der Schyf *et al.* (1986).

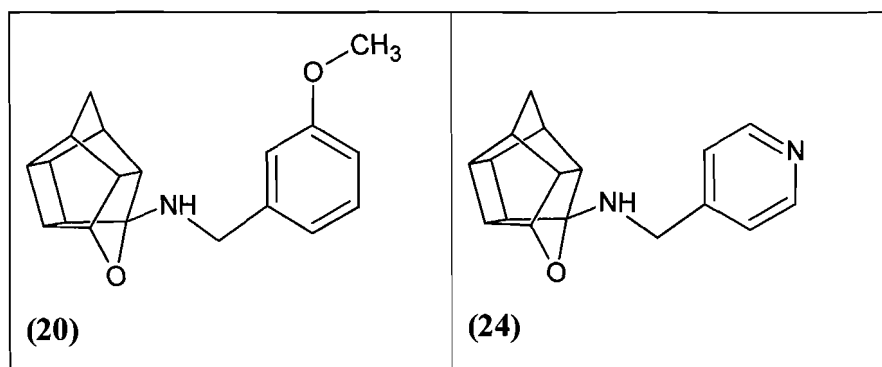


Figure 4.1: Pentacycloundecanes (**20**) **H3** or 8-(3-methoxybenzylamino)-8,11-pentacyclo[5.4.0.0^{2,6}.0^{3,10}.0^{5,9}]undecane and (**24**) **H2** or 8-[(4-aminomethyl)pyridine]-8,11-pentacyclo[5.4.0.0^{2,6}.0^{3,10}.0^{5,9}]undecane, tested in addition to the triquinylamines.

4.1.2 MATERIALS AND METHODS

Procedures similar to those of published studies were used to prepare the cell cultures, cell loading and other solutions and to establish the techniques for experimental measurement of fluorescence (Crawley *et al.*, 1997; Morgan *et al.*, 1999; Morgan and Thomas, 1999; Stout and Reynolds, 1999; Takahashi *et al.*, 1999 and Grobler, 2005)

4.1.2.1 Cell cultures

Mouse N₂α neuroblastoma cells [Obtained from American Type Culture Collection (ATCC), catalogue number CCL-131] were used in this study. Cloned Neuro-2α cells

were established by R.J. Klebe and F.H. Ruddle from a spontaneous tumour of a strain A albino mouse. Cells were maintained in DMEM-F12 in a 1:1 ratio, containing 10% foetal bovine serum, 100 units penicillin/ml, 100 µg streptomycin/ml, 0.25 µg fungizone/ml and 1 mM glutamine. The cells were incubated at 37 °C in a 5% CO₂ and 95% O₂ humidified atmosphere.

Cells duplicated once every 48 hours and, when 95% confluency was reached, were sub cultivated at a ratio of 3:1. Confluent cells were detached from the flask bottom by means of trypsinisation (incubation with trypsin/versine for approximately 5-7 minutes) and seeded in new 75 mm² flasks at a density of 1/3 confluency.

4.1.2.2 Solutions

The acetoxymethyl ester (AM) derivative of Mag-fura-2, and Pluronic F-127 as a 20% solution in anhydrous DMSO, were obtained from Invitrogen (USA). Hanks balanced salt solution (HBSS), purchased from Fisher Scientific (USA) were use for cell loading and washing. Buffer constituents were obtained from commercial sources.

Fluorescent indicator stock solution (1 mM): 50 µl anhydrous DMSO/Pluronic F-127 were added to 50 µg of the calcium indicator (Mag-fura-2/AM). Pluronic F-127 are often used to facilitate cell loading and is a non-ionic dispersing agent that helps solubilise large dye molecules in physiological media. The solution was then vortexed to properly disperse fluorescent dye and covered with aluminium foil to protect from light.

Loading solution: 17.5 µl of the fluorescent indicator stock solution was dispersed in 3.5 ml HBSS to which 10% (17.5 mg) bovine serum albumin (BSA) was added. Solutions were vortexed to help disperse the indicator in the HBSS solution. The final concentration of the fluorescent indicator was 5 µM. The solution was protected from light, and only freshly made solution was used to load neurons.

Test compound loading solution: 0.1 M stock solution was prepared by dissolving the compound to be tested in anhydrous DMSO. The loading solution was prepared by diluting 1 μ l of stock solution in 1 ml of HBSS to give a 100 μ M concentration of the test compound (final concentration DMSO in incubations = 0.1%).

The depolarizing solutions: This solution was used for stimulation and comprised of 5.4 mM NaCl, 140 mM KCl, 10 mM NaHCO₃, 0.6 mM KH₂PO₄, 0.6 mM Na₂HPO₄, 1.4 mM CaCl₂, 0.9 mM MgSO₄, 5.5 mM Glucose, and 20 mM HEPES and pH was adjusted to 7.4 with NaOH.

4.1.2.3 Loading cells with calcium-sensitive fluorescent indicator

N₂ α cell monolayer was attached at less than 50% confluence to 22-mm diameter, circular no. 1 glass cover slips, coated with rat tail collagen Type 1, from BioCoat (Fisher Scientific, USA). The glass cover slips were incubated overnight in 6 well plates to allow adherence before dye loading commenced. Before dye loading, the cell media was aspirated and the cover slips were washed twice with Hanks balanced salt solution (HBSS) preheated to 37 °C. Culture medium containing serum should not be used during staining, as serum can contain esterase activity that would hydrolyze the acetoxymethyl ester (AM) derivative of Mag-fura-2. Subsequently, cells were maintained in HBSS until use and those that were not used were discarded. If incubated for use the next day, we found that cells were too confluent and led to insufficient dye loading.

The dye loading solution was prepared just before use to prevent hydrolysis due to the unstable nature of Mag-fura-2/AM. The work was also performed in a dark room at all times to prevent photodecomposition of the photolabile dye solution. Three cover slips were loaded simultaneously by aspirating the HBSS in which the neurons were sustained and replacing it with 1 ml of loading solution per dish. The cover slips were incubated for 30 minutes at 37 °C in a 5% CO₂ and 95% O₂ humidified atmosphere. The exact indicator concentration, incubation time, and temperature will differ for different types of neurons. Adjustment of these variables should be done to optimize for the dynamic response to stimulation, and to limit sequestration of the indicator

into intracellular compartments. We found that no more than three cover slips should be loaded at a time and that they should be used within an hour after loading to prevent compartmentalization and dye leakage. After the loading period the loading solution was removed and cells were gently washed (twice) with HBSS (37 °C) to remove excess fluorescent indicator. Cells were then incubated in 2 ml HBSS for 20-30 minutes after loading to facilitate complete de-esterification. If cells were to be loaded with compounds it was done 20 minutes into de-esterification incubation time. This still allowed an adequate amount of time for full de-esterification. After 20 minutes the HBSS was aspirated and 1 ml of the prepared test compound loading solution was added. The cover slip was incubated for 10 minutes and used immediately after incubation. Each compound was incubated just before use and the controls were incubated with 0.1% DMSO.

4.1.2.4 Experimental single-cell recording

Mag-Fura-2/AM was used for imaging studies in single cells and all experiments were conducted at room temperature. Glass cover slips were mounted in a recording chamber and the compound loading solution was added to the recording chamber. The recording chamber were placed on the stage of an Olympus IX70 (Olympus America, Center Valley, PA, USA) inverted microscope. For each experiment, to initiate depolarization, 35 µl from a 4 M stock of the depolarizing solution was manually applied into the chamber with a micropipette after approximately 20 sec. Addition was done at the side of the chamber, taking care not to disturb the surface that would consequently create a disturbance in the optical effect. A time series of 120 sec was recorded with a 3,000 ms delay between each image set. Excitation wavelengths of Mag-Fura-2/AM were at 340 and 380 nm, and emission light was detected at 510 nm. Illumination was *via* a Spectra-MASTER monochromator (Perkin Elmer) with a 100 W Xenon arc lamp, coupled to a microscope fitted with a 40×/1.35 oil-immersion objective. The images were recorded on an OlymPix CCD camera, and image processing and analyses were performed using the supplied MERLIN Olympus system software. In each experiment 6 single neurons in the microscopic field were analyzed and experiments were repeated at least 3 times in neuronal preparations from different cultures. Control experiments, conducted in the absence of test compounds, comprised of 10 minute incubation with 0.1% DMSO in test compound loading

solution followed by the application of depolarizing solution in a similar method as described for experiments with test compounds.

4.1.3 RESULTS

4.1.3.1 Statistical analysis

Statistical analysis was performed by using InStat 2.0 (GraphPad Software, San Diego, CA, USA) and Microsoft Office Excel 2003. Bonferroni's Multiple Comparison, one way analysis of variance (ANOVA) was performed on all data to indicate significant differences between test compounds and control (* $p < 0.05$ and ** $p < 0.001$ were considered to be a statistically significant difference). Data in bar chart are presented as % values of initial fluorescence with each bar representing the mean \pm S.E.M.

4.1.3.2 Fluorescent calcium flux experiments

Six neurons within the microscopic field were selected as regions of interest (ROI) for each experiment. Fluorescence intensity histograms were generated at both 340 nm and 380 nm for the selected ROI over a 120 second time series. Histograms were analysed and the ratio of 340 nm to 380 nm, which indicates the average decrease in fluorescence in the presence of each of the derivatives, was calculated (Fig. 4.4 and 4.5).

Figures 4.2 – 4.3 show examples of representative experiments in the presence and absence of test compounds (100 μ M). Cells were incubated with the respective compound for 10 minutes before recording commenced. High concentration potassium solution (140 mM) was applied 20 – 40 seconds after the first image was recorded. Three images in the time series of 120 sec are presented. Slide (a) shows the ROI selected before application of KCl, the image in slide (b) was taken just after application of KCl and the image in slide (c) was taken at 120 seconds.

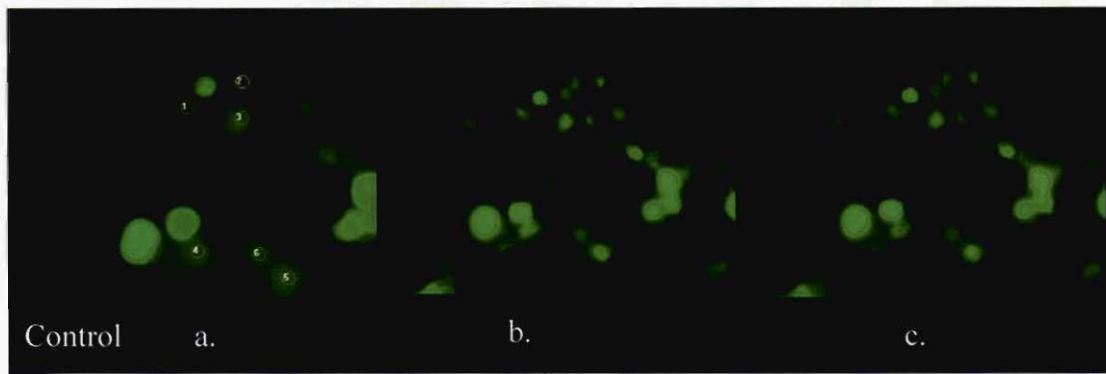
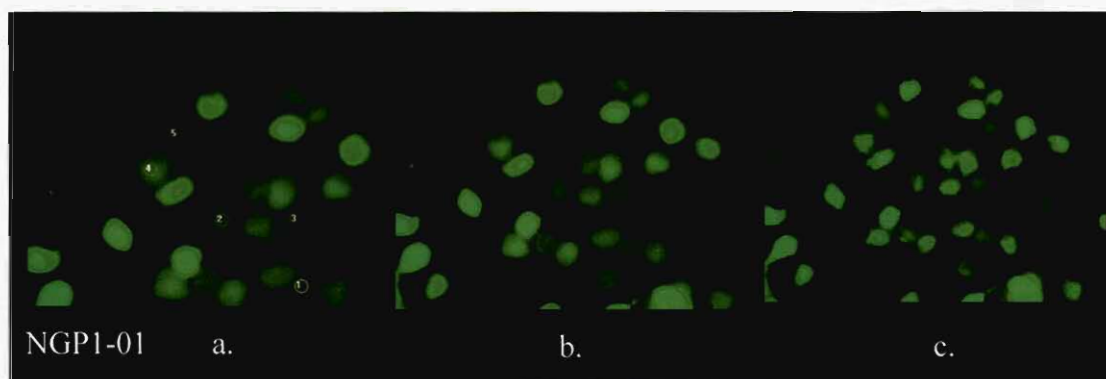
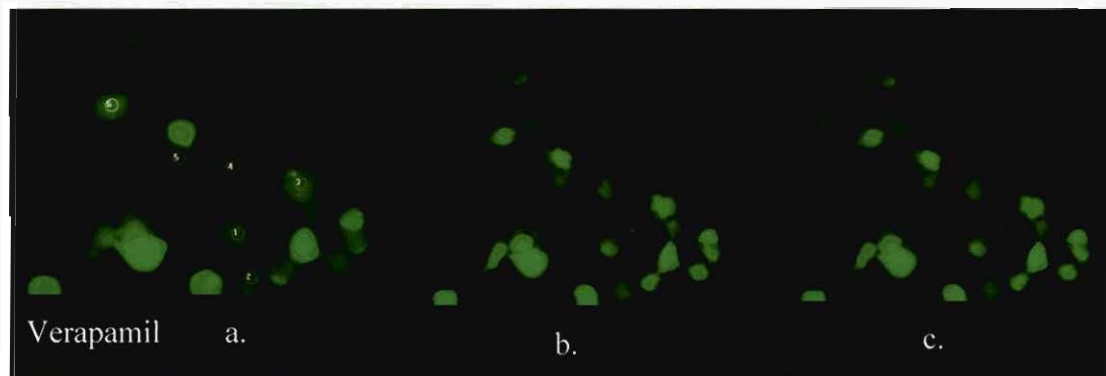
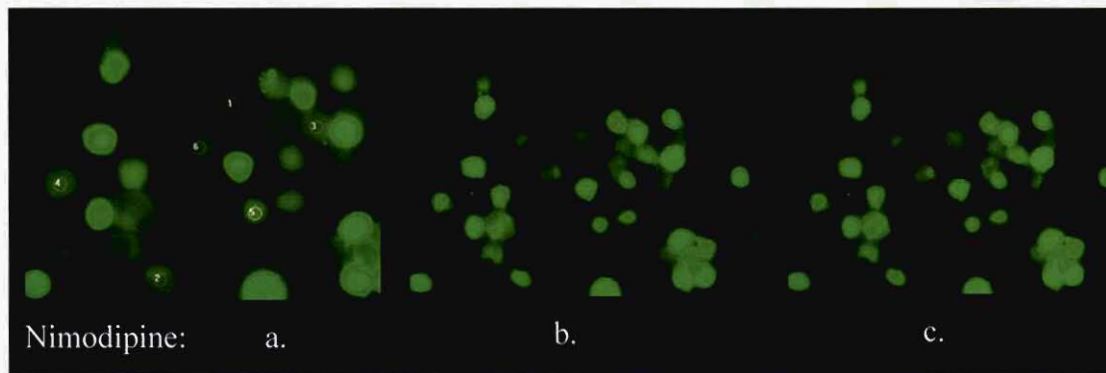
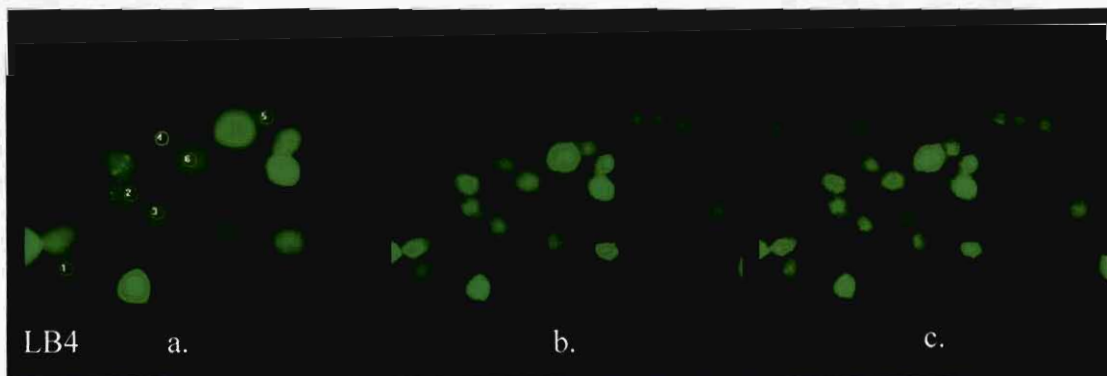
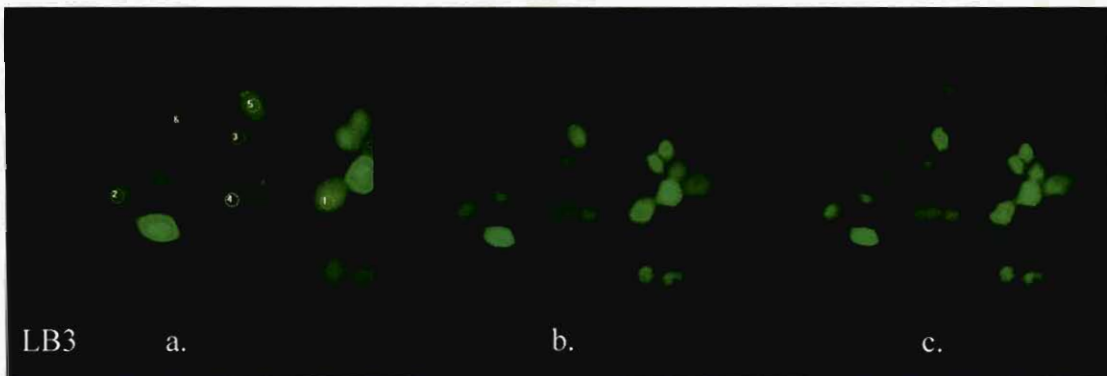
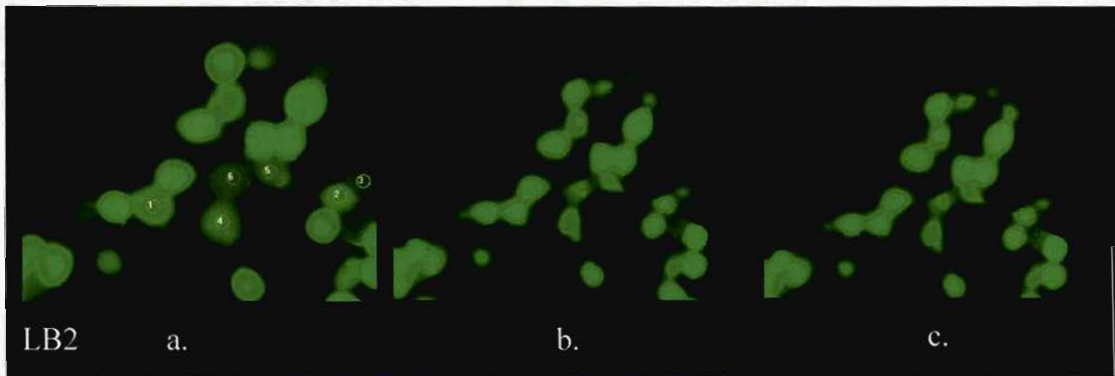
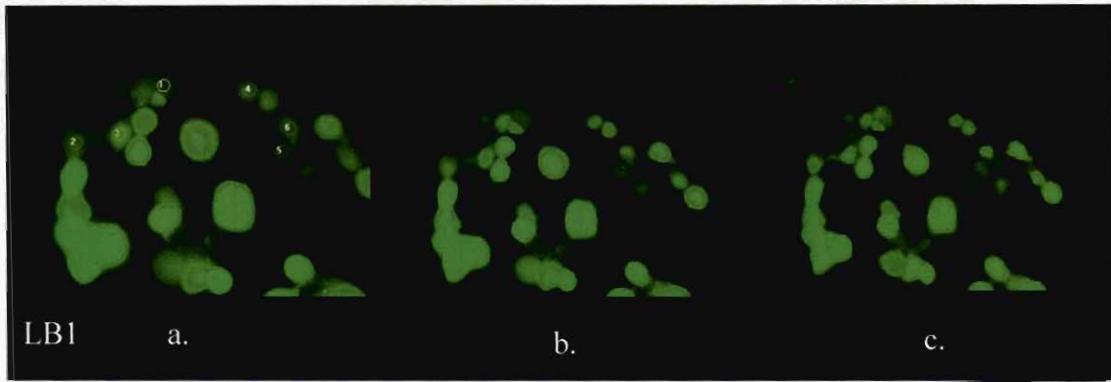


Figure 4.2: Representative frames from the time series of control experiment where cells were incubated with 0.1% DMSO followed by application of high concentration of potassium (140 mM).





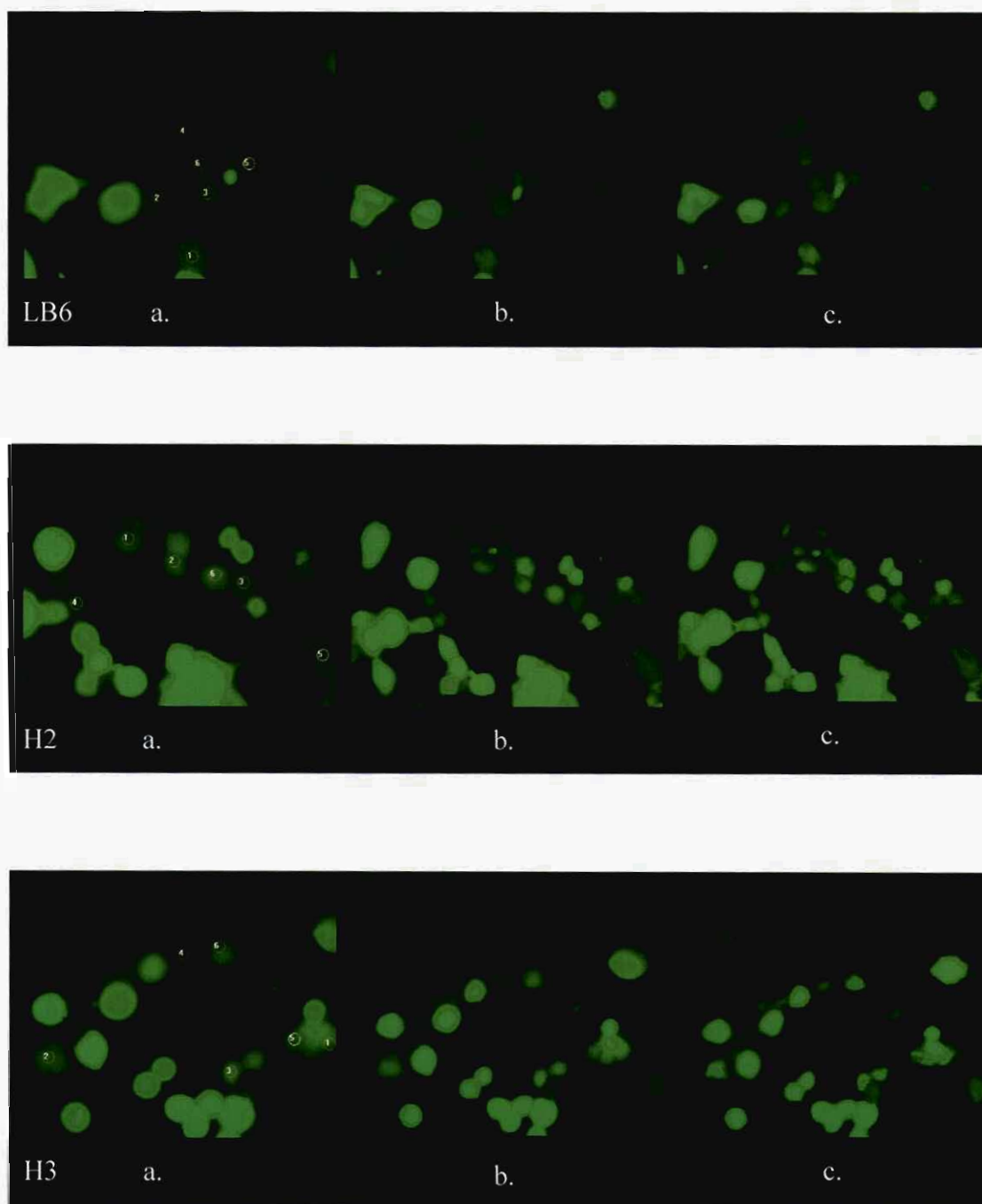


Figure 4.3: Representative frames from the time series of cells incubated with test compounds (100 μM) followed by application of high concentration of potassium (140 mM).

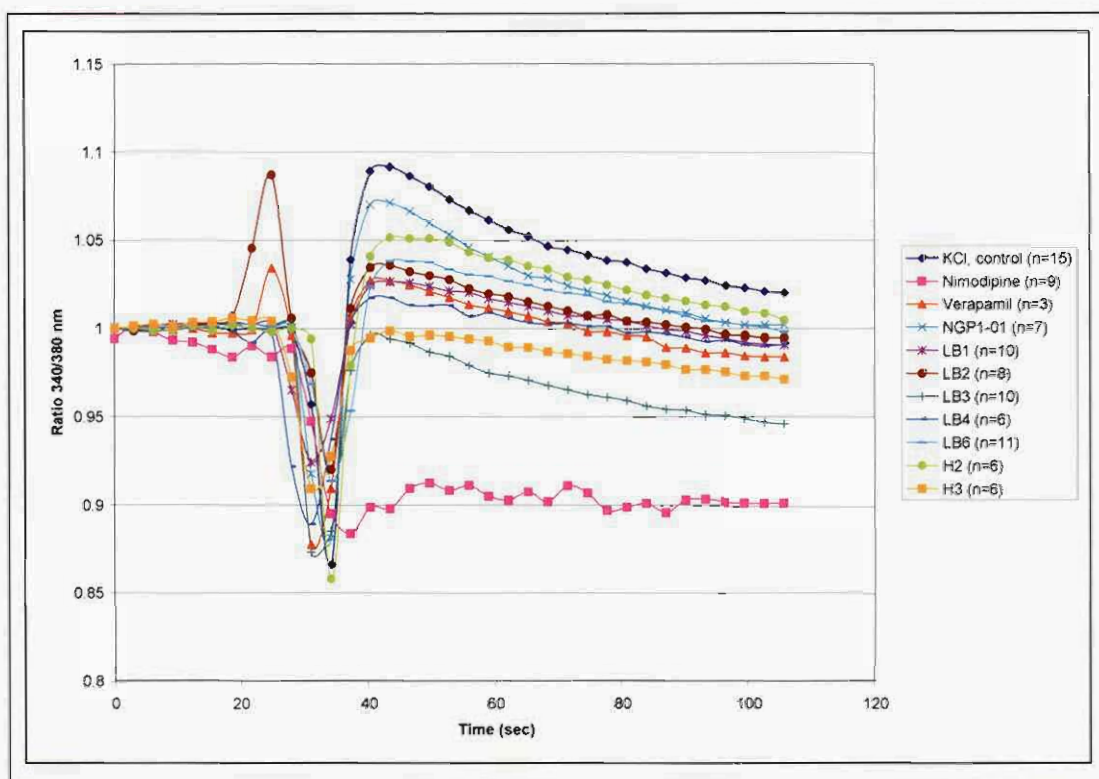


Figure 4.4: Summary of experiments demonstrating the effect of depolarisation with KCl (140 mM) in the absence and presence of test compounds (100 μ M) and controls.

In ratiometric imaging experiments using Mag-fura-2/AM as fluorescent calcium indicator, application of a high concentration potassium (140 mM) resulted in an increase in the fluorescent ratio in the presence of extracellular calcium. The increase in fluorescence indicates an influx of calcium through the ion channels. The graph in figure 4.4 shows the fluorescent ratios calculated for each of the test compounds (LB1-6, H2 and H3) compared to the controls (KCl, nimodipine, verapamil and NGP1-01).

The initial transient decrease in fluorescent ratio 340/380 observed from 1.00 to 0.85 nm might be due to an artefact created when the high concentration potassium solution was manually added by means of micropipette. To resolve this problem a perfusion chamber could be used that will allow gradual introduction of the high concentration potassium solution.

To allow for better comparison we grouped the graphs for each test compound with the graphs for the reference compounds and control in figure 4.5 (a-f). To view larger representations of these graphs refer to Appendix B.

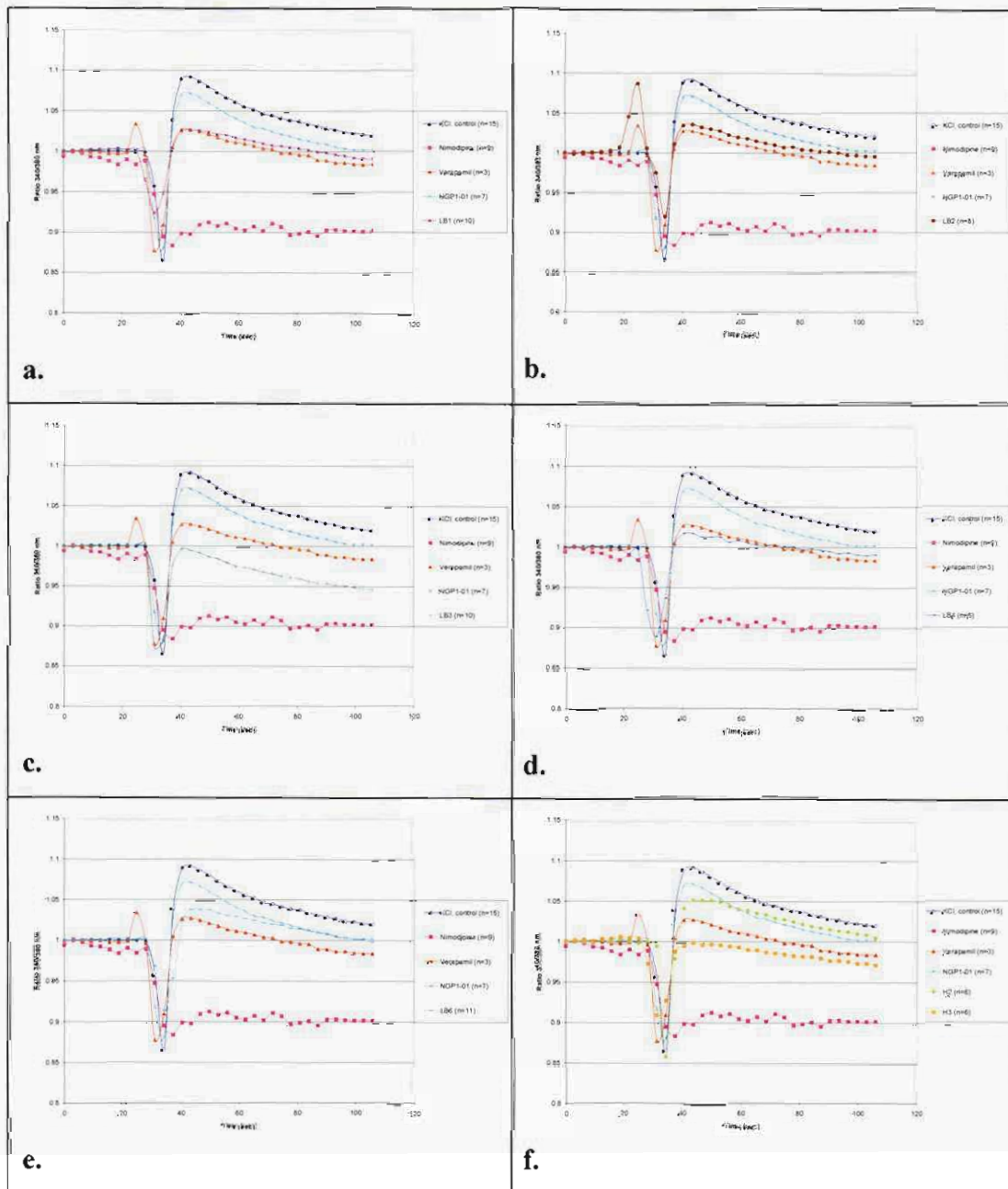


Figure 4.5: Experiments demonstrating the effect of depolarisation with KCl (140 mM) in the presence of individual test compounds (100 μM) compared to reference compounds (100 μM) and control.

To gain a more accurate interpretation of the results, the initial average fluorescence values before application of high concentration potassium (base line) were subtracted from the maximum increase in fluorescence for representative experiments in cells incubated with test compounds, reference compounds and controls. Standard errors of mean (\pm SEM) values were incorporated as error bars and compounds **LB3**, **LB4**, and **H3** presented the best profiles (Fig. 4.6).

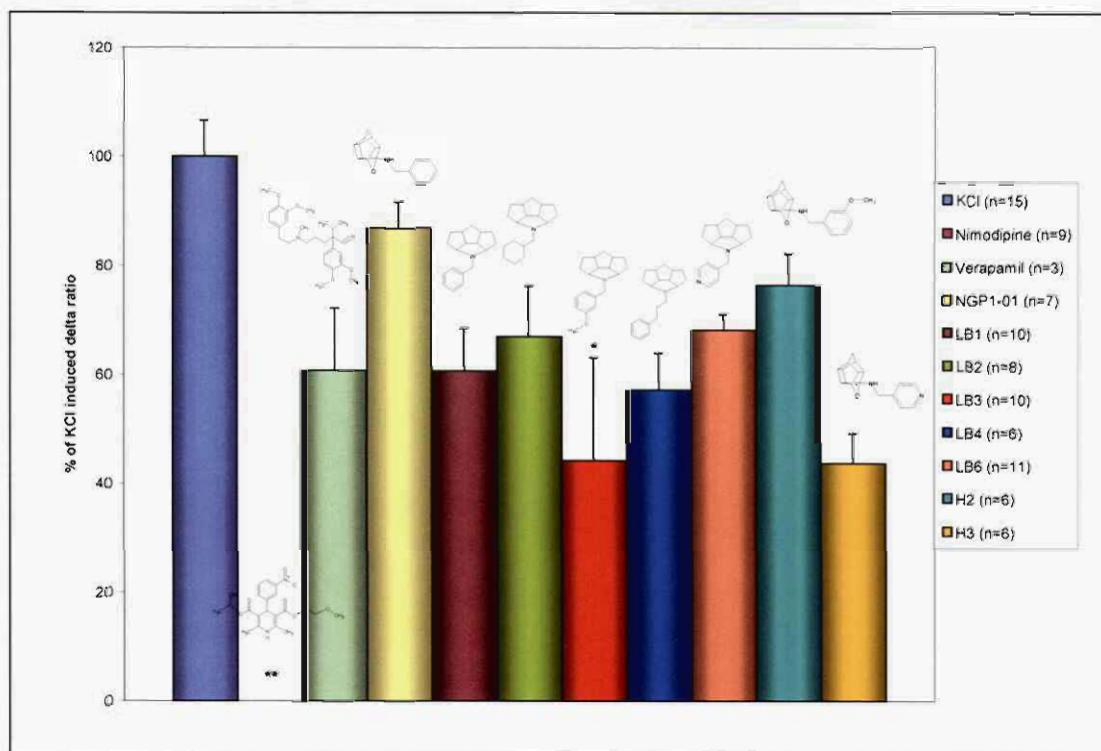


Figure 4.6: Summary of experiments demonstrating the effect of depolarisation with KCl (140 mM) in the absence and presence of test compounds and controls. Statistical analyses (see Section 4.1.3.1) were performed on raw data, with asterisks signifying significant inhibitory effect (*) $p < 0.05$, (**) $p < 0.001$ when compared to KCl as control.

Taking the KCl-induced increase in fluorescence as 100% and the nimodipine induced decrease in fluorescence (blockade of the VGCC) as 0%, the percentage that each test compound blocks the calcium flux, subsequently reducing the fluorescence, can be compared among the reference compounds. The reference compounds verapamil and NGP1-01 show an average decrease in fluorescence to $60.72 \pm 11\%$

(n=3) and $86.89 \pm 5\%$ (n=7), respectively when compared to the KCl-alone treated cells. Cells incubated with compounds **LB3** and **H3** showed a significant decrease in fluorescence to $44.11 \pm 19\%$ (n=10) and $43.66 \pm 6\%$ (n=6) respectively. Compound **LB4** also showed a noticeable decrease in fluorescence to $57.11 \pm 7\%$ (n=6). Compounds **LB1**, **LB2**, **LB6** and **H2** showed fluorescence decrease to $60.57 \pm 8\%$ (n=10), $66.86 \pm 9\%$ (n=8), $68.12 \pm 3\%$ (n=11) and $76.36 \pm 6\%$ (n=6) respectively (Fig. 4.6).

4.1.4 DISCUSSION

From the results it can be seen that compounds **LB3**, **LB4** and **H3** decreased the fluorescence to a greater extent than the other compounds evaluated, with only **LB3** showing a statistically significant difference ($p < 0.05$, ANOVA) when compared to the control. All of the tested compounds decreased the fluorescence to a greater extent than the reference compound NGP1-01, but none showed a statistically significant decrease in fluorescence. **LB1** showed a reduction in fluorescence to $60.57 \pm 8\%$, which was comparable to the reduction shown by verapamil ($60.72 \pm 11\%$), although this was not considered a statistically significant difference. Nimodipine however, did show a statistically significant decrease in fluorescence ($p < 0.001$, ANOVA). All test compounds reduced the extent of Ca^{2+} influx due to KCl-induced depolarisation.

Inhibition of the Ca^{2+} flux through the L-type calcium channels reported in this study is consistent with findings for a set of pentacycloundecanes with similar side chains studied by Malan *et al.*, (2000). The compounds investigated by this group included oxa-bridgehead compounds, in contrast to the aza-bridgehead compound used in this study. The side chains that were also included in that study were benzylamine (NGP1-01), 3-methoxybenzylamine and 4-methylpyridine. These authors investigated the mechanism of action for these compounds on L-type calcium channels through whole cell clamping on guinea-pig ventricular myocytes and structure-activity relationship studies. In their study NGP1-01 was also used as lead compound and showed good inhibition of the calcium current. In contrast to the findings of this group, NGP1-01 did not significantly inhibit calcium flux in our study. This compound is structurally related to **LB1** that showed a noticeable decrease in fluorescence in our study,

although it was not the largest decrease amongst the compounds tested and also not statistically significant ($p > 0.05$, ANOVA). Furthermore, where Malan *et al.*, (2000) found the activity for the methoxybenzylamine compound to be higher than when the aromatic benzylamine was substituted with aminomethylpyridine on the pentacycloundecane skeleton. We found that the methoxybenzylamine substituted compound (**H2**) showed weaker activity than the aminomethylpyridine substituted compound (**H3**). For the triquinylamines tested however, the methoxybenzylamine substituted compound (**LB3**) showed greater activity than the aminomethylpyridine substituted compound (**LB6**), which correlated with the study done by Malan *et al.*, 2000. As previously stated, **LB3** showed the best overall activity and was also the only test compound that showed a statistically significant decrease in fluorescence ($p < 0.05$, ANOVA). The above differences could be attributed to the difference in cells and techniques used in the two studies and the fact that additional channels might possibly have an effect in the current study.

The cyclohexylmethylamine side chain was selected for compound **LB2** to evaluate the importance of an aromatic substituent for activity. As expected, the activity decreased (though not significantly; $p > 0.05$, ANOVA) with the unsaturated cyclohexylamine moiety. This correlated with a study done on calcium-mediated action potentials in guinea-pig papillary muscle by Liebenberg *et al.*, (2000), who found that compounds with aromatic substitutions showed an increase in activity compared to their aliphatic counterparts. These findings indicate that lipophilicity plays a role in the activity of these compounds.

The phenylpropylamine side chain selected for compound **LB4**, when compared to compound **LB1**, demonstrated that an increase in side-chain length leads to a slight increase (though not significant; $p > 0.05$, ANOVA) in calcium channel blocking activity. This also correlated with the study by Liebenberg *et al.*, (2000), that found that an increase in chain length led to an increase in calcium channel antagonistic activity. Liebenberg's study concluded that bulky substituents that contributed to greater molecular surface area were essential to for calcium channel antagonistic activity. Thus we can argue that an increase in chain length might indicate that a deeper immersion into the calcium channel may be necessary for stronger interaction with the putative binding site.

4.2 SCREENING OF THE TRIQUINYLAMINES FOR ACTIVITY AT THE NMDA RECEPTOR

4.2.1 INTRODUCTION

To gain insight into the site of interaction on the NMDAR channel for the triquinylamine compounds, we used radioligand binding studies with [³H]MK-801, to measure the displacement of radiolabelled MK-801. The same series of compounds tested in the fluorescence experiments was evaluated in this study. Murine synaptoneurosomes isolated from mice striata were used for this experiment and [³H]MK-801 displacement was measured after stimulation with NMDA (100 μM) and Gly (100 μM). Dose-response curve analyses were performed on the compound that showed the highest affinity in the binding study, to determine the IC₅₀ value for that compound.

4.2.2 MATERIALS AND METHODS

4.2.2.1 Animals

ICR male mice (20 – 26 g, 6 – 8 weeks old) were obtained from Harlan, Dublin, VA. All animal care and experimental protocols were approved by the Texas Tech University HSC Institutional Animal Care and Use Committee in accordance with guidelines established by the United States Public Health Service and Texas Tech University.

4.2.2.2 Materials

(+)MK-801 (maleate) was purchased from Research Biochemicals Incorporated (Natick, MA, USA). [³H]MK-801 (17.1 Ci/mmol) was purchased from Perkin-Elmer (Boston, MA, USA). Buffer constituents were obtained from commercial sources.

4.2.2.3 Radioligand binding assay

Procedures similar to those of published studies were used to measure [³H]MK-801 (Filloux *et al.*, 1994) binding. Murine synaptoneuroosomes were prepared as described previously (Bloomquist and Soderlund, 1985) with minor modifications. Whole brains of male ICR mice (Harlan) were dissected out on ice and coarsely minced with scissors. The tissue was homogenized in magnesium-free incubation buffer by hand using a Dounce homogenizer. The incubation buffer contained 118 mM NaCl, 4.7 mM KCl, 0.1 mM CaCl₂, 20 mM HEPES and 30.9 mM glucose. The tissue was then centrifuged for 15 min at 928 × g and 0 °C. After centrifugation, the pellet was resuspended by hand in fresh incubation buffer using a Pasteur pipette and then centrifuged again as described above. The final pellets were resuspended in a volume of incubation buffer adequate for experimental use. The reaction mixture consisted of 380 µl of membrane preparation containing typically 0.38 mg protein, [³H]MK-801 (5 nM) as radioligand. Non-specific binding was assessed in the presence of 100 µM unlabelled MK-801. For the screening test, the compounds were applied at 100 µM final concentration and were dissolved in DMSO (final DMSO concentration in the incubations ≤ 0.1%). Control experiments received 0.1% DMSO to compensate for possible alterations caused by addition of DMSO in experiments. For the dose-response curve, the test compound selected from the screening test was incubated at different concentrations, in a log-scale. The reaction was initiated by the addition of 20 µl incubation buffer containing NMDA (100 µM) and Gly (100 µM) to the membrane preparation. Incubation of the mixture was for 2 h at 25 °C. The reaction was terminated by the addition of ice cold wash buffer and filtration on Whatman GF/B filters. Following air drying, the filters were placed into scintillation liquid and radioactivity retained on the filters was determined by liquid scintillation counting, using a Beckam scintillation counter.

4.2.3 RESULTS

4.2.3.1 Statistical analysis

Radioligand binding data were analyzed with InStat 2.0 and plotted with Prism 4 software (both from GraphPad Software, San Diego CA, USA). Compounds were screened at a concentration of 100 μM to assess displacement of [^3H]MK-801. Each bar represents the mean \pm S.E.M. of three experiments, each done in triplicate. Student's t-tests were performed on mean response of test compound vs. control and $P < 0.05$ (*) was considered statistically significant. Concentration-response data were analyzed by non-linear least squares curve fitting, with IC_{50} values for **LB1**, calculated using Prism 4. Statistical significance of the results was calculated with the unpaired Student's t-test and $P < 0.05$ (*) was considered statistically significant.

4.2.3.2 Radioligand binding experiments

We examined the characteristics of NMDA stimulated displacement of radiolabelled MK-801 from the PCP binding site within the NMDA receptor on murine synaptoneuroosomes. Several compounds were screened for their ability to displace labelled MK-801 and the results of the screening assay are presented in figure 4.7. The addition of NMDA (100 μM) and Gly (100 μM) resulted in activation of the NMDA channel and if possible, displacement of labelled and unlabelled MK-801 by test compounds.

Specific [^3H]MK-801 binding to the homogenate can be estimated by subtracting non-specific binding (NS) obtained in the presence of 100 μM unlabelled MK-801 from the total binding. The specific binding represents 75% of the total binding and non-specific binding represents only 25% of the total binding at 5 nM [^3H]MK-801. Unlabelled MK-801 used to determine the non-specific binding also served as a reference compound. The NMDA-stimulated displacement for each tested compound was calculated as the difference between the measured value for labelled MK-801, in the presence of each test compound, and the total binding: the purpose of this study represents only the non-specific binding for that particular compound. Compound **LB1** significantly displaced [^3H]MK-801 by $41.09 \pm 0.7\%$. For compounds **LB2**,

LB3, **LB4** and **LB6** there were no statistically significant displacement of [³H]MK-801 and displacement values were calculated to be $16.93 \pm 4.1\%$, $14.35 \pm 7.9\%$, $20.85 \pm 11.7\%$ and $9.28 \pm 6.17\%$ respectively.

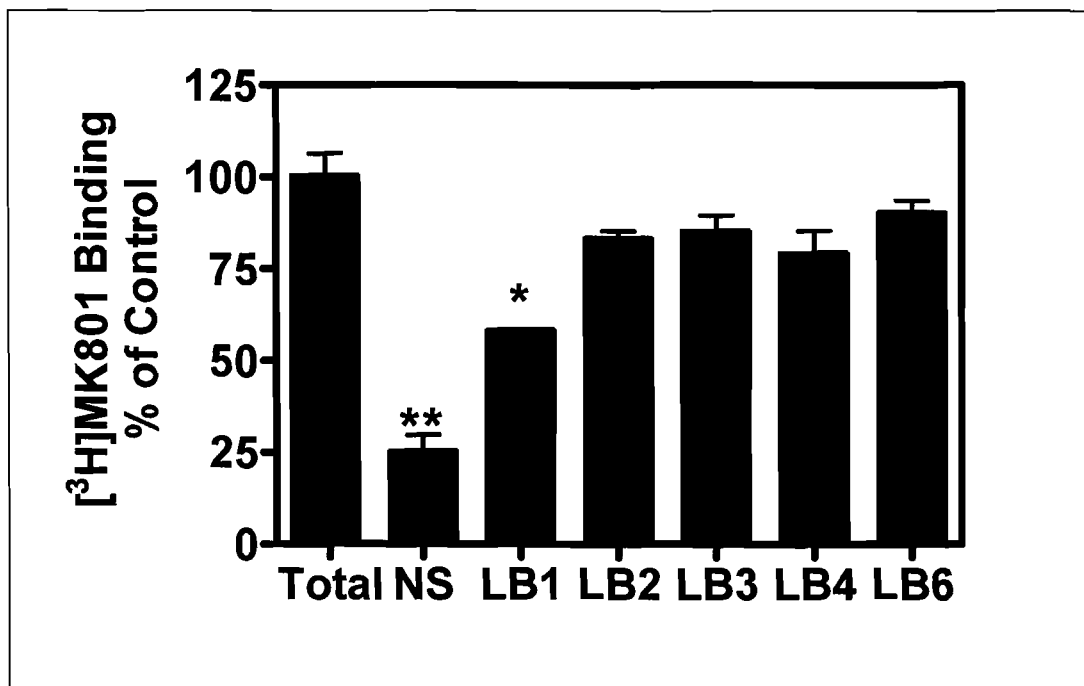


Figure 4.7: Competition binding of compounds **LB1-4** and **6** with [³H]MK-801 in the presence of NMDA/Gly. Abbreviations are: Total binding of radiolabelled MK-801 (Total), non-specific binding of unlabelled MK-801 (NS), compounds **LB1-4** and **6** all at 100 μ M. Statistical significance (see Section 5.2.3.1) compared to total binding in a t-test, (*) $p < 0.05$, (**) $p < 0.001$.

4.2.3.3 Dose-response curve

Dose-response curve fitting (Fig. 4.8) was performed to determine the IC_{50} value for the most potent inhibitor (**LB1**) among the compounds screened in the radioligand binding experiment. The IC_{50} value for **LB1** was reported to be $1.93 \pm 0.018 \mu$ M, and was considered to be statistically significant. All fittings of the dose-response relationship to a sigmoidal curve were good, with r^2 value of 0.9988. The Hill slope values for compounds with high-affinity as NMDA antagonists (MK-801, memantine,

and NGP1-01) are near unity, with lower potency compounds having greater Hill slope values. The Hill slope value for **LB1** was -1.157 ± 0.052 .

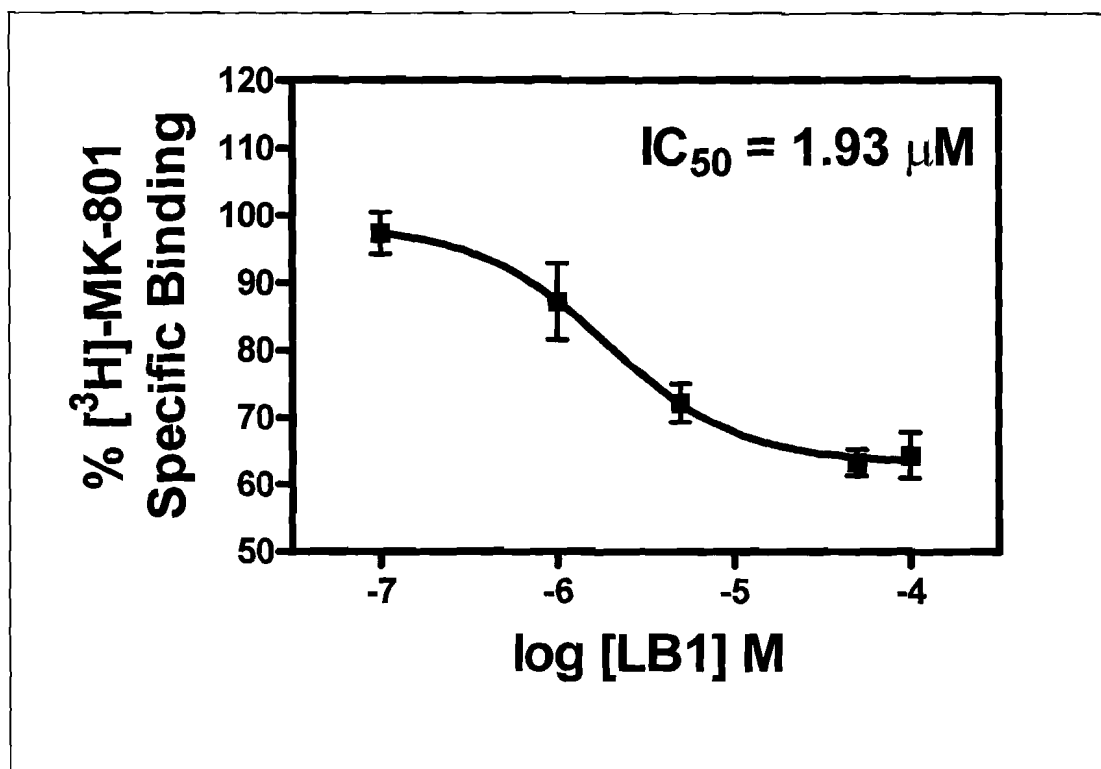


Figure 4.8: Dose-dependent effect of **LB1** on [³H]MK-801 binding in the presence of NMDA (100 μM) and Gly (100 μM).

4.2.4 DISCUSSION

From the results it can be ascertained that only compound **LB1** showed a statistically significant displacement of labelled MK-801 from the PCP binding site within the NMDA receptor. The dose-response curve indicated **LB1** to be a very potent NMDA channel blocker competing with MK-801 for the PCP binding site. The IC_{50} value ($1.93 \pm 0.018 \mu\text{M}$) of **LB1**, is comparable to that reported for the cage amine memantine ($0.54 \mu\text{M}$; Kroemer *et al.*, 1998). This indicates a mode of action similar to that of memantine and MK-801, consistent with uncompetitive antagonism at the PCP binding site. Although the remainder of compounds in this series showed an average of 20-30% displacement, none of these values were considered to be

statistically significant. This indicates that these compounds do not strongly interact with the PCP binding site and possibly have a different site of interaction within the NMDA receptor/ion channel complex. The binding characteristics reported for this study are similar to those found for a set of pentacycloundecanes with similar side chains studied by Geldenhuys *et al.*, (2006). The compounds investigated by this group included oxa-bridgehead compounds, in contrast to the aza-bridgehead compound used in this study. The side chains that were also included in that study were benzylamine, 3-methoxybenzylamine, 4-methylpyridine and phenylethylamine, which has a close resemblance to phenylpropylamine included in our study. These authors investigated the mechanism of action for these compounds through $^{45}\text{Ca}^{2+}$ flux, radioligand binding studies with [^3H]MK-801 and [^3H]TCP, and structure-activity relationship studies. In their study the benzylamine (NGP1-01) was found to be the most potent compound with an IC_{50} of 2.98 μM , but showed no significant displacement of either [^3H]MK-801 or [^3H]TCP. This compound is structurally related to **LB1** which proved to be the most potent compound in this study with an IC_{50} of 1.93 μM and showed statistically significant displacement of [^3H]MK-801. The 3-methoxybenzylamine in the study by Geldenhuys *et al.*, (2006), with an IC_{50} of 20.65 μM showed no significant activity overall and neither did this compound (**LB3**) in our study. The phenylethylamine with a longer side chain length is structurally related to the phenylpropylamine (**LB4**) in our study. In the study by Geldenhuys *et al.*, (2006) this compound showed potent antagonism of NMDA-stimulated $^{45}\text{Ca}^{2+}$ influx, but did not significantly displace [^3H]MK-801. This correlates with our findings in the radioligand binding study and may suggest that although these compounds have activity as NMDA receptor blockers they have a different site of binding than reported for MK-801. These results indicate that future studies are needed to further investigate the triquinylamines' mechanism of action as NMDA receptor blockers.

4.3 SUMMARY

From the experiments performed in the present study, a general structure activity relationship emerged that correlated with previous studies done on both the pentacycloundecanes and triquinylamines (Geldenhuys *et al.*, 2006; Liebenberg *et al.*,

1996; Liebenberg *et al.*, 2000 & Malan *et al.*, 2000). Compound **LB1** showed moderate activity as a VGCC blocker and although not statistically significant, it surpassed the activity observed for the reference compound NGP1-01. Compound **LB1** however, showed significant displacement of radiolabelled MK-801 from the PCP binding site which suggests that it has binding affinity for the NMDA receptor channel. The dose response curve indicated **LB1** to be a potent NMDA channel blocker with an IC₅₀ value ($1.93 \pm 0.018 \mu\text{M}$) that is comparable to the clinically used drug memantine ($0.54 \mu\text{M}$; Kroemer *et al.*, 1998).

Compound **LB2** showed a decrease in activity as expected for both the VGCC and NMDA channels. This proves that lipophilicity plays a role in the activity of these compounds and that aromatic substituents may be a requirement for activity. Compound **LB3** showed significant activity on the VGCC but showed no significant effect on the NMDA receptor. For the L-type calcium channel, it was found that the activity shown by the methoxybenzylamine (**LB3**) was greater than for the aminomethylpyridine (**LB6**) which correlated with a previous study (Malan *et al.*, 2000). Compound **LB4**, when tested on the VGCC, demonstrated that an increase in chain length (though not significant) led to an increase in activity. However, the same was not observed in the NMDA receptor studies. Although the effect observed for **LB4** on the NMDA receptor was not greater when compared to **LB1**, it had a greater effect than any of the other compounds tested. Thus it appears that chain length plays an important role in the activity of the compounds evaluated for both the VGCC and NMDA receptor.

As reported by Malan *et al.*, 2000 and Liebenberg *et al.*, 2000 we also found that the structure-active relationships observed for this series of compounds appear to be dominated by geometric or steric constraints rather than by electronic considerations and that an increase in activity can be observed with an increase in molecular volume. This study also confirmed the hypothesis that the pentacycloundecane skeleton only serves as a bulk contributor and that modifying the structure did not diminish the activity of this series.

CHAPTER 5

CONCLUSION

The focus of the current study was to develop novel therapeutic agents to attenuate excitotoxicity, a process that results in neuronal injury as a result of excessive influx of Ca^{2+} primarily through the NMDAR channel, and secondarily through the L-type calcium channel (Sattler & Tymianski, 2000; Arundine & Tymianski, 2003; Pringle, 2004).

This study is part of an ongoing investigation into the biological activity of polycyclic amine derivatives and their possible role as neuroprotective or neurorescue agents. Several groups have contributed to the investigation of pentacycloundecane structures for activity on both the L-type calcium channel and NMDAR channel (Van der Schyf *et al.*, 1986; Van der Walt *et al.*, 1988; Malan *et al.*, 2000; Liebenberg *et al.*, 2000; Geldenhuys *et al.*, 2003; Grobler *et al.*, 2006; Geldenhuys *et al.*, 2006; Kiewert *et al.*, 2006). From these studies NGP1-01 was established as a promising lead structure for a new class of multifunctional drugs with great potential in the treatment of neurodegenerative diseases (Kiewert *et al.*, 2006). The “dual-mechanism” nature of NGP1-01 (as a blocker of both the NMDAR and the L-type calcium channel) is an example of a new approach in the treatment of diseases – including neurodegenerative disorders – that exhibit multiple etiological causes resulting in the observed pathological characteristic of the disease in question (Christiaans & Timmerman, 1996; Morphy *et al.*, 2004; Roth *et al.*, 2004; Morphy & Rankovic, 2005; Youdim & Buccafusco, 2005a,b; Van der Schyf *et al.*, 2006).

Elucidation of the mechanism by which NGP1-01 and its derivatives exert their pharmacological action led to the establishment of structure-activity relationship correlations for NGP1-01 and related compounds for both the L-type calcium channel and NMDAR channel, peripherally and in the CNS (Malan *et al.*, 2000; Liebenberg *et*

al., 2000; Geldenhuys *et al.*, 2006). These structure-activity relationships suggest that the pentacycloundecane skeleton may serve only as a bulk contributor for the biological activity of NGP1-01 and other polycyclic cage compounds (Van der Schyf *et al.*, 1986; Malan *et al.*, 2000; Liebenberg *et al.*, 2000). In order to investigate the validity of this hypothesis Liebenberg *et al.* (1996), synthesised thermal ring-opened derivatives of NGP1-01. The possibility that yet another group of polycyclic compounds – the unique *cis-syn-cis* triquinane system obtained through the procedure of Liebenberg *et al.* (1996) – could be identified as multimodal drug scaffolds, was an important concept lending impetus to the justification of this study. The series of triquinylamines investigated by Liebenberg *et al.* (1996), showed favourable activity as calcium channel antagonists and the authors concluded that ring opening of the cage moiety did not diminish these compounds' potential to block the L-type calcium channel. However, at the time of these investigations, the activity of triquinylamines as potential NMDAR antagonists still remained to be investigated.

In the current study we aimed to: (1) synthesise a series of triquinylamine compounds, and (2) evaluate these compounds as possible L-type calcium channel and NMDAR antagonists in the central nervous system. Part of the first aim required focus on designing and building a suitable pyrolysis apparatus that would be necessary to perform the thermal fragmentation reaction. Design specifications of the pyrolysis apparatus were based on several earlier descriptions in the literature, and resulted in the development of a unique apparatus, which produced excellent results with optimised pyrolysis reaction yields approaching 80%. The product of the thermal fragmentation reaction furnished the desired unique *cis-syn-cis* triquinane structure that can only be obtained from the thermal [2 + 2] cycloreversion reaction of pentacyclo[5.4.0.0^{2,6}.0^{3,10}.0^{5,9}]undecane-8,11-dione (Mehta *et al.*, 1981).

However, subsequent attempts at synthesising several derivatives from the triquinane scaffold afforded much lower yields and attempts to isolate the methylamine derivative (N-methyl-3,11-azatricyclo[6.3.0.0^{2,6}]undecane), failed. We initiated a computational study in an attempt to explain the apparent preferential formation of the benzylamine derivative over the methylamine derivative. For this study *ab initio* Hartree-Fock (HF) and density functional theory (DFT) calculations predicted a significantly lower energy of formation for the benzylamine derivative than for the

methylamine derivative. Frontier molecular orbital theory (FMO) analyses suggested a stronger HOMO-LUMO overlap for the 3-benzyliminotricyclo[6.3.0.0^{2,6}]undecane-11-one intermediate than for the 3-methyliminotricyclo[6.3.0.0^{2,6}]undecane-11-one intermediate, indicating the formation of a stronger covalent bond between the carbonylic oxygen and the imine. The HOMO-LUMO overlap may also further account for the preferential formation of the benzylamine derivative over the methylamine derivative.

The second aim of this study was to evaluate the activities of the synthesised triquinylamines on both the L-type calcium channel and the NMDAR. Utilizing the N₂α murine neuroblastoma cell line, fluorescence microscopy was utilized to measure calcium influx through the L-type calcium channel after KCl-induced depolarisation (KCl at 140 mM). The affinity of the compounds for the NMDAR channel was measured by radioligand binding studies wherein the displacement of [³H]MK-801 from murine synaptoneurosomes was used to evaluate channel block in the presence and absence of the triquinylamine derivatives. This technique allowed us to evaluate whether these compounds compete with MK-801 for interaction at this ligands' specific binding site(s) inside the NMDAR channel.

From these experiments a general structure activity relationship emerged that correlated with previous studies done on both the pentacycloundecanes and triquinylamines (Geldenhuis *et al.*, 2006; Liebenberg *et al.*, 1996; Liebenberg *et al.*, 2000 and Malan *et al.*, 2000). Compound **LB1** showed moderate activity as a VGCC blocker and although not in a statistically significant way, it nonetheless surpassed the activity observed for the reference compound NGP1-01. Compound **LB1** however, showed considerable displacement of radiolabelled MK-801 from the PCP binding site, which suggests that this compound has significant affinity for the NMDAR and will show activity as an NMDA receptor channel blocker. The dose response curve indicated **LB1** to be a potent NMDA channel blocker with an IC₅₀ value (1.93 ± 0.018 μM) that is comparable to the clinically used drug memantine (0.54 μM; according to Kroemer *et al.*, 1998).

Compound **LB2** showed a decrease in activity on both the VGCC and NMDA channels. This behaviour was expected and suggests that lipophilicity plays a role in

the activity of these compounds, and that aromatic substituents are a requirement for activity on both the L-type calcium channel and NMDAR channel. These findings correlated with the study by Liebenberg *et al.*, (2000) that indicated aliphatic derivatives of the pentacycloundecane moiety to be inactive on L-type calcium channels in the periphery. In a study by Kroemer *et al.*, (1998) the proposed pharmacophore for the NMDAR indicated that a third point of hydrophobic interaction acts as a high affinity binding site. Interactions at this site was determined to be both sterically directed, and requiring an aromatic ring, which may explain the weak affinity observed for **LB2** compared to **LB1** for the NMDAR channel.

Compound **LB3** showed significant activity on the VGCC but no significant affinity for the NMDA receptor. For the L-type calcium channel, it was found that the activity shown by the methoxybenzylamine (**LB3**) was greater than for the aminomethylpyridine (**LB6**) which correlated with a previous study (Malan *et al.*, 2000). The study by Malan *et al.*, (2000) indicated that compounds with aromatic substitution in the *meta* position were more active, with the *meta*-methoxy substituted compound showing increased activity compared to the (*para*-substituted) 4-pyridine compound. A study by Geldenhuys *et al.*, (2006) also indicated that a *meta*-methoxy substituent imparts more activity to the molecule than a *para*-substituted pyridine. However, in the present study, the 4-pyridine substituted compound (**LB6**), was observed to be slightly more active. These findings may be the results of different experimental conditions for in the present study fluorescent calcium imaging techniques were used in an immortalised neuroblastoma cell line. The study by Malan *et al.*, (2000) utilised whole cell voltage clamping on guinea-pig ventricular myocytes to examine the L-type calcium blocking effect and the study by Geldenhuys *et al.*, (2006) utilised ligand-stimulated $^{45}\text{Ca}^{2+}$ influx into synaptoneurosome to measure the NMDAR channel block. Interestingly, the study by Geldenhuys *et al.*, (2006) concluded that although the pentacycloundecylamines had activity as NMDAR channel blockers, they interacted with a unique binding site distinct to that reported for MK-801 or PCP. Such a distinction may also explain why the triquinylamine derivatives tested in this study (with exception of **LB1**), showed no significant displacement of radiolabelled MK-801.

Although the pharmacological data were not statistically significant, findings for **LB4** when tested on the VGCC, again suggest that an increase in chain length leads to an increase in channel blocking activity. Such a trend was also observed in the study by Liebenberg *et al.*, (2000) where the authors reported that an increase in chain length led to increased suppression of calcium-mediated action potential in isolated guinea-pig papillary muscle. However, the same trend was not observed in the NMDA receptor studies. Although the activity observed for **LB4** on the NMDA receptor was not greater than that of **LB1**, the former compound had greater affinity than any of the other compounds tested. A similar trend was observed in later radioligand binding studies by Geldenhuys *et al.*, (2006). In this report, the ethylamine derivative of the pentacycloundecane scaffold displayed more activity than any of the substituted aromatic amine derivatives with the exception of NGP1-01. Thus, it appears that chain length plays an important role in the activity of the compounds evaluated for both the VGCC and NMDA receptor.

The binding characteristics reported in this study are similar to those found during evaluation of the pentacycloundecylamines for activity on both the L-type calcium and NMDAR channels (Liebenberg *et al.*, 1996; Kroemer *et al.*, 1998; Malan *et al.*, 2000; Liebenberg *et al.*, 2000 & Geldenhuys *et al.*, 2006). Also, for the triquinylamines, we found that the structure-activity relationships appear to be dominated by geometric or steric constraints rather than by electronic considerations, and that an increase in activity can be observed in concert with an increase in molecular volume. For activity on the VGCC, aromatic substitution appears to be of crucial importance, with an increase in activity observed for *meta*-methoxy substitution on the aromatic moiety. An increase in chain length also led to a slight increase in activity. Both aromatic substitution and an increase in chain length resulted in an increased activity as blockers of the NMDAR channel. However, manipulation of electronic effects with *meta*-methoxy substitution on the aromatic moiety did not result in any significant change of effect at the NMDAR. The current study therefore, confirms the hypothesis that the pentacycloundecane skeleton only serves as a bulk contributor and that modifying the structure did not diminish the activity of this series of compounds.

5.1 FINAL REMARK

The triquinylamines tested represent a novel group of compounds that have potential as multifunctional therapeutic agents against neurodegenerative diseases such as Alzheimer's disease, Parkinson's disease and post-stroke neurodegeneration. Thus, these compounds with their unique *cis-syn-cis* triquinane system represent yet another group of polycyclic compounds, the scaffold of which may serve as the basis for multimodal drug design. The triquinylamines demonstrated activity as blockers of both the L-type calcium channel and the NMDAR, and attenuated excessive Ca^{2+} influx through both receptors. Future studies are thus warranted to further investigate these potential multifunctional therapeutic agents for a role as neuroprotective agents in the treatment of an array of neurodegenerative diseases.

REFERENCES

ARUNDINE, M. & TYMIANSKI, M. 2003. Molecular mechanisms of calcium-dependent neurodegeneration in excitotoxicity. *Cell Calcium*. 34:325-337.

ARUNDINE, M. & TYMIANSKI, M. 2004. Molecular mechanisms of glutamate-dependent neurodegeneration in ischemia and traumatic brain injury. *Cellular and Molecular Life Sciences*. 61:657-668.

BLOOMQUIST, J.R. & SODERLUND, D.M. 1985. Neurotoxic insecticides inhibit GABA-dependent chloride uptake by mouse brain vesicles. *Biochemical and Biophysical Research Communications*. 133(1): 37-43.

BROWN, R.F.C. 1980. Pyrolytic methods in organic chemistry: Application of flow and flash vacuum pyrolytic techniques. Vol. 41. New York: Academic Press. 347p.

CHEN, H.V. & LIPTON, S.A. 2006. The chemical biology of clinically tolerated NMDA receptor antagonists. *Journal of Neurochemistry*. 97:1611-1626.

CHOI, D.W. 1985. Glutamate neurotoxicity in cortical cell cultures is calcium dependent. *Neuroscience Letters*. 58:293-297.

CHOI, D.W., MAULUCCI-GEDDE, M. & KRIEGSTEIN, A.R. 1987a. Glutamate neurotoxicity in cortical cell culture. *Journal of Neuroscience*. 7:357-368.

CHOI, D.W. 1987b. Ionic dependence of glutamate neurotoxicity. *Journal of Neuroscience*. 7:369-379.

CHOI, D.W. 1988a. Calcium-mediated neurotoxicity: relationship to specific channel types and role in ischemic damage. *Trends in Neuroscience*. 11:465-467.

CHOI, D.W. 1988b. Glutamate neurotoxicity and diseases of the nervous system. *Neuron*. 1(8):623-634.

- CHOI, D.W. 1995. Calcium: still center-stage in hypoxic-ischemic neuronal death. *Trends in Neuroscience*. 18:58-60.
- CHRISTIAANS, J.A.M. & TIMMERMAN, H. 1996. Cardiovascular hybrid drugs: Combination of more than one pharmacological property in one single molecule. *European Journal of Pharmaceutical Sciences*. 4:1-22.
- COOKSEN, R.C., GRUNDWELL, E., HUDEC, J. 1958. Synthesis of cage-like molecules by irradiation of Diels-Alders adducts. *Chemistry and Industry*. 1003-1004.
- CRAWLEY, J.N., GERFEN, C. R., ROGAWSKI, M. A., SIBLEY, D. R., SKOLNICK, P. & WRAY, S. 1997. Current protocols in neuroscience. [Web] <https://catalog.invitrogen.com/index.cfm?fuseaction=iProtocol.home> [Date of access: 11 July 2006].
- DAVIES, W.L., GRUNERT, R.R., HAFF, R.F., MCGAHEN, J.W., NEUMAYER, E.M., PAULSHOCK, M., WATTS, J.C., WOOD, T.R., HERMANN, E.C. & HOFFMAN, C.E. 1964. Antiviral activity of 1-adamantanamine (amantadine). *Science*. 144:862-863.
- DOCKENDOLF, G. 1992. Struktuurvereistes van polisikliese amiene vir kalsiumantagonistiese werking. North-West University: Potchefstroom campus. (Dissertation – M.Sc.) 83p.
- EROWID. 2004. Neuropharmacology of DXM from DXM FAQ. [Web:] http://www.erowid.org/chemicals/dxm/faq/dxm_neuropharm.shtml [Date of access: 13 March 2004].
- FEIGIN, V.L., RINKEL, G.J.E., ALGRA, A., VERMUELEN, M. & VAN GIJN, J. 1998. Calcium antagonist in patients with aneurismal subarachnoid hemorrhage. A systematic review. *Neurology*. 50:876-883.

- FILLOUX, F.M., FITTS, R.C., SKEEN, G.A. & WHITE, H.S. 1994. The dihydropyridine nitrendipine inhibits [^3H]MK-801 binding to mouse brain sections. *European Journal of Pharmacology*. 269(3):325-330
- FLECKENSTEIN, A. 1977. Specific pharmacology of calcium in myocardium, cardiac pacemakers, and vascular smooth muscle. *Annual Reviews of Pharmacology and Toxicology*. 17:149-166
- GARTHWAITE, G., HAJOS, F. & GARHTWAITE, J. 1986. Ionic requirements for neurotoxic effects of excitatory amino acid analogues in rat cerebellar slices. *Neuroscience*. 18:437-447.
- GELDENHUYS, W.J., MALAN, S.F., BLOOMQUIST, J.R., MARCHAND, A.P. & VAN DER SCHYF, C.J. 2005. Pharmacology and structure-activity relationships of bioactive polycyclic cage compounds: A focus on pentacycloundecane derivatives. *Medical Research Reviews*. 25(1):21-48
- GELDENHUYS, W.J., MALAN, S.F., MURUGENSAN, T., VAN DER SCHYF, C.J. & BLOOMQUIST, J.R. 2004. Synthesis and biological evaluation of pentacyclo[5.4.0.0^{2,6}.0^{3,10}.0^{5,9}]undecane derivatives as potential therapeutic agents in Parkinson's disease. *Bioorganic and Medical Chemistry*. 12:1799-1806.
- GELDENHUYS, W.J., TERRE'BLANCHE, G., VAN DER SCHYF, C.J. & MALAN, S.F. 2003. Screening of novel pentacyclo-undecylamines for neuroprotective activity. *European Journal of Pharmacology*. 458:73-79.
- GÖBEL, A., KRAUSE, E., FEICK, P. & SCHULZ, I. 2001. IP3 and cyclic ADP-ribose induced Ca^{2+} release from intracellular stores of pancreatic acinar cells from rat in primary culture. *Cell Calcium*. 29(1):29-37.
- GODOY-ALCÁNTAR, C., YATSIMIRSKY, .A.K. & LEHN, J.M. 2005. Structure stability correlations for imine formation in aqueous solution. *Journal of Physical Organic Chemistry*. 18:979-985.

GREENE, J.G. & GREENAMYRE, J.T. 1996. Bioenergetics and glutamate excitotoxicity. *Progress in Neurobiology*. 48:613-634.

GROBLER, E. 2005. The influence of polycyclic amines on calcium homeostasis of neuronal cells. North-West University: Potchefstroom campus. (Dissertation – M.Sc.) 81p.

GRYNKIEWICZ, G., POENIE, M. & TSIEN, R.Y. 1985. A new generation of Ca^{2+} indicators with greatly improved fluorescence properties. *The Journal of Biological Chemistry*. 260:3440-3450.

GURNEY, A.M., DRUMMOND, R.M. & FAY, F.S. 2000. Calcium signalling in sarcoplasmic reticulum, cytoplasm and mitochondria during activation of rabbit aorta myocytes. *Cell Calcium*. 27(6):339-351.

HANSCH, C., LEO, A., & TAFT, R.W. (1991). A Survey of Hammett Substituent Constants and Resonance and Field Parameters. *Chemical Reviews*. 91:165-195.

HANSCH, C., LEO, A., & HOEKMAN, D. (1995). Exploring QSAR - Hydrophobic, Electronic, and Steric Constants. American Chemical Society, Washington, D.C.

HARDINGHAM, G.E. & BADING, H. 2002. The yin and yang of NMDA receptor signalling. *Trends in Neurosciences*. 26:81-89.

HOCKERMAN, G.H., PETERSON, B.Z., JOHNSON, B.D. & CATTERALL, W.A. 1997. Molecular determinants of drug binding and action on L-type calcium channels. *Annual Review of Pharmacology & Toxicology*. 37:361-396.

- HOFER, A.M. & SCHULZ, I. 1996. Quantification of intraluminal free $[Ca^{2+}]$ in the agonist-sensitive internal calcium store using compartmentalized fluorescent indicators: some considerations. *Cell Calcium*. 20(3):235-242.
- HORN, J. & LIMBURG, M. 2001. Calcium antagonists for ischemic stroke: a systematic review. *Stroke*. 32:570-576.
- HYRC, K.L., BOWNIK, J.M. & GOLDBERG, M.P. 2000. Ionic selectivity of low-affinity ratiometric calcium indicators: Mag-Fura-2, Fura-2FF & BTC. *Cell Calcium*. 27(2):75-86.
- JANIS, R.A., SILVER, P. & TRIGGLE, D.J. 1987. Drug action and cellular calcium regulation. *Advance Drug Research*. 16:309-591.
- JOHNSTON, G.A.R., CURTIS, D.R., DAVIES, J. & McCULLOCH, R.M. 1974. Spinal interneurone excitation by conformationally restricted analogues of L-glutamic acid. *Nature, London*. 248:804-805.
- KEMP, J.A. & McKERNAN, R.M. 2002. NMDA receptor pathways as drug targets. *Nature Neuroscience*. 5:1039-1042.
- KIEWERT, C., HARTMANN, J., STOLL, J., THEKKUMKARA, T.J., VAN DER SCHYF, C.J. & KLEIN, J. 2006. NGP1-01 is a brain-permeable dual blocker of neuronal voltage- and ligand-operated calcium channels. *Neurochemistry Research*. 31:395-399.
- KOBAYASHI, T. & MORI, Y. 1998. Ca^{2+} channel antagonists and protection from cerebral ischemia. *European Journal of Pharmacology*. 363:1-15.
- KORNHUBER, J. & WELLER, M. 1997. Psychotogenicity and N-methyl-D-aspartate receptor antagonism: Implications for neuroprotective pharmacotherapy. *Biological Psychiatry*. 41:135-144.

KROEMER, R.T., KOUTSILIERI, E., HECHT, P., LIEDL, K.R., RIEDERER, P. & KORNHUBER, J. 1998. Quantitative Analysis of the Structural Requirements for Blockade of the *N*-Methyl-D-aspartate Receptor at the Phencyclidine Binding Site. *Journal of Medicinal Chemistry*. 41:393-400.

KUPSCH, A., LÖSCHMANN, P.A., SAUER, H., ARNOLD, G., RENNER, P., PUFAL, D., BURG, M., WATCHEL, H., TEN BRUGGENCATE, G. & OERTEL, W.H. 1992. Do NMDA receptor antagonists protect against MPTP-toxicity? Biochemical and immunocytochemical analysis in black mice. *Brain Research*. 592:74-83.

LAURIE, D.J., PUTZKE, J., ZIEGLGANSBERGER, W., SEEBURG, P.H. & TOLLE, T.R. 1995. The distribution of splice variants of the NMDR1 subunit mRNA in adult rat brain. *Molecular Brain Research*. 32:94-108.

LIEBENBERG, W. 1986 Stikstofbevattende derivate van pentasiklo-undekaan – ‘n nuwe reeks kalsium kanaalblokkers. North-West University (University for CHE): Potchefstroom campus. (Dissertation – M.Sc.) 100p.

LIEBENBERG, W. 1989. Die sintese, konformasie en biologiese aktiwiteit van trikwanielamiene en verwante verbindings. North-West University (University for CHE): Potchefstroom campus. (Thesis-Ph.D) 129p.

LIEBENBERG, W., VAN ROOYEN, P.H. & VAN DER SCHYF, C.J. 1996. The biological activity of two symmetric amine derivatives of the *cis-syn-cis* triquinane system. *Pharmazie*. 51:20-24.

LIEBENBERG, W., VAN DER WALT, J.J. & VAN DER SCHYF, C.J. 2000. Effects of derivatives of NGP 1-01, a putative calcium channel antagonist, on electrically stimulated guinea-pig papillary muscle. *Pharmazie*. 55:833-836.

LIMBRICK Jr., D.D., CHURN, S.B., SOMBATI, S. & DeLORENZO, R.J. 1995. Inability to restore resting intracellular calcium levels as an early indicator of delayed neuronal cell death. *Brain Research*. 690:145-156.

- LIPTON, P. 1999. Ischemic cell death in brain neurons. *Physiological Reviews*. 79:1431-1568.
- LU, H. 2002. Potential antiepileptic drugs acting on glutaminergic receptors. Department of Biopharmaceutical Science at University of Illinois. [Web:] www.uic.edu/classes/phar/phar402/Potential%20... [Date of access: 13 March 2004]
- McLEAN, A.E.M., McLEAN, E., & JUDA, J.D. 1965. Cellular necrosis in the liver induced and modified by drugs. *International Review of Experimental Pathology*. 4:127-157.
- McMURRY, J. 1996. Organic Chemistry. 4 th ed. Brooks/Cole Publishing Company. 1243p.
- MALAN, S.F. 1997. Polisikliese amienderivate: nuwe moontlikhede vir kalsiumkanaalaktiwiteit. North-West University (University for CHE): Potchefstroom campus. (Thesis-Ph.D) 199p.
- MALAN, S.F., DOCKENDOLF, G., VAN DER WALT, J.J., VAN ROOYEN, J.M. & VAN DER SCHYF, C.J. 1998. Enantiomeric resolution of the calcium channel antagonist 8-benzylamino-8,11-oxapentacyclo[5.4.0.0^{2,6}.0^{3,10}.0^{5,9}]undecane (NGP1-01). *Pharmazie*. 53:859-862.
- MALAN, S.F., VAN DEN HEEVER, I. & VAN DER SCHYF, C.J. 1996. Screening of polycyclic amines for calcium channel antagonism. *Journal of Pharmaceutical Medicine*. 6:125-135.
- MALAN, S.F., VAN DER WALT, J.J. & VAN DER SCHYF, C.J. 2000. Structure-activity relationships of polycyclic aromatic amines with calcium channel blocking activity. *Archive der Pharmazie, Pharmaceutical and Medical Chemistry*. 333:10-17.

- MALONE, T.C., ORTWINE, D.F., JOHNSON, G. & PROBERT Jr., A.W. 1993. Synthesis and biological activity of conformationally constrained 4_a-Phenantreneamine antagonists. *Bioorganic and Medical Chemistry Letters*. 3:49-54.
- MARCHAND, A.P., ARNEY, B.E., DAVE, P.R., SATYANARAYANA, N., WATSON, W.H. & NAGL, A. 1988. Transannular cyclizations in the pentacyclo[5.4.0.0^{2,6}.0^{3,10}.0^{5,9}]undecane-8,11-dione system: a reinvestigation. *Journal of Organic Chemistry*. 53:2644-2647.
- McNAB, H. 2004. Chemistry without reagents: Synthetic applications of flash vacuum pyrolysis. *Aldrichimica Acta*. 37:19-26.
- MEADOR-WOODRUFF, J.H. 1999. Neurochemical Circuitry of Schizophrenia. Mental Health Research Institute, Department of Psychiatry, University of Michigan. [Web:] <http://www.med.umich.edu/mhri/researchfaculty/meador-woodruff.htm> [Date of access: 13 March 2004].
- MEHTA, G. & RAO, K.S. 1985. Reductive carbon-carbon cleavage in caged systems: a new general synthesis of linearly fused *cis-syn-cis* triquinanes. *Journal of Organic Chemistry*. 50:5537-5543.
- MEHTA, G., SRIKRISHNA, A., REDDY, A.V. & NAIR, M.S. 1981. A novel, versatile synthetic approach to linearly fused tricyclopentanoids *via* photo-thermal olefin metathesis. *Tetrahedron*. 37:4543-4559
- MICHAELIS, E.K. 1998. Molecular biology of glutamate receptors in the central nervous system and their role in excitotoxicity, oxidative stress and aging. *Progress in Neurology*. 54:369-415.
- MORGAN, A. J. & THOMAS, A. P. 1999. Single cell and subcellular measurement of intracellular Ca²⁺ concentration. In: Lambert, D. G. *eds*. Methods in molecular biology, Vol. 114: Calcium signaling protocols. USA. Humana Press Inc. p93-123.

- MORGAN, L. C., GORMALLY, J., HUBBARD, A. R. D., d'LACEY, C. & OCKLEFORD, C. D. 1999. Confocal Microscopy: Theory and Applications. In: Lambert, D. G. *eds.* Methods in molecular biology, Vol. 114: Calcium signaling protocols. USA. Humana Press *Inc.* p51-74.
- MORPHY, R. & RANKOVIC, Z. 2005. Designed multiple ligands. An emerging drug discovery paradigm. *Journal of Medicinal Chemistry.* 48:6523-6543.
- MORPHY, R., KAY, C. & RANKOVIC, Z. 2004. From magic bullets to designed multiple ligands. *Drug Discovery Today.* 9:641-651.
- NEUROBIOLOGICAL TECHNOLOGIES, *Inc.* 2002. Neuroprotection. [Web:] <http://www.ntii.com/products/neuroprotection.shtml> [Date of access: 13 March 2004].
- OGURA, A., MIYAMOTO, M. & KUDO, Y. 1988. Neuronal death *in vitro*: parallelism between survivability of hippocampal neurones and sustained elevation of cytosolic Ca²⁺ after exposure to glutamate receptor agonist. *Brain Research.* 73:447-458.
- OKAMOTO, Y., KANEMATSU, K., FUJIYOSHI, T. & OSAWA, E. 1983. Remarkably fast [2+2] cycloreversion in methoxy substituted Cookson's cage ketones assisted by the capto-dative substituent effects and by the through-bond interaction. *Tetrahedron Letters.* 24:5645-5648.
- OLNEY, J.W. 1969. Brain lesion, obesity and other disturbances in mice treated with monosodium glutamate. *Science.* 164:719-721.
- OLNEY, J.W. 1978. Neurotoxicity of excitatory amino acids. *In:* McGeer, E.G., Olney, J.W. & McGeer, P.L. *eds.* Kainic Acid as a Tool in Neurobiology. New York: Raven Press. p95-121.

- OZYURT, E., GRAHAM, D.I., WOODRUFF, G.N. & McCULLOCH, J. 1988. Protective effect of the glutamate antagonist, MK-801 in focal cerebral ischemia in the cat. *Journal of Cerebral Blood Flow and Metabolism*. 8:138-143.
- PARSONS, C.G., DANYSZ, W. & QUACK, G. 1999. Memantine is a clinically well tolerated N-methyl-D-aspartate (NMDA) receptor antagonist – Review of preclinical data. *Neuropharmacology*. 38:735-767.
- PIZZI, M., RIBOLA, M., VALERIO, A., MEMO, M. & SPANO, P. 2002. Various Ca^{2+} entry blockers prevent glutamate-induced neurotoxicity. *European journal of Pharmacology*. 209:169-173.
- PRINGLE, A.K. 2004. In, out, shake it all about: elevation of $[\text{Ca}^{2+}]_i$ during acute cerebral ischemia. *Cell Calcium*. 36:235-245.
- ROGAWSKI, M.A. & WENK, G.L. 2003. The neuropharmacological basis for the use of memantine in the treatment of Alzheimer's disease. *CNS Drug Reviews*. 9:275-308.
- ROTH, B.L., SHEFFLER, D.J. & KROEZE, W.K. 2004. Magic shotguns versus magic bullets: selectively non-selective drugs for mood disorders and schizophrenia. *Nature Reviews and Drug Discovery*. 3:353-359.
- SASAKI, T., EGUCHI, S., KIRIYAMA, T. & HIROAKI, O. 1974. Studies of hetero-cage compounds, VI: transannular cyclization in pentacyclo-[6.2.1.0^{2,7}.0^{4,10}.0^{5,9}]undecan-3,6-dione system. *Tetrahedron*. 30:2707-2712.
- SATTLER, R. & TYMIANSKI. 2000. Molecular mechanisms of calcium-dependent excitotoxicity. *Journal of Molecular Medicine*. 78:3-13.
- SCHWAB, R.S., POSKANZER, D.C., ENGLAND, A.C., Jr. & YOUNG, R.R. 1972. Amantadine in the treatment of Parkinson's disease. Review of more than two years' experience. *Journal of American Medical Association*. 222:792-795.

- SILVA, M.A., PELLEGRINET, S.C. & GOODMAN, J.M. 2003. A DFT study on the regioselectivity of the reaction of dichloropropynylborane with isoprene. *Journal of Organic Chemistry*. 68:4059-4066.
- SIMON, R.P., GRIFFITHS, T., EVANS, M.C., SWAN, J.H., MELDRUM, B.S. 1984. Calcium overload in selectively vulnerable neurons of the hippocampus during and after ischemia: an electron microscopy study in the rat. *Journal of Cerebral Blood Flow and Metabolism*. 4(3):350-361.
- SIMON, R.P., SWAN, J.H. & MELDRUM, B.S. 1984. Blockade of N-methyl-D-aspartate receptors may protect against ischemic damage in the brain. *Science*. 244:798-800.
- SIMPSON, A.W.M. 1999. Fluorescent measurement of $[Ca^{2+}]_c$. Basic practical considerations. In: Lambert, D. G. *eds.* Methods in molecular biology, Vol. 114: Calcium signalling protocols. USA. Humana Press Inc. p3-30.
- SOBOLEVSKY, A.I., KOSHELEV, S.G. & KHODOROV, B.I. 1999. Molecular size and hydrophobicity as factors which determine the efficacy of the blocking action of amino-adamantane derivatives on NMDA channels. *Membrane and Cell Biology*. 13(1):79-93.
- STOUT, A. K. & REYNOLDS, I. J. 1999. High-affinity calcium indicators underestimate increases in intracellular calcium concentrations associated with excitotoxic glutamate stimulations. *Neuroscience*. 89(1):91-100.
- SWANEPOEL, S. 1991. Antimikrobiese aktiwiteit van die trikwinielamiene. North-West University (University for CHE): Potchefstroom campus. (Dissertation – M.Sc.) 133p.
- TAKAHASHI, A., CAMACHO, P., LECHLEITER, J.D. & HERMAN, B. 1999. Measurement of intracellular calcium. *Physiological Reviews*. 79:1089-1125.

- TATSUTA, K., AKIMOTO, K. & KINOSHITA, M. 1981. The total synthesis of (\pm)-coriolin. *Tetrahedron*. 37:4365-4369.
- TIMIN, E.N., BERJUKOW, S. & HERING, S. 2004. Concepts of state-dependent pharmacology of calcium channels. In: McDonough, S.I. *eds*. *Pharmacology of Calcium Channels*. New York: Kluwer Academic/Plenum Publishing.
- TRIGGLE, D.J. 2003. Drug targets in the voltage-gated calcium channel family: why some are and some are not. *Assay and Drug Development Technologies*. 1:719-733.
- TRIGGLE, D.J. 2006. L-Type Calcium Channels. *Current Pharmaceutical Design*. 12:443-457.
- TURSKI, L., BRESSLER, K., RETTIG, K.J., LÖSCHMANN, P.A. & WACHTEL, H. 1991. Protection of substantia nigra from MPP⁺ neurotoxicity by N-methyl-D-aspartate antagonists. *Nature*. 349:414-418.
- TYMIANSKI, M. & TATOR, C.H. 1996. Normal and abnormal calcium homeostasis in neurons: a basis for the pathophysiology of traumatic and ischemic injury. *Neurosurgery*. 38(6):1176-1195.
- UMEZAWA, H. 1985. Low-molecular-weight immunomodifiers produced by micro-organisms. *Biotechnology and genetic engineering reviews*. 3:255-273.
- VAN DER SCHYF, C.J., SQUIER, G.J. & COETZEE, W.A. 1986. Characterisation of NGP1-01, an aromatic polycyclic compound, as a calcium antagonist. *Pharmacological Research Communications*. 18:407-417.
- VAN DER SCHYF, C.J., LIEBENBERG, W., BORNMAN, R., DEKKER, T.G., VAN ROOYEN, P.H., FOURIE, T.G., MATTHEE, E. & SNYCKERS, F.O. 1989. The polycyclic calcium antagonist, NGP1-01, has an oxa rather than an aza bird-cage structure: evidence from n.m.r. spectroscopy and the X-ray crystal structure. *South African Journal of Chemistry*. 42:46-48.

- VAN DER SCHYF, C.J., GELDENHUYS, W.J. & YODIM, M.B.H. 2006. Multifunctional drugs with different CNS targets for neuropsychiatric disorders. *Journal of Neurochemistry*. 99(4):1033-1048.
- VAN DER WALT, J.J., VAN DER SCHYF, C.J., VAN ROOYEN, J.M., DE JAGER, J. & VAN AARDE, M.N. 1988. Calcium current blockade in the cardiac myocytes by NGP1-01, an aromatic polycyclic amine. *South African Journal of Science*. 84:448-450.
- VENTER, H.J. 1988. Die sintese en pirolise van polisikliese organiese sulfiete. North-West University (University for CHE): Potchefstroom campus. (Thesis-Ph.D) 267p.
- VIEHE, H.G., MERENYI, R., STELLA, L. & JANOUSEK, Z. 1979. Captop-dative substituent effects in synthesis with radicals and radicophiles. *Angewandte Chemie*. 18:917-932.
- VIGNON, J., CHICHEPORTICHE, R., CHICHEPORTICHE, M., KAMENKA, J.M., GENESTE, P. & LAZDUNSKI, M. 1983. [³H]TCP: a new tool with high affinity for the PCP receptor in rat brain. *Brain Research*. 280(1):194-197
- WENKERT, E. & YODER, J.E. 1970. Zinc reduction of γ diketones. *Journal of Organic Chemistry*. 35:2986-2989.
- YODIM M.B.H. & BUCCAFUSCO J.J. 2005(a). CNS Targets for multifunctional drugs in the treatment of Alzheimer's and Parkinson's diseases. *Journal of Neural Transmission*. 112:519-537.
- YODIM M.B.H. & BUCCAFUSCO J.J. 2005(b). Multi-functional drugs for various CNS targets in the treatment of neurodegenerative disorders. *Trends in Pharmacological Sciences*. 26:27-35.

ZAH, J. 2002. Physicochemical parameters as descriptors of blood-brain barrier permeability in polycyclic amines. North-West University: Potchefstroom campus. (Dissertation – M.Sc.) 123p.

ZAH, J., TERRE'BLANCE, G., ERASMUS, E. & MALAN, S.F. 2003. Physicochemical prediction of a brain-blood distribution profile in polycyclic amines. *Bioorganic and Medical Chemistry*. 11:3569-3578.

Acknowledgements

Thanks to God for my Redeemer,
Thanks for all Thou dost provide!
Thanks for times now but a memory,
Thanks for Jesus by my side!
Thanks for pleasant, balmy springtime,
Thanks for dark and stormy fall!
Thanks for tears by now forgotten,
Thanks for peace within my soul!

Thanks for prayers that Thou hast answered,
Thanks for what Thou dost deny!
Thanks for storms that I have weathered,
Thanks for all Thou dost supply!
Thanks for pain, and thanks for pleasure,
Thanks for comfort in despair!
Thanks for grace that none can measure,
Thanks for love beyond compare!

Thanks for roses by the wayside,
Thanks for thorns their stems contain!
Thanks for home and thanks for fireside,
Thanks for hope, that sweet refrain!
Thanks for joy and thanks for sorrow,
Thanks for heav'nly peace with Thee!
Thanks for hope in the tomorrow,
Thanks through all eternity!

The words of *August L. Storm*, in the *Swedish Salvation Army paper Strids-Ropet*, 1891; translated from Swedish to English by *Carl E. Backstrom*, 1931. These words were based on scripture in *1Thessalonians 5:18* "...in everything give thanks; for this is the will of God in Christ Jesus for you."

I would like to express my gratitude to the following people for their valuable input, motivation and support:

- Prof. S.F. Malan, my supervisor, for your guidance and support.
- Prof. C.J. van der Schyf for all the opportunities you have given me as well as inspiring me to be the best I can be.
- Prof. W. Liebenberg for your assistance.
- Dr. W.J. Geldenhuys for your generous help, sharing your expertise, support, friendship and guidance.
- Dr. J.P. Petzer for teaching me so much of what I know today. You have also been a wonderful friend.
- The very competent team from the instrument making facility at the Northwest University (Potchefstroom campus). Without their skills, building of the pyrolysis apparatus would not have been possible.
- All the personnel and student at the department of Pharmaceutical Chemistry at the Northwest University.
- Special thanks to my parents, Piet and Mercia Bezuidenhout for raising me to be a confident young woman with lots of vigour for life, a positive spirit and a humble soul. You both have set such great examples: my dad with your practical approach to life; you can make anything work, never got discouraged and never gave up. My mom who always gave so much of herself, thank you for teaching me what it is to love and give generously.
- My sisters, Mercia and Cornia Bezuidenhout. You guys are such a joy in my life and I love you dearly.
- The wonderful man in my life, Chris Young. You are such an amazing man and have taught me so much about life and love. You inspire me with your wisdom, compassion, calm and gentle nature. I have never had so much respect for a man as I have for you and I love you with all that I have.

I also want to give thanks to:

- Dr. T.J. Thekkumkara at Texas Tech University for allowing us the use of his fluorescent microscope.
- Potchefstroom University, Department of Pharmaceutical Chemistry, South Africa
- National Research Foundation (NRF), South Africa, for financial support.
- Texas Tech University, School of Pharmacy, USA
- Northeast Ohio University College of Pharmacy (NEOUCOP), USA

APPENDIX A

ABBREVIATIONS

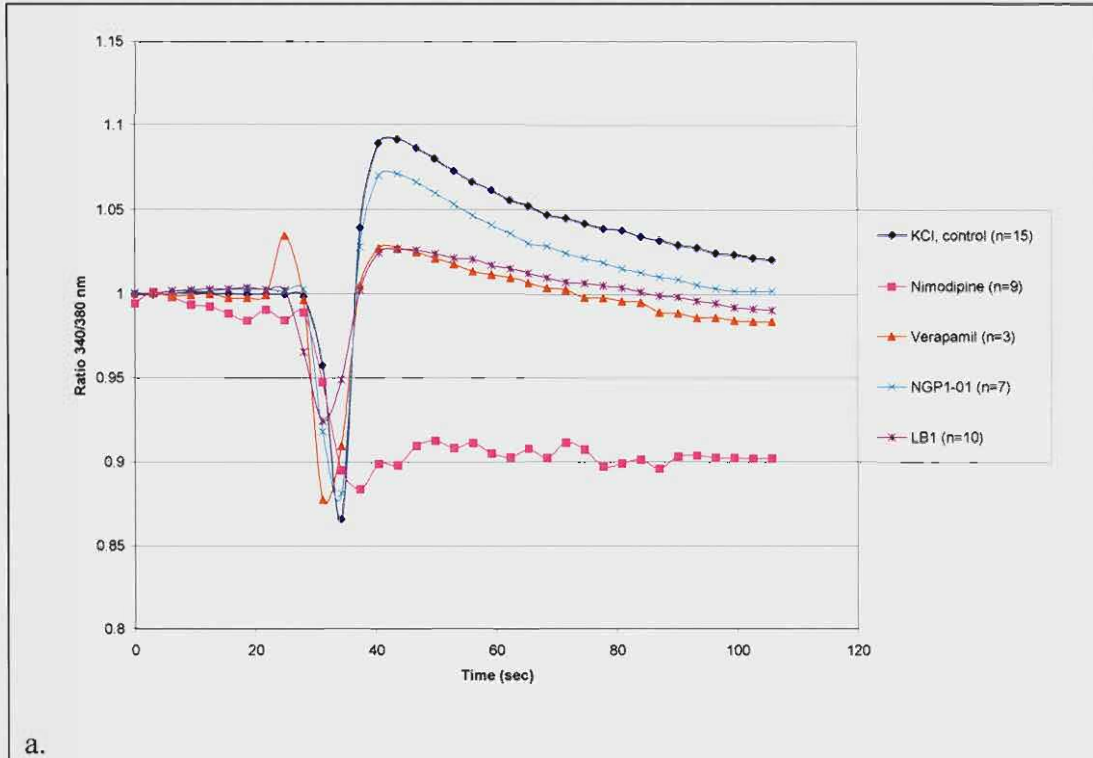
AC	adenyl cyclase	
AMPA	α -amino-3-hydroxy-5-methylisoxazole-4-propionic receptor (also known as the quisqualate receptor)	acid
AM	acetoxymethyl ester	
AM1	Austin model 1	
ANOVA	analysis of variance	
AP	action potential	
ATP	adenyl triphosphate	
BSA	bovine serum albumin	
cAMP	cyclic adenosine-monophosphate	
[Ca²⁺]_i	intracellular calcium concentration	
[Ca²⁺]_e	extracellular calcium concentration	
CNS	central nervous system	
DMEM	dulbecco's modified eagle's medium	
DMSO	dimethylsulphoxide	
DSC	differential scanning calorimetry	
DTF	density functional theory	
EAA	excitatory amino acid	
ER	endoplasmic reticulum	
FMO	frontier molecular orbital theory	
FVP	flash vacuum pyrolysis	
Glu	glutamate	
Gly	glycine	
GTP	guanosine triphosphate	

HBSS	Hanks balanced salt solution
HEPES	<i>N</i> -2-Hydroxyethylpiperazine- <i>N'</i> -2-ethanesulphonic acid
HF	Hartree-Fock
IR	infrared spectroscopy
KA	kainate
LUMO	lowest unoccupied molecular orbital
Mag-Fura-2/AM	2-[5-[2-[(acetyloxy)methoxy]-2-oxoethoxy]-6-[bis[2-[(acetyloxy) methoxy]-2-oxoethyl]amino]-2-benzofuranyl]- (acetyloxy)methyl ester
MK-801	dizocilpine
HOMO	highest occupied molecular orbital
Mp	melting point
MS	mass spectrometry
NMDA	<i>N</i> -methyl-D-aspartate
NMDAR	<i>N</i> -methyl-D-aspartate receptor
NMR	nuclear magnetic resonance spectroscopy
NOS	nitric oxide synthases
PCP	phencyclidine
PKC	protein kinase-C
PLC	phospholipase-C
ppm	parts per million
ROI	region of interest
ROS	reactive oxygen species
SAR	structure-activity relationship
SEM	standard error of mean
TCP	<i>N</i> -(1-[2-thienyl]cyclohexyl)3,4-piperidine
THF	tetrahydrofuran
TLC	thin-layer chromatography
TMS	tetramethylsilane
Triq	triquinane
UV	ultra-violet
VGCC	voltage gated calcium channels

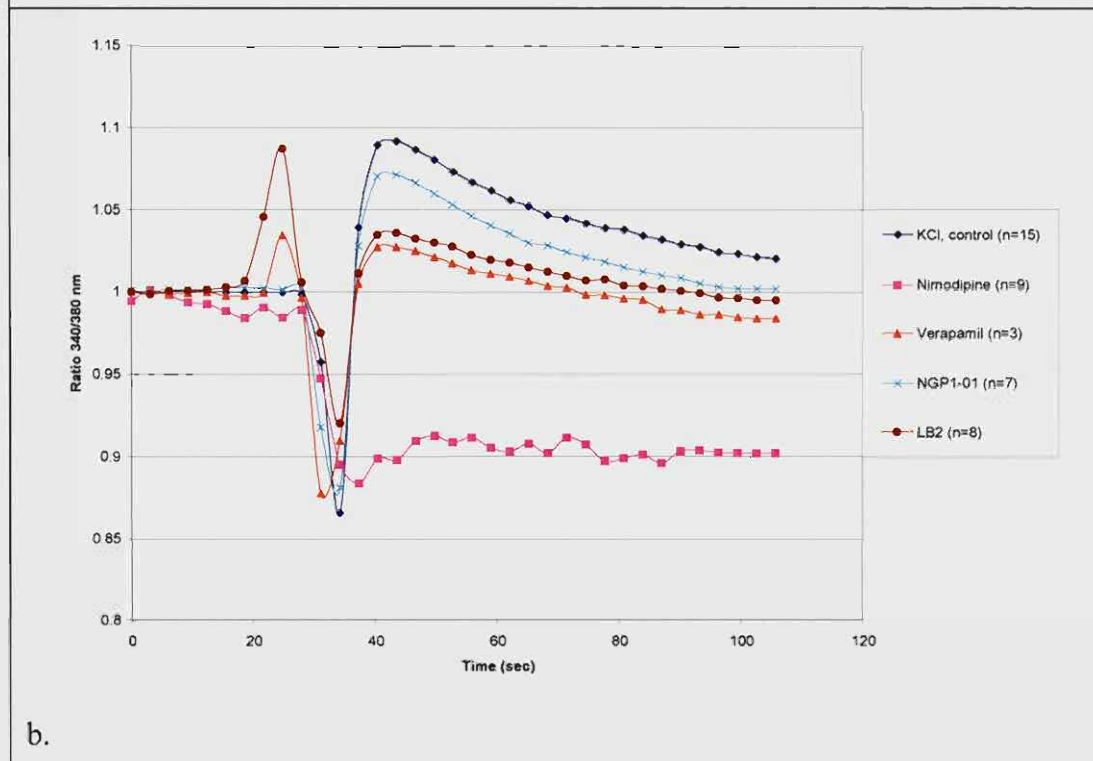
APPENDIX B

EXPERIMENTAL GRAPHS

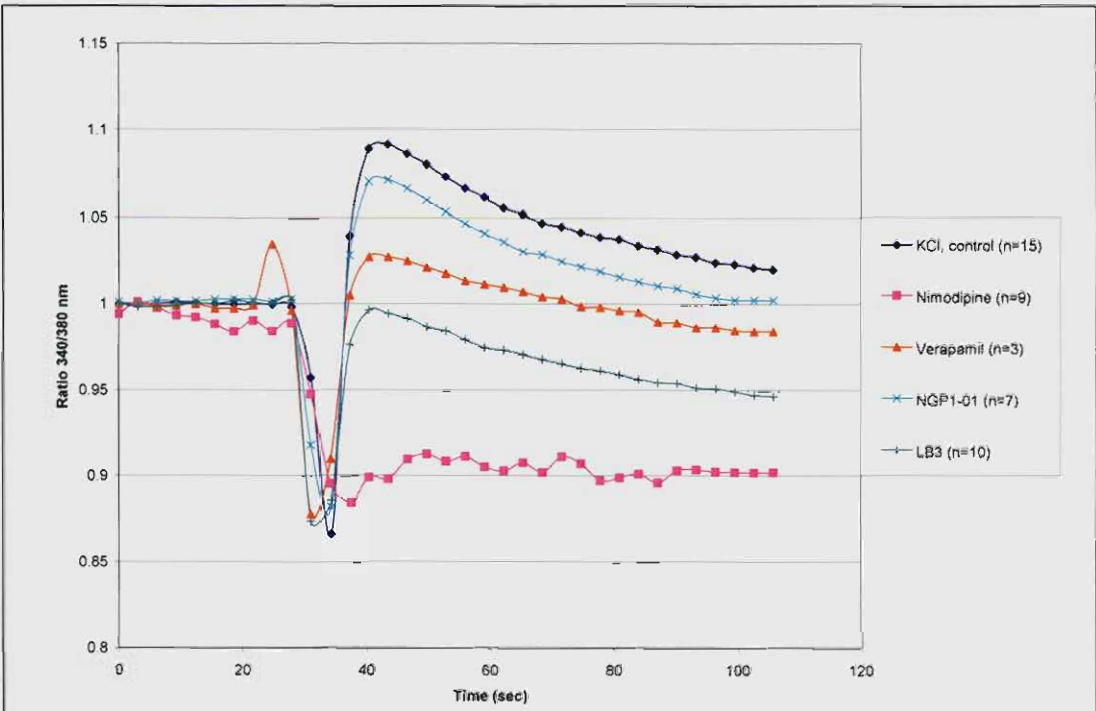
- KCl-induced depolarisation in the presence of test compounds and controls.



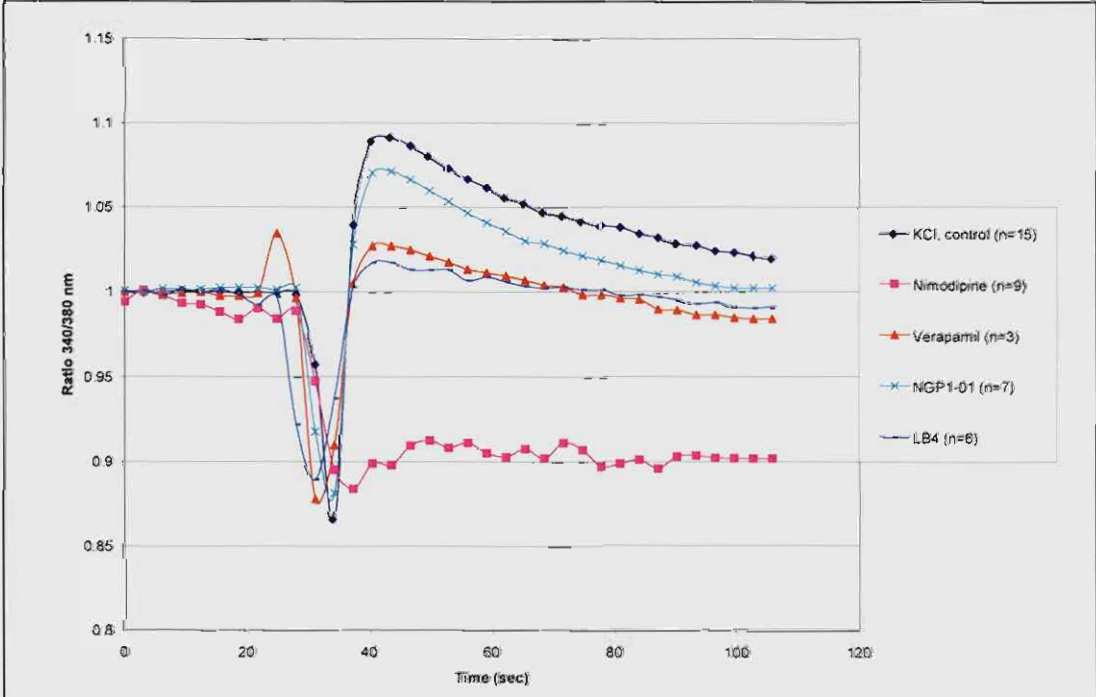
a.



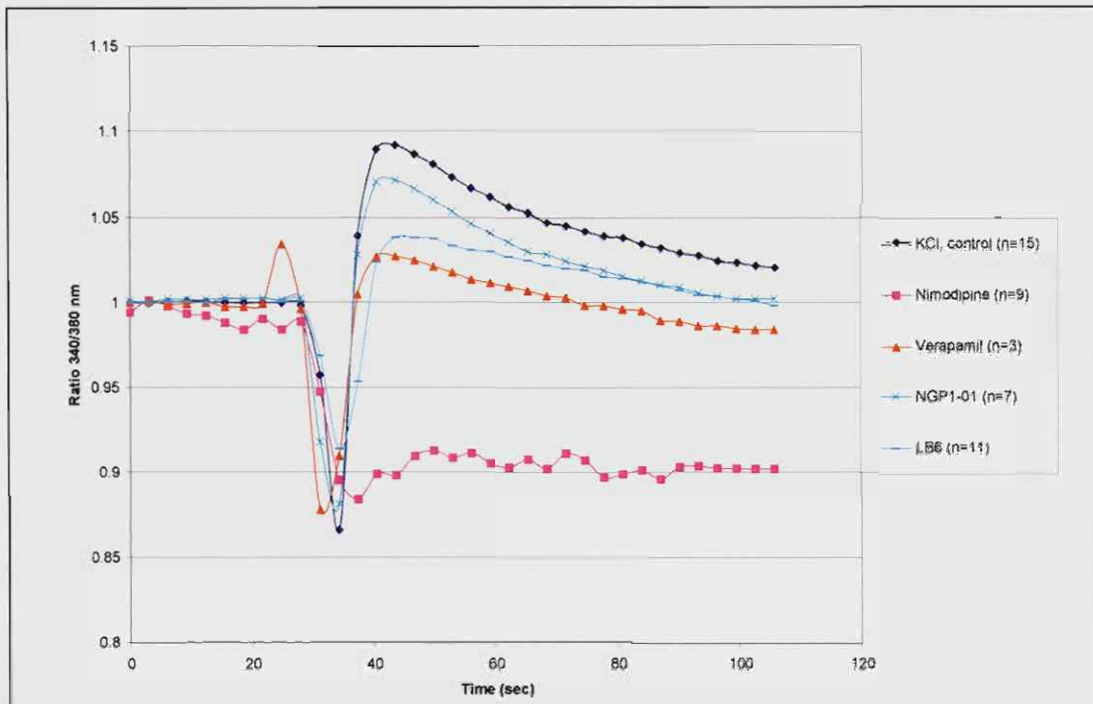
b.



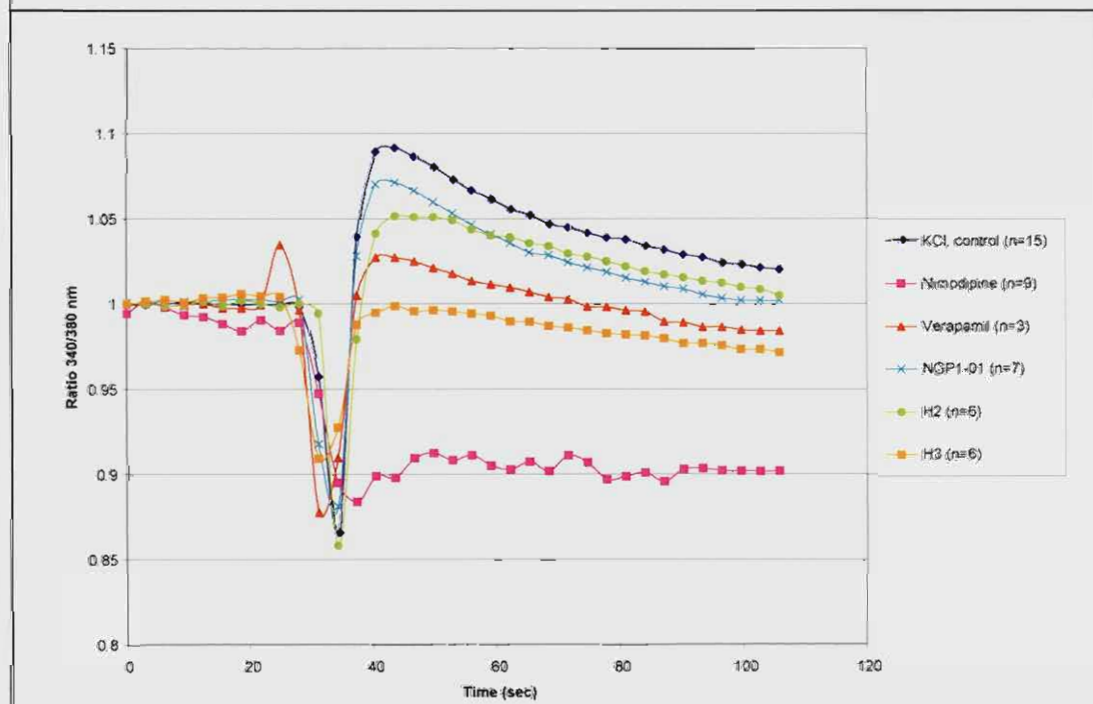
C.



d.



e.



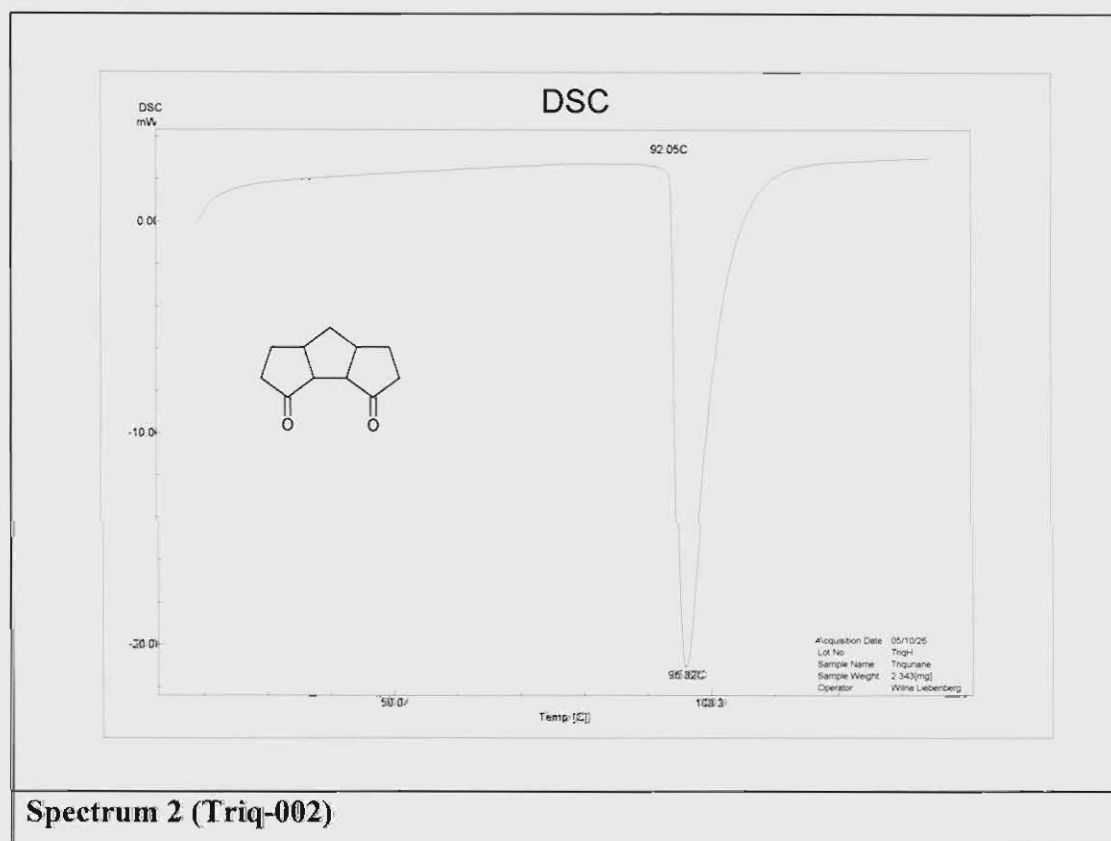
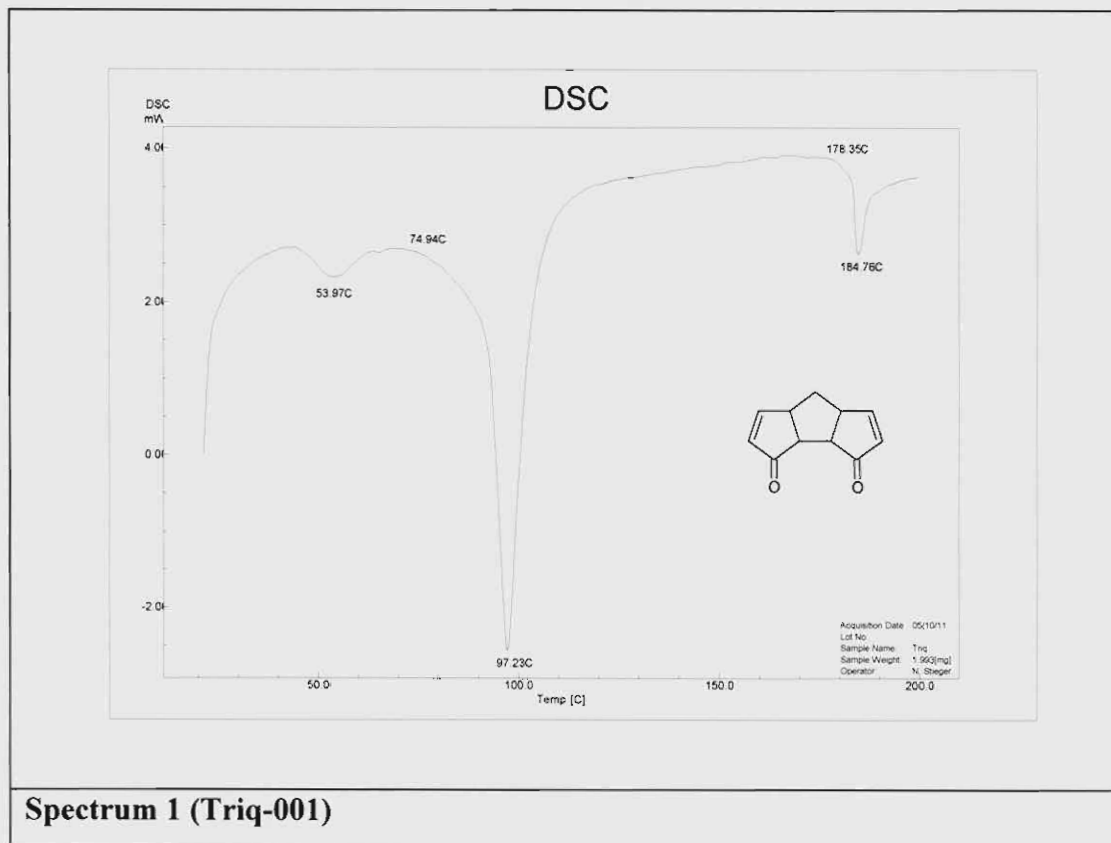
f.

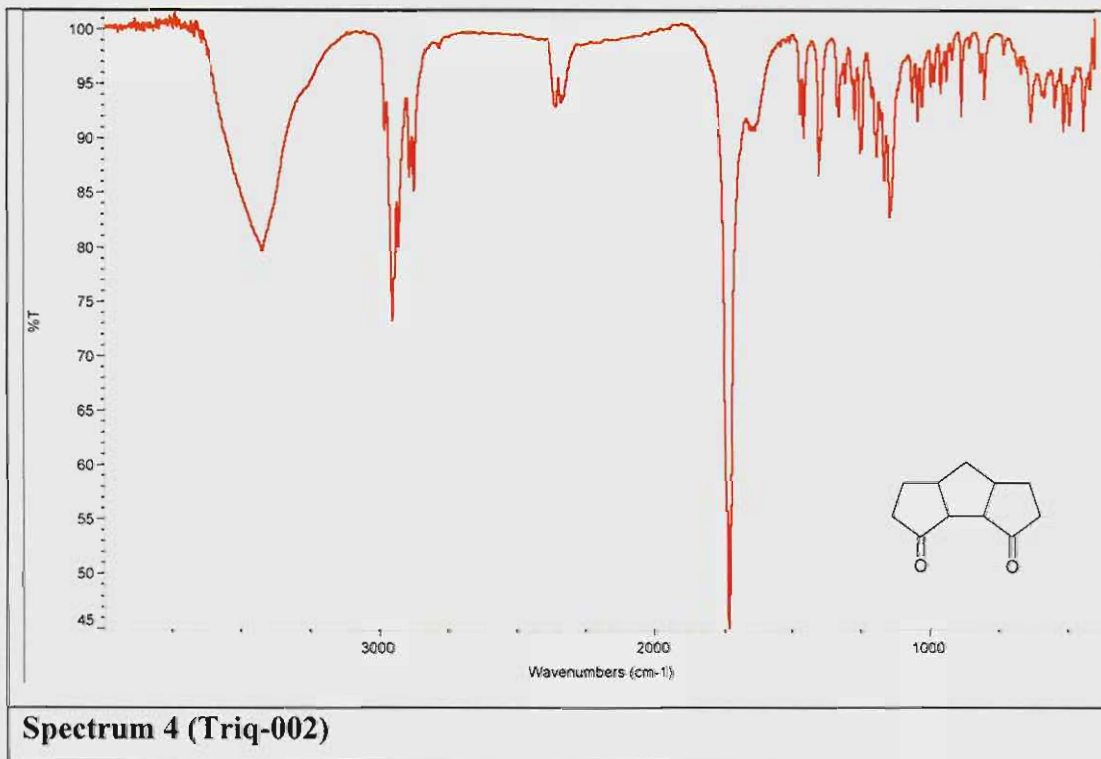
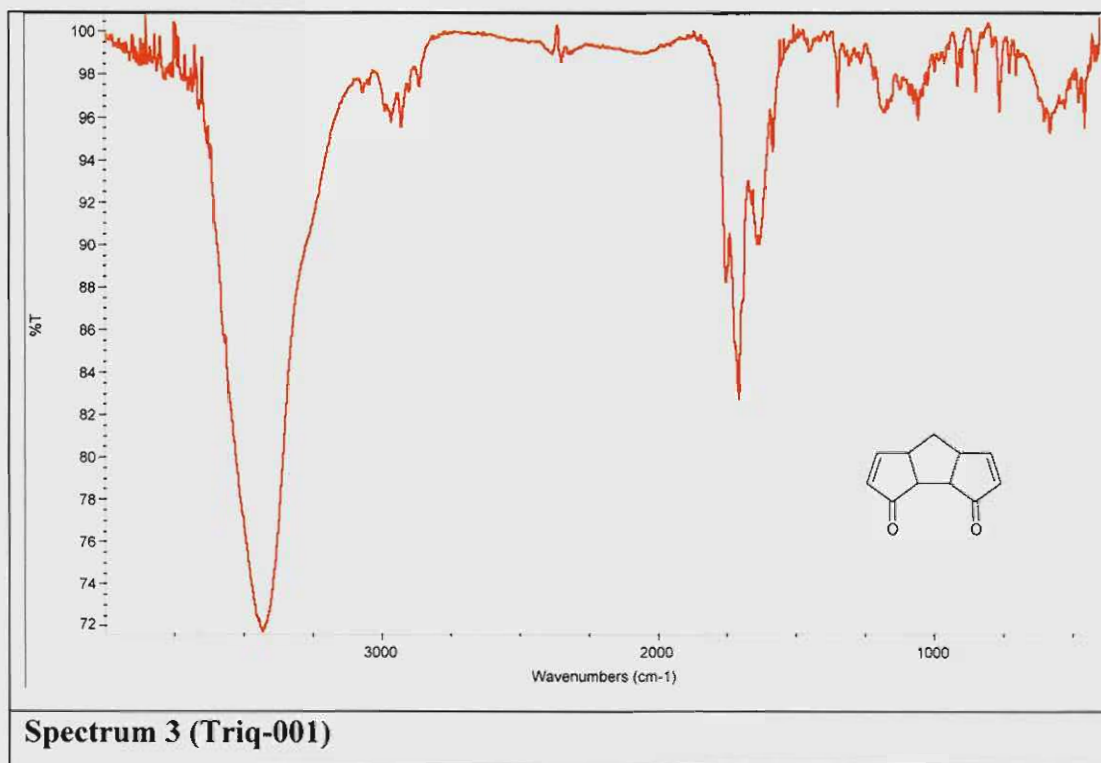
Experiments demonstrating the effect of depolarisation with KCl (140 mM) in the presence of individual test compounds (100 μ M) compared to reference compounds (100 μ M) and control (Fig. 5.5, section 5.1.3.2, chapter 5).

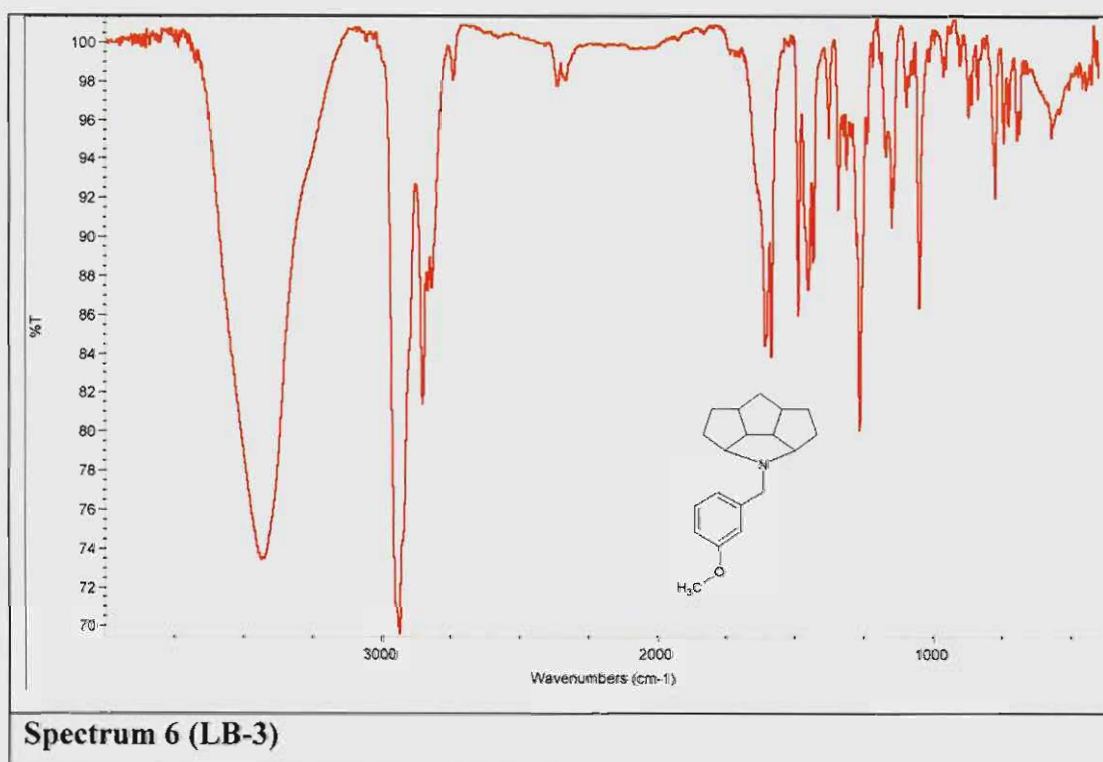
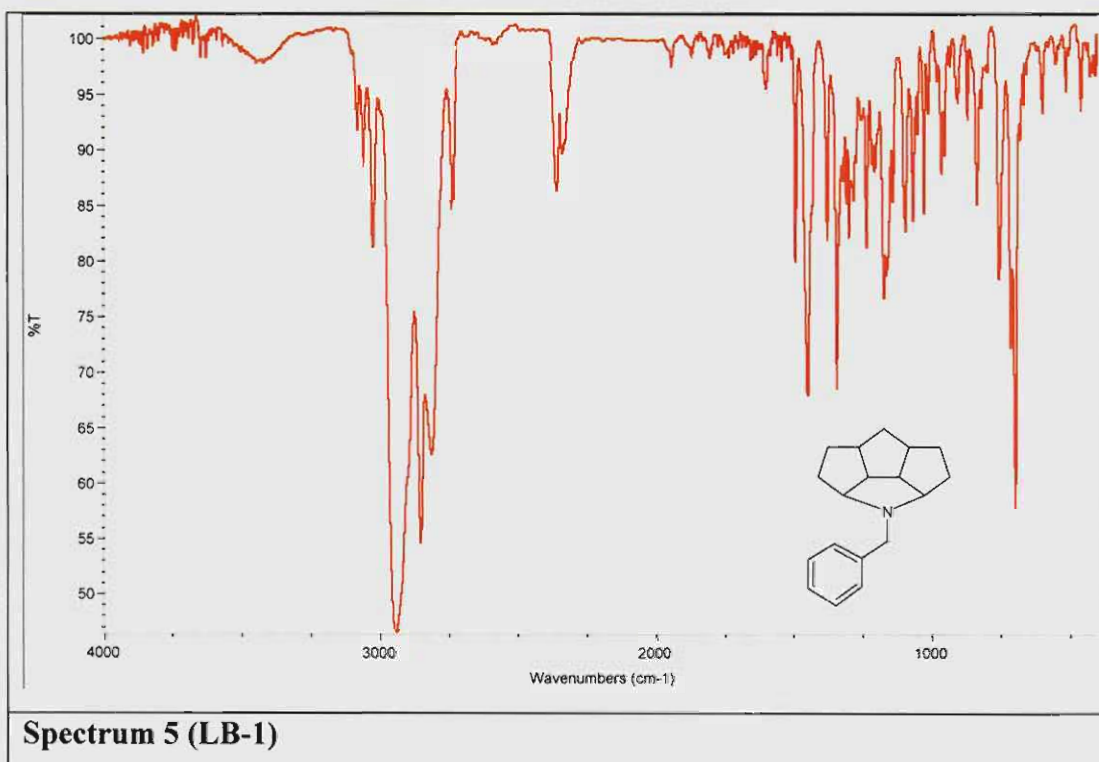
APPENDIX C

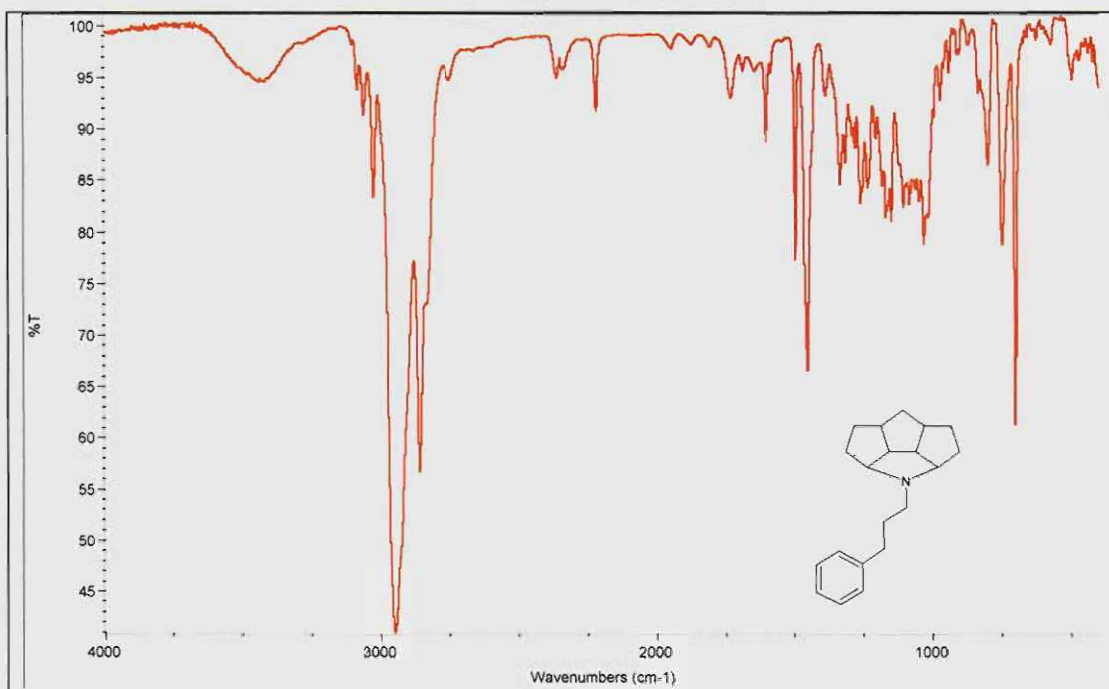
SPECTRAL DATA

- DSC
- INFRARED SPECTROSCOPY
- MASS SPECTROMETRY
- ^1H NUCLEAR RESONANCE SPECTROMETRY
- ^{13}C NUCLEAR RESONANCE SPECTROSCOPY

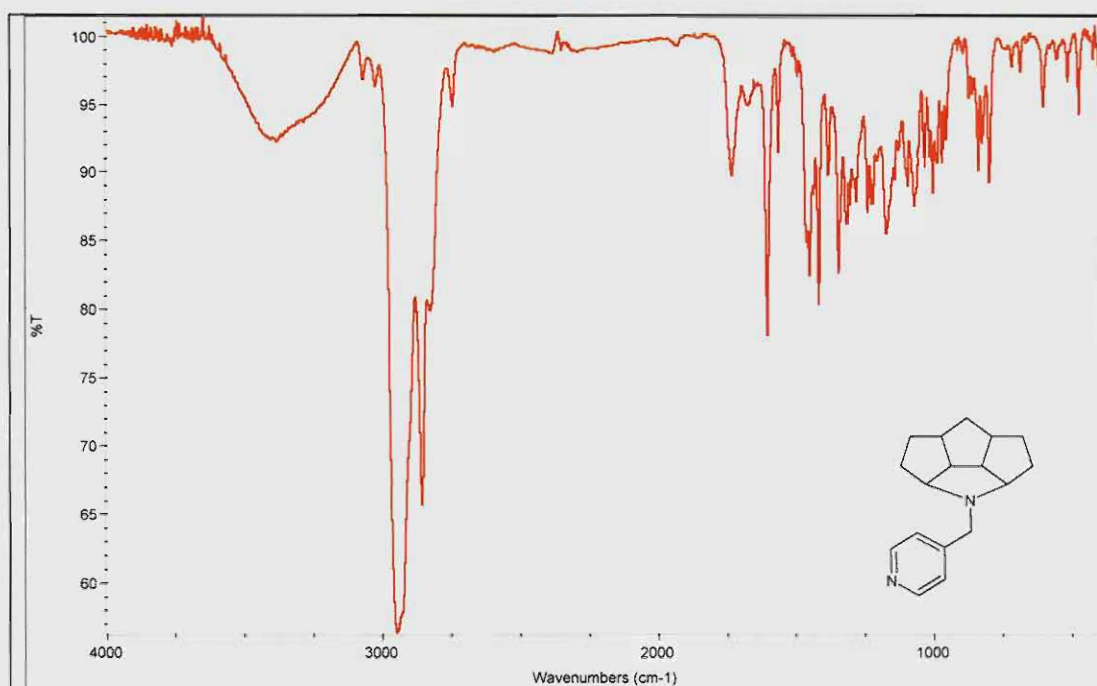
DSC

INFRARED SPECTROSCOPY

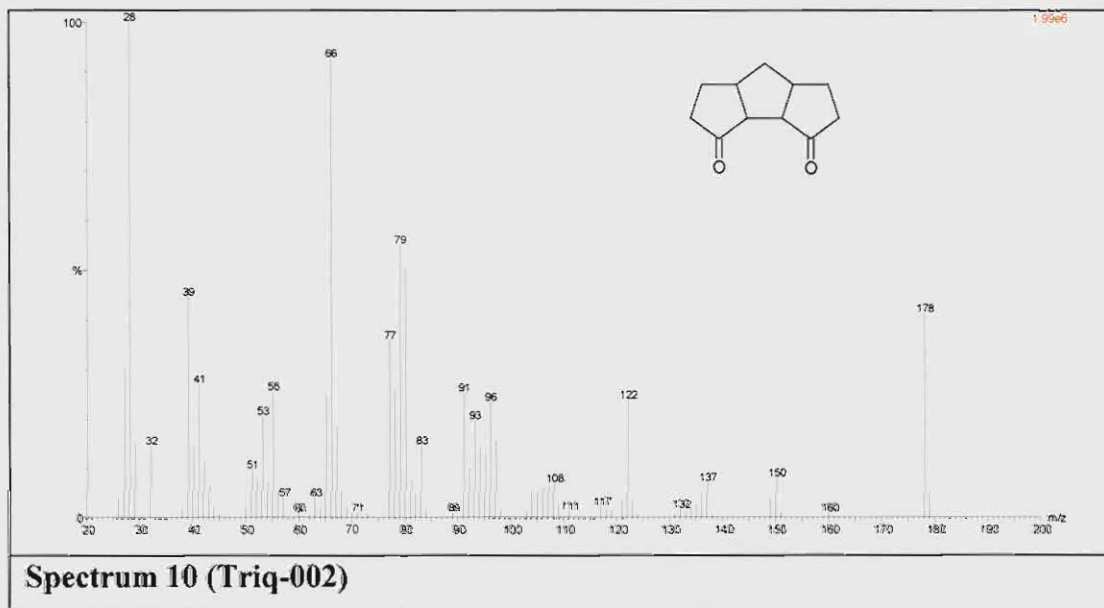
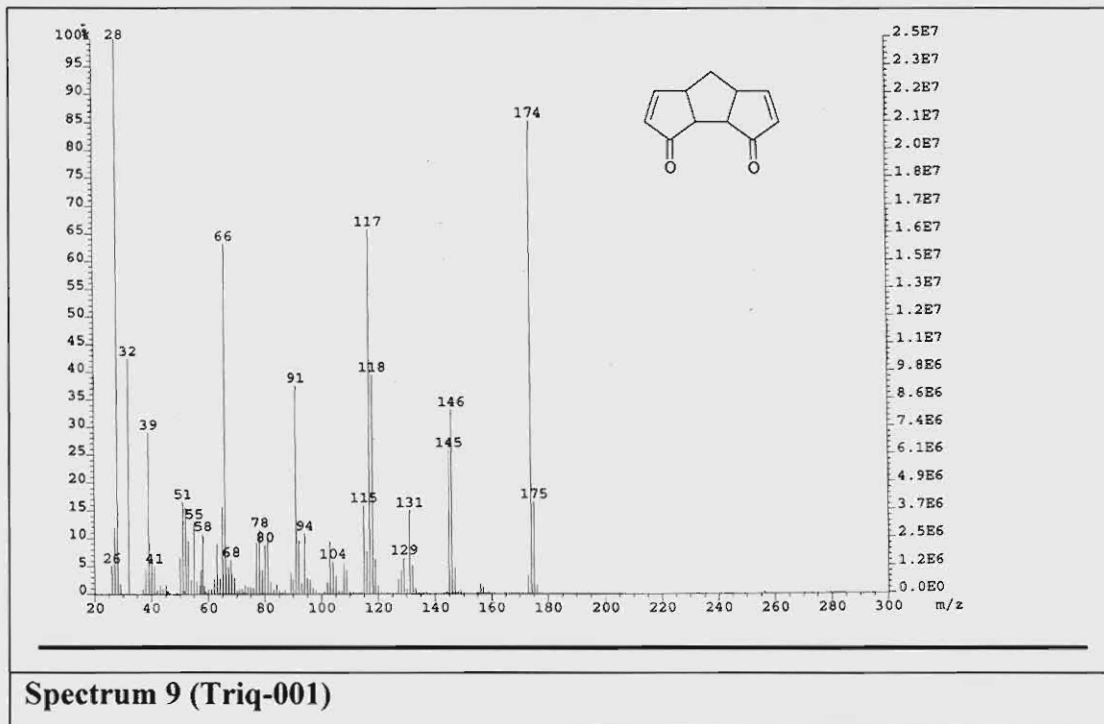


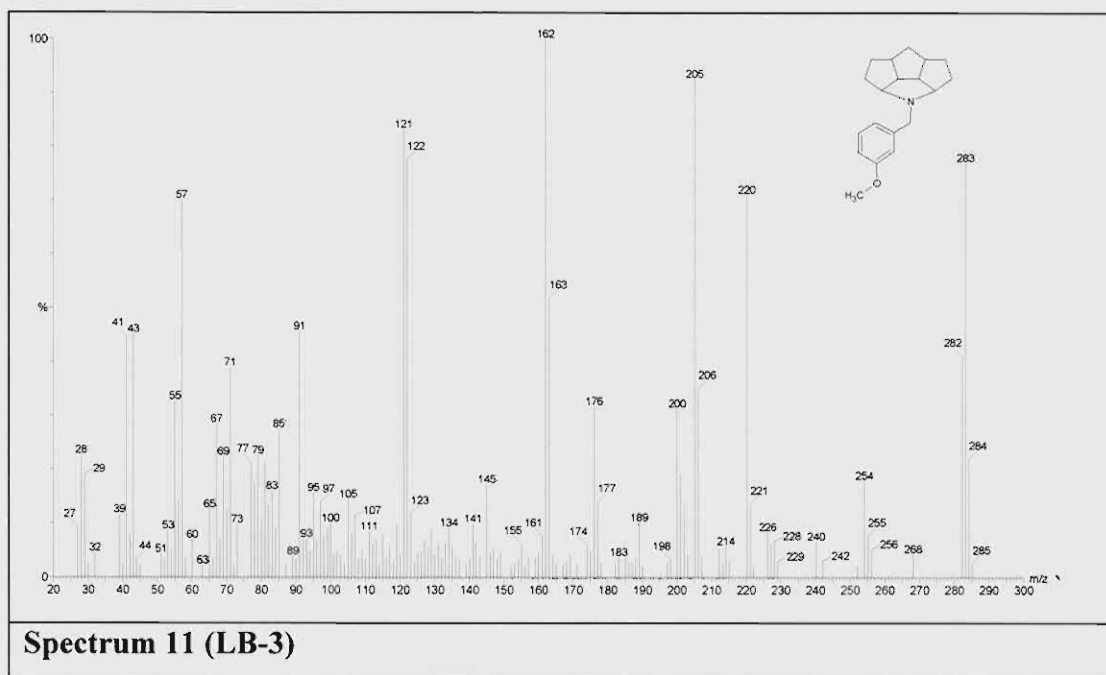
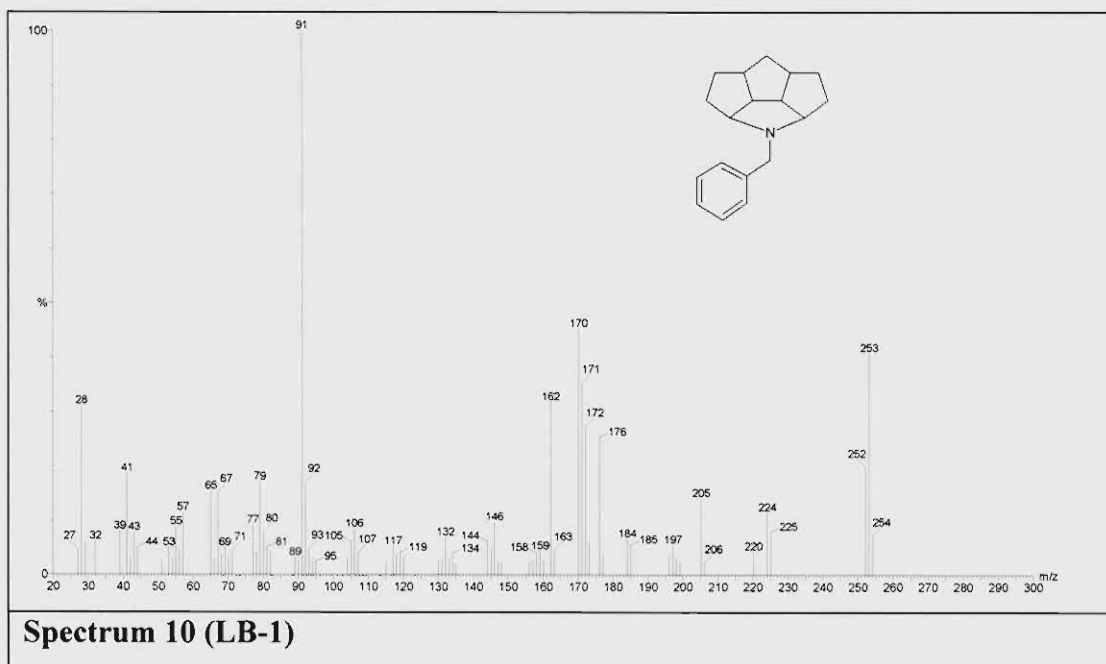


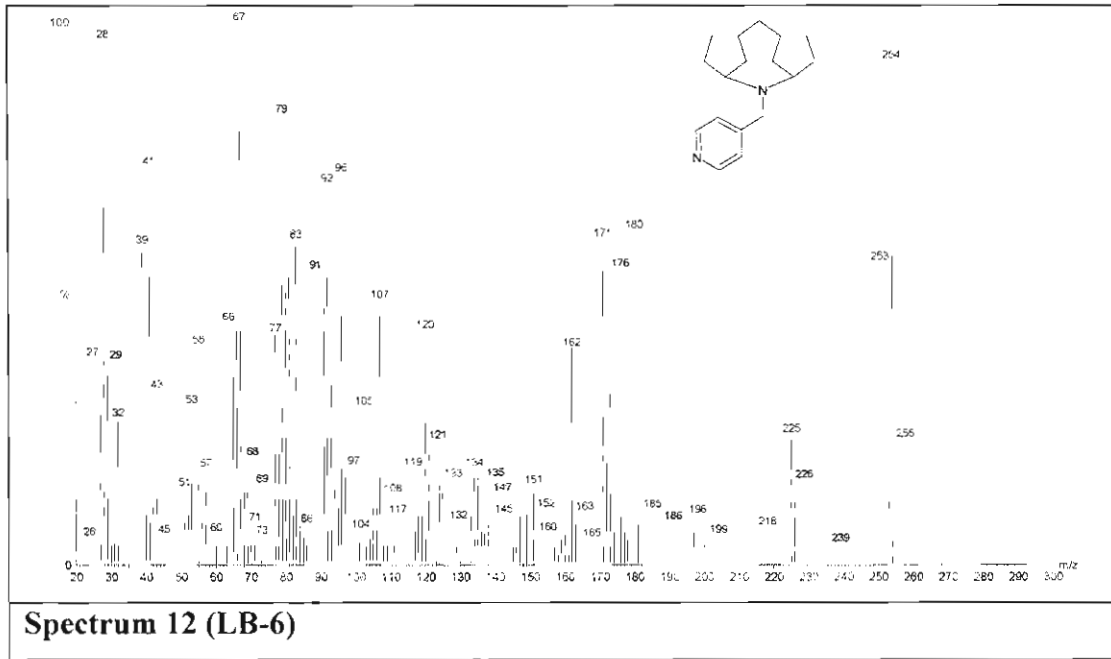
Spectrum 7 (LB-4)

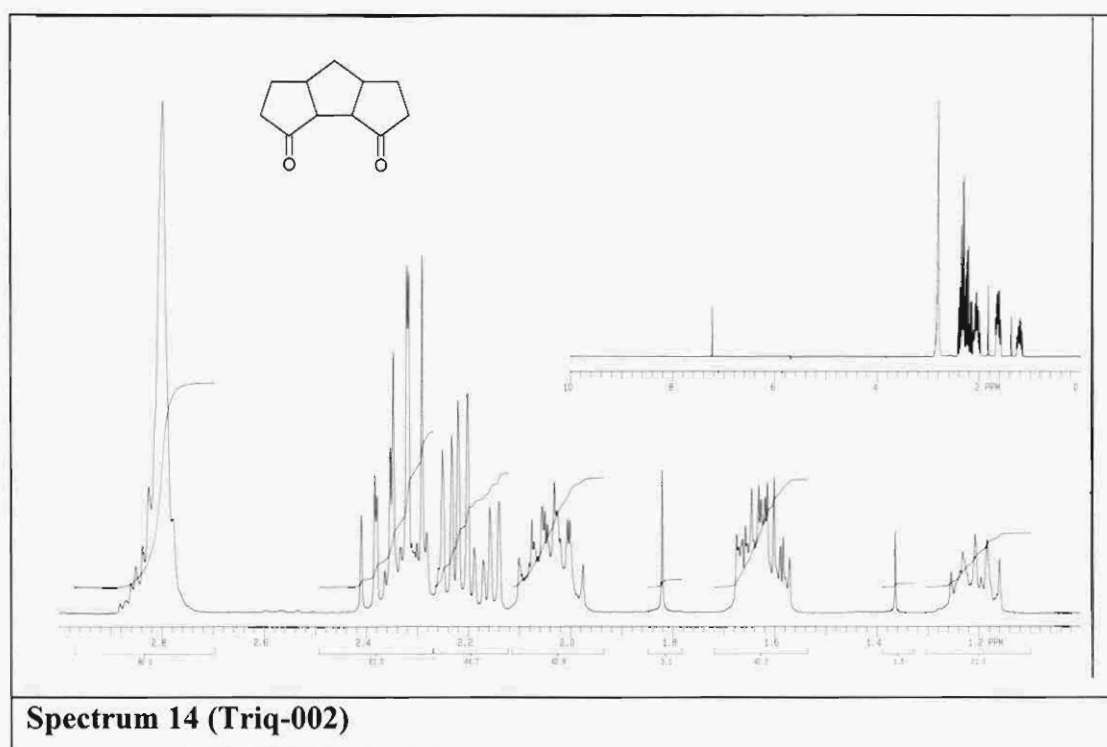
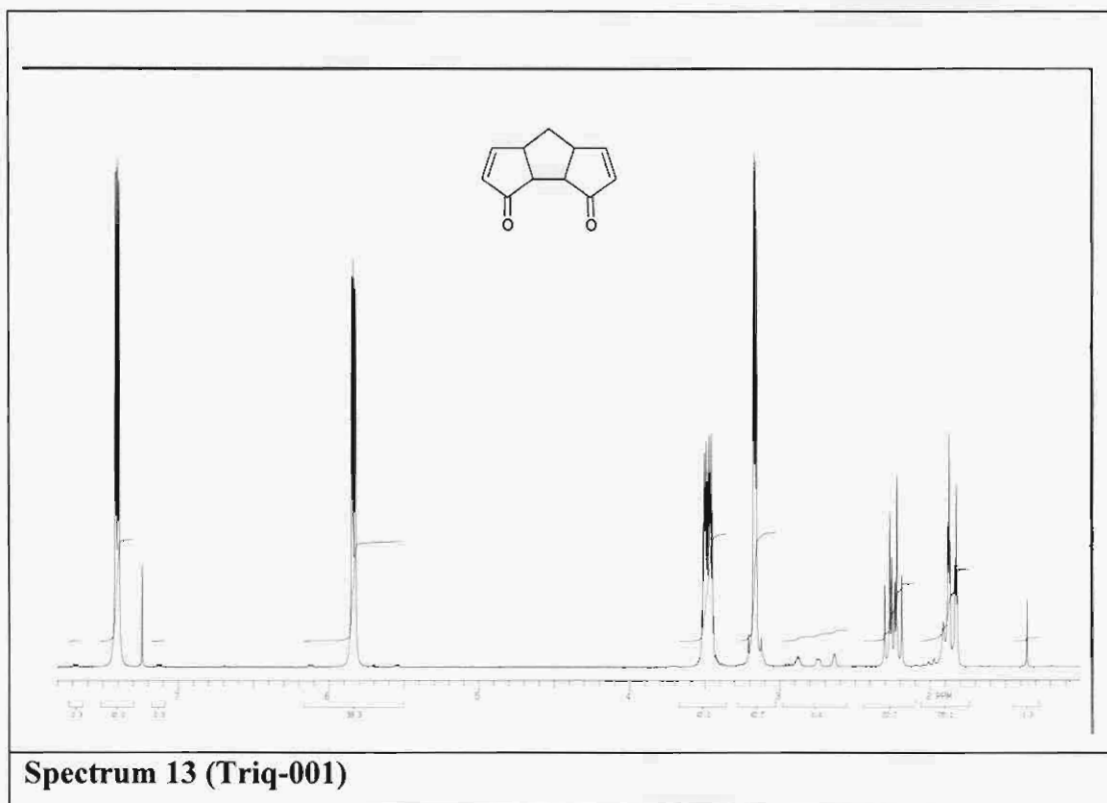


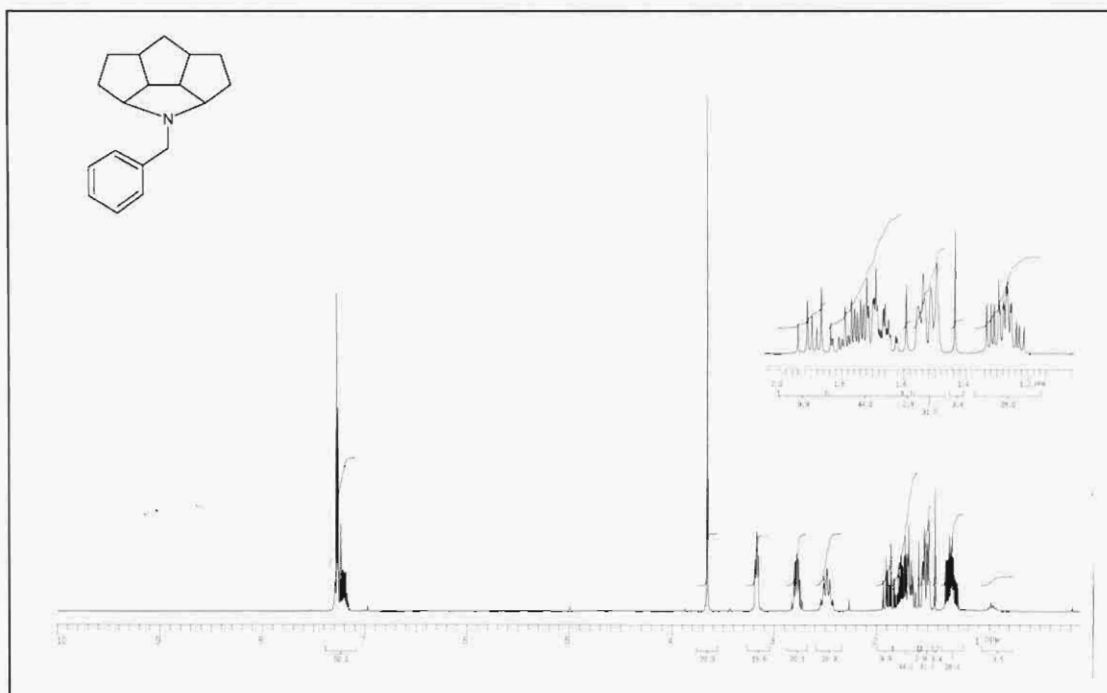
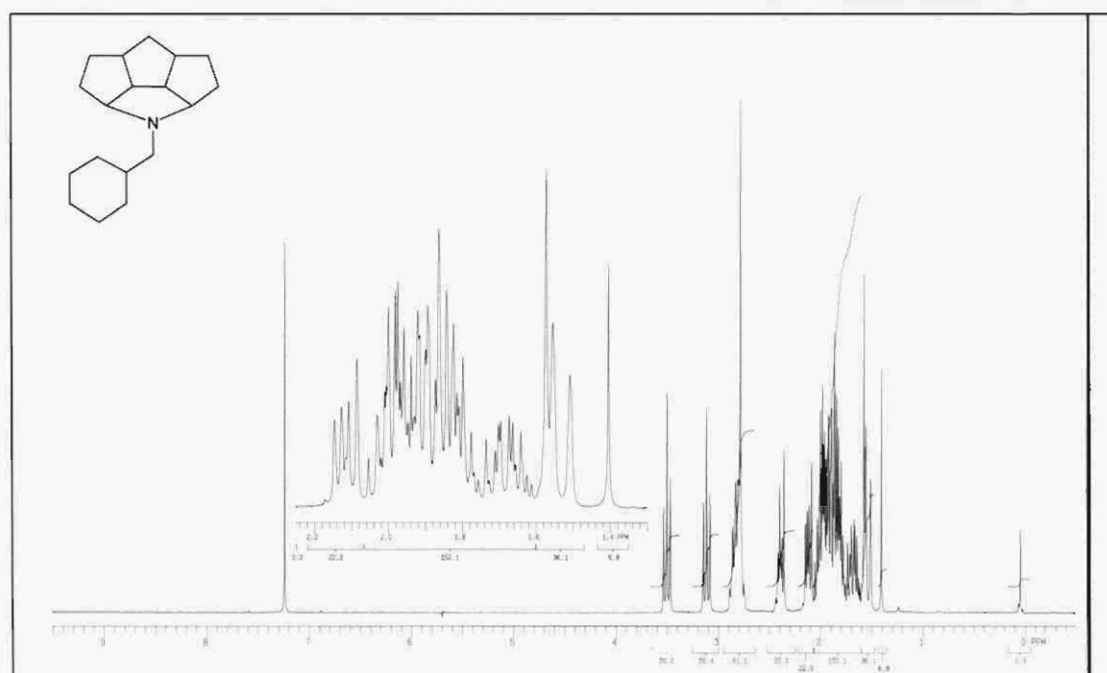
Spectrum 8 (LB-6)

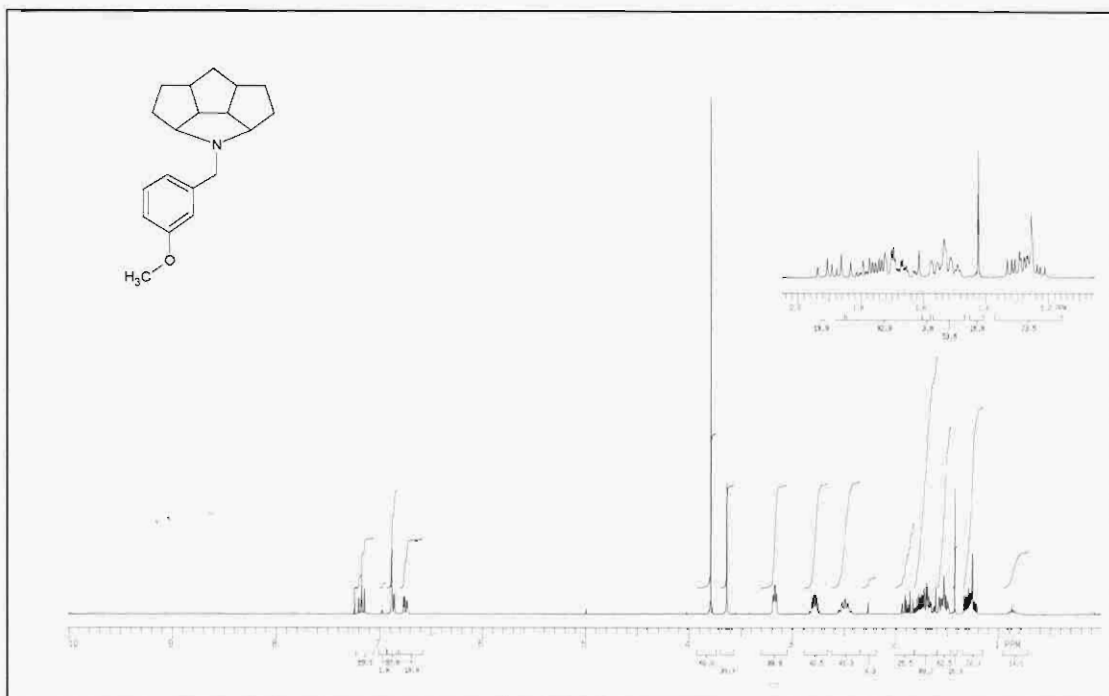
MASS SPECTROMETRY



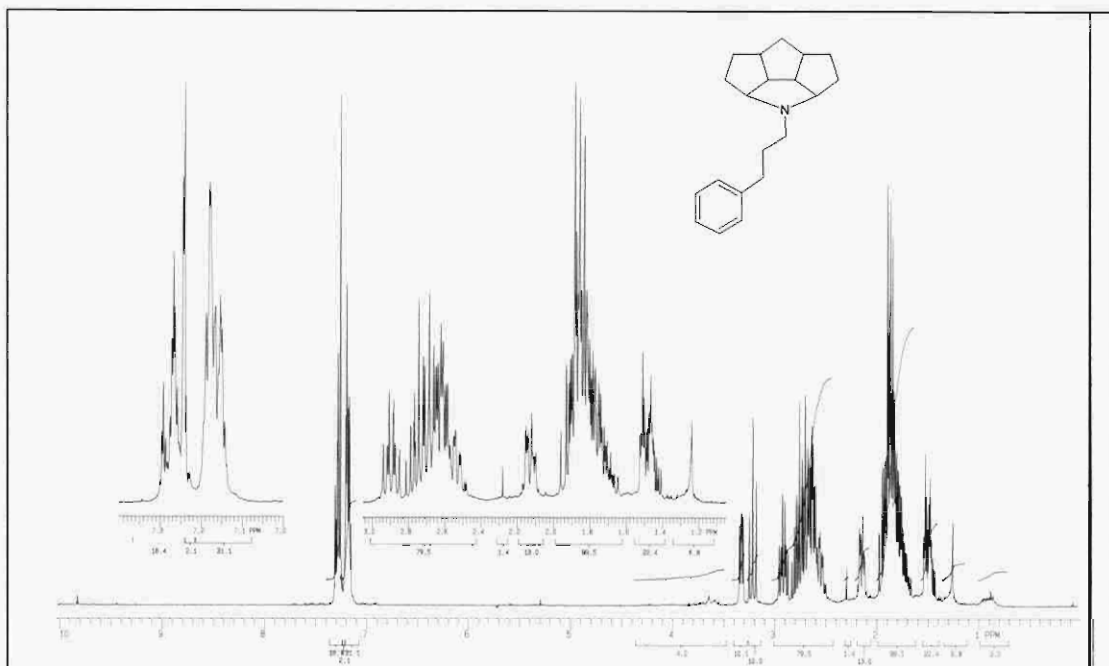


^1H NUCLEAR RESONANCE SPECTROMETRY

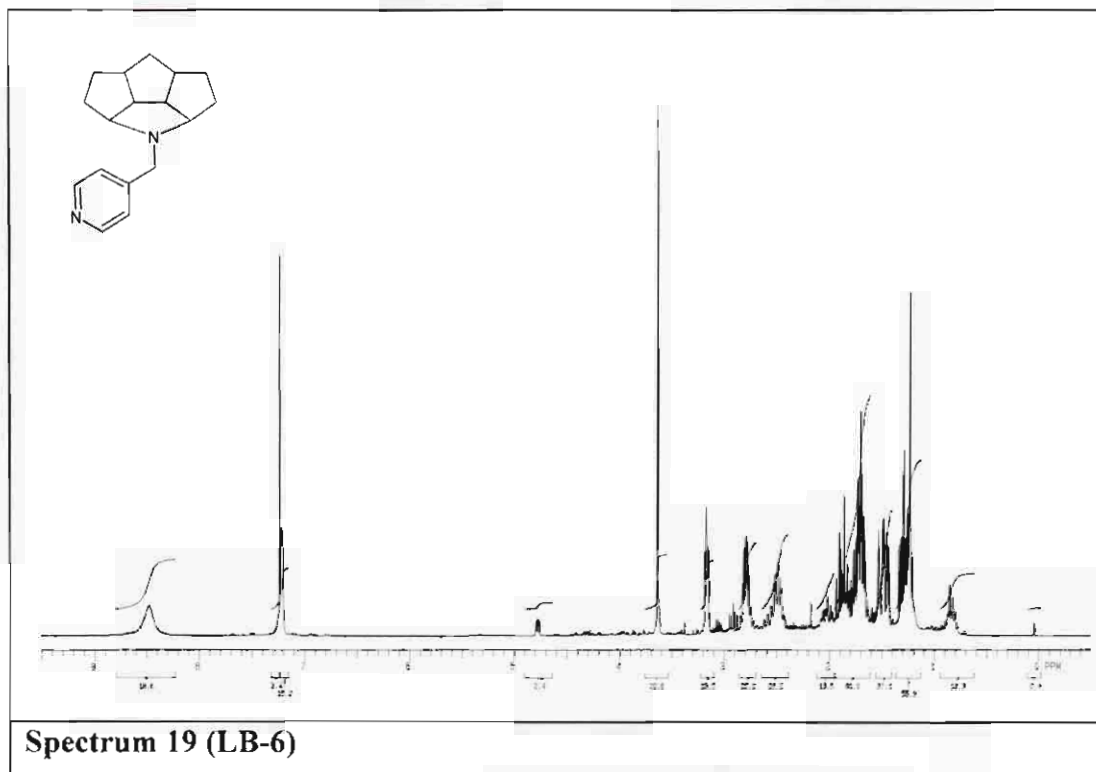
**Spectrum 15 (LB-1)****Spectrum 16 (LB-2)**



Spectrum 17 (LB-3)



Spectrum 18 (LB-4)



^{13}C NUCLEAR RESONANCE SPECTROSCOPY